

## **Copyright Warning & Restrictions**

The copyright law of the United States (Title 17, United States Code) governs the making of photocopies or other reproductions of copyrighted material.

Under certain conditions specified in the law, libraries and archives are authorized to furnish a photocopy or other reproduction. One of these specified conditions is that the photocopy or reproduction is not to be “used for any purpose other than private study, scholarship, or research.” If a user makes a request for, or later uses, a photocopy or reproduction for purposes in excess of “fair use” that user may be liable for copyright infringement,

This institution reserves the right to refuse to accept a copying order if, in its judgment, fulfillment of the order would involve violation of copyright law.

**Please Note: The author retains the copyright while the New Jersey Institute of Technology reserves the right to distribute this thesis or dissertation**

Printing note: If you do not wish to print this page, then select “Pages from: first page # to: last page #” on the print dialog screen

The Van Houten library has removed some of the personal information and all signatures from the approval page and biographical sketches of theses and dissertations in order to protect the identity of NJIT graduates and faculty.

## ABSTRACT

Title of Thesis: Thermal Decomposition of Dichloromethane/  
1,1,1-Trichloroethane Mixture in an  
Atmosphere of Hydrogen

Yang Soo Won, Master of Science in Environmental Science,  
1988

Thesis Directed by Dr. J .W. Bozzelli

The thermal decomposition of a dichloromethane/1,1,1-trichloroethane mixture diluted in hydrogen was conducted in tubular flow reactors at 1 atmosphere total pressure. The thermal degradation of each species was analyzed systematically over temperature ranges from 475 - 810 °C, residence times of 0.05 - 2.0 seconds and three different surface to volume ratio flow reactors.

It was found that the conversions of each species in the mixture were a function of both temperature and residence time. Complete decay occurs at about 810 °C for dichloromethane and around 570 °C for 1,1,1-trichloroethane at 1 second residence time. The major products observed were dichloroethylene, vinyl chloride, methyl chloride and dichloroethane at about 570 °C. Ethylene, methane, ethane, methyl chloride and HCl were the products at more complete conversions which occurred near 810 °C and above. The hydrocarbon production increased approximately linearly with temperature. An increase in surface to volume ratio of the reactor tube was observed to accelerate the species

decomposition in hydrogen, but it had no effect on the distribution of major products.

This study demonstrated that selective formation of HCl can result from thermal reaction of dichloromethane/1,1,1-trichloroethane mixture and showed that synergistic effects of 1,1,1-trichloroethane decomposition accelerate the rate of dichloromethane decomposition. A detailed kinetic reaction mechanism was developed and used to model results obtained from the experimental reaction system. The detailed kinetic reaction mechanism was based on thermochemical principle and transition state theory.

Rate constants obtained for initially important decomposition of dichloromethane and 1,1,1-trichloroethane over the temperature range 475 to 810 °C are:

	A (1/s)	Ea (Kcal/mol)
$\text{CH}_2\text{Cl}_2 \text{ ----> CH}_2\text{Cl} + \text{Cl}$	1.1E16	82.8
$\text{CH}_3\text{CCl}_3 \text{ ----> CH}_2\text{CCl}_2 + \text{HCl}$	3.8E13	47.9
$\text{CH}_3\text{CCl}_3 \text{ ----> CH}_3\text{CCl}_2 + \text{Cl}$	2.4E16	73.2

THERMAL DECOMPOSITION  
OF DICHLOROMETHANE/1,1,1-TRICHLOROETHANE MIXTURE  
IN AN ATMOSPHERE OF HYDROGEN

BY  
YANG SOO WON

Thesis submitted to the faculty of the Graduate School of  
the New Jersey Institute of Technology in partial  
fulfillment of the requirements for the degree of  
Master of Science in Environmental Science

1988

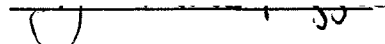
Blank Page

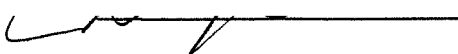
APPROVAL SHEET


Title of Thesis: Thermal Decomposition of Dichloromethane/  
1,1,1-Trichloroethane in an Atmosphere of  
Hydrogen

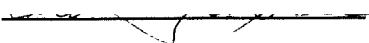
Name of Candidate: Yang Soo Won  
Master of Science in Environmental  
Science, 1988

Thesis and Abstract Approved:

 Aug 12 1988  
Joseph W. Bozzelli  
Professor  
Dep. Chemical Engineering,  
Chemistry and Environmental  
Science

 Aug 15, 1988  
Henry Shaw  
Professor  
Dep. Chemical Engineering,  
Chemistry and Environmental  
Science

 Aug 15, 1988  
Piero Armenante  
Assistant Professor  
Dep. Chemical Engineering,  
Chemistry and Environmental  
Science

 9/13/88  
Dr. Anthony M. Dean  
Exxon Research & Engineering  
Clinton Township, Annandale,  
New Jersey

VITA

Name: Yang Soo Won

Permanent Address:

Degree and Date to be conferred: Master of Science in  
Environmental Science 1988

Date of Birth:

Place of Birth:

Collegiate Institutions attended	Dates	Degree	Date
Yonsei University, Korea	75-79	B.S.	Feb., 79.
Korea Advanced Institute of Science and Technology	79-81	M.S.	Feb., 81
Major: Chemical Engineering			
New Jersey institute of Technology	86-88	M.S.	Sep., 88
Major: Environmental Science			



## Acknowledgement

I wish to express appreciation to Dr. Joseph W. Bozzelli for his advice and encouragement. I am deeply indebted to him for the opportunities which he made available to me. I acknowledge the helpful corrections and productive comments by Dr. H. Shaw, Dr. P. Armenante and Dr. A. M. Dean ( Exxon Research and Engineering ).

For love and inspiration I shall be eternally grateful to my wife, Jeong Yeon and my parents.

It is my pleasure to thank my colleagues at Kinetics Research Laboratory of the New Jersey Institute of Technology: Dr. Javad Tavakoli for his support and guidance.

## CONTENTS

	page
I. Introduction	1
II. Previous Studies	6
III. Theory	10
A. Transition-State and Collision Theory	11
B. Tubular Flow Reactor Theory	15
C. Decoupling of The Wall and Bulk Reaction Rate Constants	18
D. Prediction of Rate Constants for Radical Addition and Combination Reactions by Bimolecular QRRK Theory	19
IV. Experimental Method	28
A. Temperature Control and Measurment	30
b. Quantitative Analysis of Reaction Products	32
C. Hydrochloric Acid Analysis	37
V. Results and Discussion	39
A. Reaction of $\text{CH}_2\text{Cl}_2/\text{CH}_3\text{CCl}_3$ mixture with $\text{H}_2$	39
B. Reagent Conversion and Product Distribution	51
C. Comparison of $\text{CH}_2\text{Cl}_2/\text{CH}_3\text{CCl}_3$ Mixture Reaction with Each Pure Compound Reactions of Previous Studies	63
D. Quantum RRK	69
E. Detailed Kinetic Mechanism and Modeling	76
VI. Conclusion	96
VII. References	98
Appendix	

## LIST OF TABLES

1. Average Retention Time of Product	35
2. Relative Response Factors for FID	36
3. Chlorine Material Balance	56
4. Carbon Material Balance	57
5. Product Maxima Formation Temperatures and Bond Energies between Carbon and Chlorine in This Reaction System	60
6. Thermal Reaction Product Distribution with Temperature	61
7. Thermal Reaction Product Distribution with Time	62
8. Detailed Mechanism for $\text{CH}_2\text{Cl}_2/\text{CH}_3\text{CCl}_3/\text{H}_2$ Reaction System	85

## LIST OF FIGURES

1. Energy Diagram for Pressure-dependent Reaction	22
2. Experimental Set Up	29
3. Reactor Temperature Profile (axial)	31
4. Sample Chromatogram of $\text{CH}_2\text{Cl}_2$ / $\text{CH}_3\text{CCl}_3$ / $\text{H}_2$ Decomposition	33
5. Decay of $\text{CH}_2\text{Cl}_2$ and $\text{CH}_3\text{CCl}_3$ Decomposition versus Time	41
6. 1st Order Kinetics Fit of $\text{CH}_3\text{CCl}_3$ Decomposition	43
7. 1st Order Kinetics Fit of $\text{CH}_2\text{Cl}_2$ Decomposition	44
8. Reagent Decay vs. Reaction Time: Comparison of Different Reactor Tube Diameters	45
9. Arrhenius Behavior of $k_{\text{exp}}$ for $\text{CH}_3\text{CCl}_3$	46
10. Arrhenius Behavior of $k_{\text{exp}}$ for $\text{CH}_2\text{Cl}_2$	47
11. Arrhenius Behavior of $k_b$ & $k_w$ for $\text{CH}_3\text{CCl}_3$	49
12. Arrhenius Behavior of $k_b$ & $k_w$ for $\text{CH}_2\text{Cl}_2$	50
13. Product Distribution versus Temperature in $\text{CH}_2\text{Cl}_2$ / $\text{CH}_3\text{CCl}_3$ / $\text{H}_2$ System	52
14. Product Distribution versus Time in $\text{CH}_2\text{Cl}_2$ / $\text{CH}_3\text{CCl}_3$ / $\text{H}_2$ System	53
15. Dechlorinated Hydrocarbon Product Distribution versus Temperature	55
16. $\text{CH}_2\text{CCl}_2$ Formed per mole of Feed	59
17. Comparison of Pure and Mixed System for $\text{CH}_2\text{Cl}_2$	65
18. Comparison of Pure and Mixed System for $\text{CH}_3\text{CCl}_3$	68
19. Energies of Activation Relative to the Stabilized $\text{CH}_3\text{CHCl}_2$	72
20. Results of Activated Complex Theory Calculation for Reaction $\text{CH}_3\text{CCl}_2 + \text{H}$	73

21. Energies of Activation Relative to the Stabilized $\text{CH}_2\text{CHCl}_2$	74
22. Results of Activated Complex Theory Calculation for Reaction $\text{CH}_2\text{CCl}_2 + \text{H}$	75
23. $\text{CH}_3\text{CHCl}_2$ and $\text{CH}_3\text{Cl}$ Formation Cycle with H Radical	79
24. Structure of the CHEMKIN Package	81
25. Model Prediction: Product Distribution versus Temperature	93
26. Modified Experimental Product Distribution versus Temperature	94
27. Model Prediction: Product Distribution vs Time	95

## I. INTRODUCTION

Controlled, high-temperature incineration has been identified as a desirable method for disposal of hazardous organic waste. This approach avoids many of the problems associated with storage of hazardous materials in landfills or impoundments<sup><1></sup>. Theoretically, incineration could result in the total conversion of hazardous organic compounds to innocuous thermodynamic end-products, such as carbon dioxide and water, and other simple compounds such as HCl which are easily scrubbed with existing pollution control equipment. In practice, total conversion to innocuous materials cannot be achieved without considerable expense, and for an incinerator of less than optimum design or operating conditions, the most thermally stable components in the waste feed may not be totally decomposed. Also of concern is the formation of stable toxic combustion products that are both stable and toxic.

Commercialized incineration at high temperature with excess oxygen has been made the chosen method<sup><2></sup>, and is available, as there are a number of hazardous waste incinerators around the country. For chlorinated hydrocarbons, this technique may destroy all the initial parent species, but reaction products are not all converted to carbon dioxide, as these combustion facilities are run in an oxygen-rich environment where is no stable and desirable

end adduct for chlorine. Chlorine oxide and  $\text{Cl}_2$  are not acceptable end products for discharge to atmosphere, nor are they formed in a selective or quantitative manner for complete collection or neutralization. One preferred chloride product is hydrogen chloride, which can be quantitatively neutralized or collected. If an incinerator with excess oxygen operates under less than optimum conditions, the chlorine containing carbon products can usually be found as effluent which include partially decomposed and oxidized fragments of the initial chlorocarbon. These incomplete combustion product can and often are more stable and more toxic than the parent compound<sup><3,4></sup>. The O-H bond in water is, however, stronger than the H-Cl bond,  $\text{O}_2$ -rich conditions therefore limit hydrogen availability. Another way of looking at the problem is that oxygen and Cl are both competing for the available fuel hydrogen and this is one reason that chlorocarbons serve as flame inhibitors. The C-Cl bond is the next strongest compared with other possible chlorinated products such as Cl-Cl, N-Cl or O-Cl bonds. Consequently, C-Cl may persist in a oxygen rich or hydrogen limited atmosphere<sup><3></sup>. This is one reason why emission of toxic chlorine-containing organic products persists through an oxygen-rich incineration, as carbon species are one of the more stable sinks for chlorine.

Instead of detoxifying chlorocarbons in an oxidizing

atmosphere, one alternative approach to incineration is detoxication of chlorinated hydrocarbon by reductive reactions using hydrogen<sup><3,5,6,7></sup>, water vapor<sup><3></sup> or methane<sup><8></sup>. Methane reductive reaction process was developed and patented by S.W. Benson<sup><9></sup>. In this process, methane is added to chlorine containing compound and the mixture is heated in the absence of air to about 1000 °C. That converts all the chlorine into hydrochloric acid which can then combine with lye to form sodium chloride and hydrodechlorinated hydrocarbons which are usable fuel gas.

Chlorocarbons can also be detoxicated (destroyed) with a hydrogen reductive reaction. One desired and thermodynamically favorable product from a chlorocarbon process is HCl, providing there exists sufficient H<sub>2</sub> to achieve stoichiometric formation of HCl and other desired product-C<sub>n</sub>H<sub>m</sub>. One possible method to obtain quantitative formation of HCl as one of the desired and thermodynamically favorable products from chlorocarbon, might be straight forward thermal conversion of these compounds under a more reductive atmosphere of hydrogen. Other products expected are gaseous hydrocarbon and solid carbon. Also, the choice of pure hydrogen in research work is based on the conviction that leads to less complex chemical systems compared with carbon based on other hydrogen source. It also provides a fundamental and more readily interpreted series of reactions.

The chlorocarbon conversion studies in hydrogen



reductive atmosphere which have been done so far, examined global kinetic information, such as kinetic parameters, reaction product distribution and overall mechanism, on pure chlorocarbon compounds. In this study, we performed the detailed experimental studies on the dichloromethane and 1,1,1-trichloroethane mixed system and developed a detailed reaction mechanism to describe the results.

The objectives of this work are ;

- . examine the high temperature hydrodechlorination and thermal reactions of a  $\text{CH}_2\text{Cl}_2/\text{CH}_3\text{CCl}_3$  mixture in a tubular flow system.
- . characterize product distributions and synergistic effects of the mixed chlorocarbon reaction system.
- . determine if complete and facile conversion to HCl is achievable.
- . enhance understanding of thermal reaction kinetics of chlorocarbons (C,H,Cl systems).
- . formulate a detailed reaction mechanism based on fundamental thermochemical and kinetic principles for this system.

In the present study, Activated Complex Quantum RRK analysis is involved stable compounds and free radical species under going :

- . addition
- . beta scission
- . recombination

these type reactions for evaluation of the reacting system over a wide range temperature and pressure. A detailed kinetic reaction mechanism was developed and used to model results obtained from the experimental reaction system.

## II. Previous Studies

Remarkably little work has been done in the field on reaction studies of hydrogen with chlorinated hydrocarbon.

Relevant studies have been done thoroughly and systematically in the laboratories of NJIT, under the guidance of Dr. Bozzelli, since the initial work of Chuang (1982 )<sup><10></sup>.

Chuang studied the thermal decomposition of chloroform and 1,1,2-trichloroethane with hydrogen or water vapor, over temperature range of 550 to 1100 °C. Chang<sup><11></sup> in his work on the estimation of homogeneous and wall rate constants from laminar flow analysis has presented data on the reaction of hydrogen with 1,1,1-trichloroethane. The thermal reaction of chloroform and trichloroethylene with hydrogen was investigated by Mahmood<sup><12></sup> in 1985. Lee<sup><13></sup> investigated the thermal decomposition of 1,2-dichloroethane with hydrogen in 1986. Ritter<sup><14></sup> performed studies on the thermal decomposition of chlorobenzene in an atmosphere of hydrogen. More recently, the thermal reaction of hydrogen with methyl chloride and carbon tetrachloride at high temperature was examined by Tsao<sup><15></sup> ( 1987 ). The thermal decomposition of dichlorobenzene with hydrogen by Hung<sup><16></sup> was performed at atmospheric pressure, using tubular reactor and a hydrogen atmosphere.

The thermal decomposition of pure single chlorinated hydrocarbons both neat and in inert atmosphere has also been

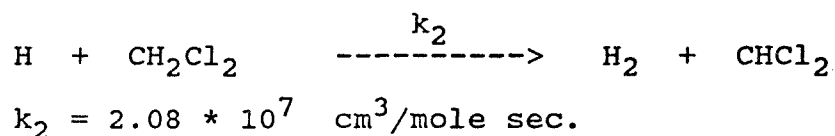
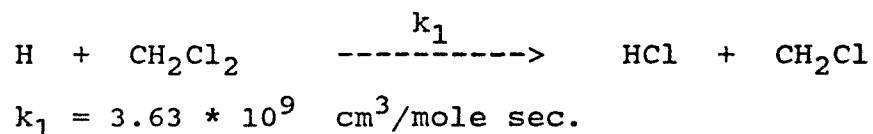
studied. A number of reports were found on the thermal decomposition of pure dichloromethane and 1,1,1-trichloroethane.

#### A. DICHLOROMETHANE

Tsao<sup><15></sup> studied the thermal decomposition of dichloromethane with hydrogen over the temperature range of 700 to 950 °C, using almost same as our apparatus system. Activation energies of bulk and wall reaction on hydrogen reaction with dichloromethane are 50.0 Kcal/mole, 57.8 Kcal/mole. A factors of  $2.84 * 10^{10}$  and  $2.65 * 10^{10}$  respectively were reported. The major products of reaction of dichloromethane in between 700 to 800 °C were methylchloride and methane. The minor products were ethylene, acetylene and HCl. Trace amounts of ethane, chloroethylene, 1,2-dichloroethylene, trichloroethylene, benzene were also observed. No chlorocarbons were found over 950 °C and one second residence time where the only products were methane, hydrogen chloride, acetylene, ethane and benzene.

Huang<sup><17></sup> studied the kinetics of the reaction of atomic hydrogen with dichloromethane in a flow system at pressure of 2.1 to 2.7 mm Hg absolute and room temperature. The major products observed were hydrogen chloride and methane. The extent conversion of dichloromethane increases first to a maximum and then decreases with increasing

concentration of dichloromethane. Through the modeling of the reaction scheme and comparison with experimental data, the rate constants of the initial steps were determined as follows :

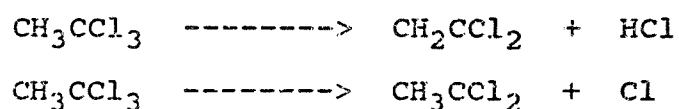


#### B. 1,1,1-TRICHLOROETHANE

Chang<sup><18></sup> who investigated the reactor modeling and calculation of homogeneous bulk and wall rate constants from laminar flow reactor analysis on the reaction of hydrogen with 1,1,1-trichloroethane in the temperature range 555 to 681 °C. The activation energies of bulk and wall reaction were determined to be 25.3 Kcal/mol and 37.9 Kcal/mole respectively. The major products from the reaction were observed to be 1,1-dichloroethylene, chloroform, 1,1-dichloroethane, trichloroethylene, dichloromethane, 1,1,1,2-tetrachloroethane and HCl.

Barton and Onyon<sup><5></sup> ( 1950 ) studied 1,1,1-trichloroethane thermal decomposition in batch reactor in temperature range 635.7 to 707.0 °K and pressure range 10 to 120 mm Hg to give 1,1-dichloroethylene and HCl. They found that the decomposition rate in packed reactor was slower

than in empty reactor. They proposed the packed reactor has a larger surface to volume ratio so the recombination of some radicals to terminate the chain reactions occurred at a faster rate and slowed the overall process. The initiation steps suggested by Barton and Onyon as follows :



Their results showed that the wall inhibited the decomposition reaction because the proposed "key" free radical  $\text{CH}_2\text{CCl}_3$  was consumed faster at the wall. They reported that the first order rate constant for homogeneous unimolecular decomposition can be represented by  $10 * \text{EXP}(-54,000/\text{RT})$  sec.

Benson and Spokes<sup><19></sup> ( 1967 ), using the very low pressure technique, covered a high temperature range 890 to 1265 °K ( so that the reactor was operated at gas flow rates from  $10^{15}$  to  $10^{16}$  molecules/sec. and most of the collisions made by reactant molecules were with wall rather than with other gas molecule ) to estimate the homogeneous rate constant of the thermal decomposition of 1,1,1-trichloroethane at high pressure limit . The corresponding high pressure rate equation is  $10^{13.8} e^{(-51,700/\text{RT})}$  sec..

### III. THEORY

The incineration of chlorocarbons is generally performed in an oxygen rich environment that contains excess  $O_2$  and  $N_2$ <sup><2></sup>, in addition to the C and Cl from the halocarbon, with relatively small amounts of available hydrogen from the limiting fuel operation. In considering products from incineration, the H-Cl bond is the strongest (thermodynamically) and has the lowest Gibbs free energy of formation per chlorine atom<sup><3></sup>. HCl is, therefore, the thermodynamically favored product for chlorine, providing there exists sufficient hydrogen for its stoichiometric formation. It is noted, however, that the O-H bond in water, specifically HO-H is stronger than the H-Cl bond, and the  $O_2$ -rich conditions limit hydrogen availability. The C-Cl bond is the next strongest compared with other possible chlorinated products such as Cl-Cl, N-Cl, or O-Cl bonds. Consequently, C-Cl may persist in a oxygen rich atmosphere. This suggests that the emission of toxic chlorine-containing organic products may persist through an oxygen-rich incineration, as it is one of the more stable sinks for the chlorine.

In order to obtain quantitative formation of HCl from chlorocarbons, it might help to convert these chlorocarbons under a more reductive atmosphere of hydrogen. The chlorocarbon plus hydrogen system contains only carbon, hydrogen, and chlorine elements and is expected to lead to

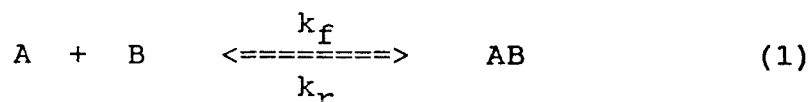
formation of light hydrocarbons, carbon(s), and hydrogen chloride at the high temperatures where complete reaction occurs<sup><3,7></sup>. It also does not have wet HCl in the effluent and is, therefore, not nearly as corrosive as the system with water vapor present.

## A. Transition-State and Collision Theory

### 1. Transition-State Theory

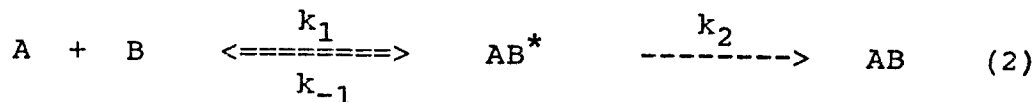
For many reactions and particularly elementary reactions the rate expression can be written as a product of a temperature dependent term and a composition term.

A more detailed explanation for the transformation of reactants into products is given by the transition-state theory. The reactants combining to form unstable intermediates called activated complexes which then decompose spontaneously into products. It assumes that an equilibrium exists between the concentration of reactants and activated complex at all times and that the rate of decomposition of complex is the same for all reactions which is given by  $kT/h$  where  $k$  is the Boltzmann constant and  $h$  is the Planck constant. Thus for the forward elementary reaction of a reversible reaction,





we have the following conceptual elementary scheme:



$$K^* = \frac{k_1}{k_{-1}} = \frac{[AB^*]}{[A][B]}$$

$$k_2 = \frac{kT}{h}$$

The observed rate of the forward reaction is then

$$\begin{aligned} r_{AB, \text{forward}} &= (\text{conc. of activated complex}) \times (\text{rate of decomposition activated complex}) \\ &= \frac{kT}{h} [AB^*] \\ &= \frac{kT}{h} K^* C_A C_B \quad (3) \end{aligned}$$

By expressing the equilibrium constant of activated complex in terms of the standard free energy,

$$\Delta G^* = \Delta H^* - T\Delta S^* = -RT \ln K^* \quad (4)$$

$$K^* = \text{EXP}(-\Delta G^*/RT) = \text{EXP}(-\Delta H^*/RT + \Delta S^*/R)$$

the rate becomes

$$r_{AB, \text{forward}} = \frac{kT}{h} \text{EXP}(\Delta S^*/R) \text{EXP}(-\Delta H^*/RT) C_A C_B \quad (5)$$

Theoretically both  $\Delta S^*$  and  $\Delta H^*$  vary very slowly with temperature. Hence, of the three terms that make up the rate

constant in Eq. 5, the middle one,  $\text{EXP}(\Delta S^*/R)$ , is so much less temperature-sensitive than the other two terms that we may take it to be constant. So for the forward reaction, and similarly for the reverse reaction of Eq. 1, we have approximately

$$k_f \propto T \text{EXP}(-\Delta H_f^*/RT) \quad (6)$$

$$k_r \propto T \text{EXP}(-\Delta H_r^*/RT)$$

$$\text{where } \Delta H_f^* - \Delta H_r^* = \Delta H_{\text{RXN}}$$

## 2. Collision Theory

The collision rate of molecules in a gas can be found from the kinetic theory of gases. For the bimolecular collisions of like molecules A we have

$$Z_{AA} = d_A^2 n_A^2 \cdot \frac{4 kT}{M_A} = d_A^2 \frac{N^2}{10^6} \cdot \frac{4 kT}{M_A} \cdot C_A^2$$

where  $d$  = diameter of molecule, cm

$M$  = mass of molecule, gm

$N$  = Avogadro's number

$C_A$  = concentration of A, mol/liter

$n_A$  = number of molecules of A/cm<sup>3</sup>

$k$  = Boltzmann constant

For bimolecular collisions of unlike molecules in mixture of A and B kinetic theory gives

$$Z_{AB} = \left( \frac{d_A + d_B}{2} \right)^2 \cdot \frac{N^2}{10^6} \cdot 8 kT \left( \frac{1}{M_A} + \frac{1}{M_B} \right) \cdot C_A \cdot C_B$$

If every collision between reactant molecules results in the conversion of reactants into product, these expressions give the rate of bimolecular reaction. The actual rate is usually much lower than that predicted, and this indicates that only a small fraction of all collisions result in reaction. This suggests that only more energetic and violent collisions, or more specifically, only those collisions that involve energies in excess of a given minimum energy  $E$  lead to reaction. From the Maxwell distribution law of molecular energies the fraction of all bimolecular collisions that involve energies in excess of this minimum energy is given approximately by  $e^{(-E/RT)}$ , when  $E \gg RT$ . Since we are only considering energetic collisions, this assumption is reasonable. Thus the rate of reaction is given by

$$\begin{aligned}
 -r_A &= k C_A C_B = (\text{collision rate}) \times (\text{fraction of collisions involving energies in excess of } E) \\
 &= Z_{AB} \frac{10^3}{N} e^{(-E/RT)} \\
 &= \left( \frac{d_A + d_B}{2} \right)^2 \frac{N}{10^3} \frac{8 kT}{\sqrt{\pi}} \left( \frac{1}{M_A} + \frac{1}{M_B} \right) e^{(-E/RT)} C_A C_B
 \end{aligned}$$

A similar expression can be found for the bimolecular collisions between like molecules. For both, in fact for all bimolecular reaction, above equation shows that the temperature dependency of the rate constant is given by

$$k \propto T^{1/2} e^{(-E/RT)}$$

### 3. Comparison of Two Theories

It is interesting to note the difference in approach between the transition-state and collision theories. Consider A and B colliding and forming an unstable intermediate which then decomposes into product, or



collision theory views the rate to be governed by the number of energetic collisions between reactants. What happens to the unstable intermediate is of no concern. The theory simply assumes that this intermediate breaks down rapidly enough into products so as not to influence the rate of the overall process. Transition-state theory, on the other hand, views the reaction rate to be governed by the rate of decomposition of intermediate. The rate of formation of intermediate is assumed to be governed by collisions plus thermodynamics and it is present on equilibrium concentrations at all times. Thus collision theory views the first step to be slow and rate-controlling, whereas transition-state theory views the second step combined with the determination of complex concentration to be the rate controlling factors.

#### B. Tubular Flow Reactor Theory

The ideal tubular flow reactor is one in which there is no mixing in the direction of flow and complete mixing

perpendicular to the direction of flow (i.e. in the radial direction)<sup><20,21></sup>. In other words, all fluid elements of the fluid have the same residence time in the reactor and there is no radial concentration gradient.

In our tubular flow reactor, radial mixing is due to molecular diffusion and axial mixing is due to fluid velocity gradients. Concentrations will vary along the length (axial) coordinate and to a smaller extent over the radial coordinate. These complications concern the flow pattern which affects our kinetic interpretations. In turbulent flow, vortices and eddies produce mixing in the longitudinal direction. In the laminar flow, the parabolic velocity profile is formed across the tube. At low temperature and high pressure condition, the molecular diffusion process is relatively slow, so the annular elements of fluid flow through the reactor are only slightly mixed in the radial direction also. The fluid near the wall will have a longer residence time in the reactor than for ideal tubular flow performance, while the fluid near the center will have a short residence time. Our higher temperature conditions give a much higher diffusion rate and therefore a well mixed axial system.

To estimate the deviation of a tubular flow reactor with axial diffusion from the plug flow assumption, Reman<sup><22></sup> has used Danckwerts solution of a differential equation which describes a plug flow reactor following

first-order kinetics. He found that  $D/vl < 0.1$  the reactor follows the plug flow assumption, and for  $D/vl > 2.0$  the reactor behaves like a well-mixed one<sup><23></sup>. Here  $D$  is diffusion coefficient,  $v$  is mean velocity,  $l$  is reactor length. For our reactor,  $D/vl$  is always below 0.1 (  $1.1 * 10^{-4} - 4.4 * 10^{-3}$  ). This would be sufficient for plug flow assumption to hold true if the Reynolds number were in the upper range of laminar flow when molecular diffusion effects in dispersion are negligible compared to the effect of the velocity<sup><24></sup>. This is, however, not true for our experiments (  $N_{RE} = 5 - 600$  ).

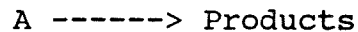
A more rigorous analysis that is applicable to our system is the paper by Poirier and Carr<sup><25></sup>. They solved the continuity equations for a tubular flow reactor with radial diffusion first-order kinetics. They propose that if  $D/kR^2$  (where  $R$  is the radius of reactor,  $k$  is homogeneous rate constant) is equal to or greater than 0.5, the plug flow approximation is satisfied. Our system has a  $D/kR^2$  values from 10 to 170, so the plug flow model is a good approximation for our present reactor.

A comparison of the kinetic values found by plug flow analysis with values obtained by applying both the numerical and analytical solution of continuity equation for first order kinetics with laminar flow done by Chang and Bozzelli<sup><18></sup>. The comparison turns out to be favourable to the plug flow assumption for our experimental system.

### C. Decoupling of the wall and Bulk Reaction Rate Constants

The decomposition of chlorinated hydrocarbons is not only a function of temperature and residence time but also of the radius of reactor. This means that, the reaction at wall in addition to the bulk reaction needs to be evaluated.

In order to simplify the formulation of governing equations for a reactor system in which both bulk and wall reactions are present, it is usually assumed that the two reactions are parallel and independent<sup><21></sup>. Hence, for the first order reaction of species A one can write:



$$\begin{aligned} \text{Rate} &= - \frac{d[A]}{dt} = k_b * [A] + k_w * [A] * [A_w] \\ &= (k_b + k_w * [A_w]) * [A] \end{aligned} \quad (1)$$

$$k_{\text{exp}} = k_b + k_w * [A_w] \quad (2)$$

Assuming a rapid radical diffusion,  $A_w$  can be written as<sup><26></sup>:

$$A_w = (S/V) \quad (3)$$

where:

$A_w$  = wall concentration

$S/V$  = surface to volume ratio

=  $2/R$  for a cylindrical reactor

From (2) and (3) one obtains:

$$K_{\text{exp}} = K_b + K_w * (2/R) \quad (4)$$

In this equation  $k_b$  is the first order reaction rate constant for the bulk or homogeneous reaction and  $k_w$  is the rate constant for the wall or heterogeneous reaction. If one uses several reactors of different radius this equation allows  $k_b$  and  $k_w$  to be evaluated. The Arrhenius behavior of each rate constant can then be determined.

#### D. Prediction of Rate Constants for Radical Addition and Recombination Reactions by Bimolecular QRRK Theory

The decomposition of a radical or molecule has a unimolecular, pressure-independent rate constant in the limit of high pressure, but as pressure is reduced the rate constant eventually falls off or decreases with pressure. In the low-pressure limit, it becomes directly proportional to the pressure. Rationalizing and qualifying these effects, first accomplished in the 1920's, again has become an active area in kinetics research.

Radical combination or radical-molecule addition to an unsaturated would seem to be simply the reverse of decomposition, having the same falloff behavior by microscopic reversibility. This is true for the specific reaction channel that leads to formation of the collisionally stabilized adduct. The reason is that the adduct species has an energy distribution in thermal equilibrium with surrounding gas molecules, just as for a species that is thermally decomposing.



However, it is very important, but not so well recognized that additional products can be formed from combination and addition reactions by this chemical activated pathway. The initially formed adduct has a chemical energy distribution, different from a thermal energy distribution because the thermal energies of the reactants are augmented by the chemical energy released by making the new bond. This chemical energy is initially the same as the energy barrier for redissociation of the collisionally stabilized adduct to the original adducts. If the energy in the chemical activation energy distribution extends above the barrier for a new dissociation ( or isomerization reaction pathway ) of the adduct, then that reaction pathway can also occur.

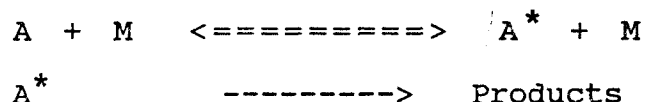
Calculation of the bimolecular rate constant involves the concept that the fate of the chemically activated adduct is determined by competition among the possible pathways; stabilization by collision, redissociation to reactants, or formation of new products by dissociation or isomerization. References are the Dean's paper<sup><27></sup>.

#### 1. Unimolecular QRRK Equation

Dean<sup><27></sup> ( 1985 ) has presented equations for bimolecular rate constants based on the Quantum-RRK or QRRK unimolecular reaction theory of Kassel ( 1928 ), which treats the storage of excess energy ( relative to the ground

state ) as quantized vibrational energy.

In the simplest form of the theory, the assumption is made that the vibrations of the decomposing molecule can be represented by a single frequency  $\nu$ , usually a geometric mean  $\langle \nu \rangle$  of the molecule's frequencies. Next, energy  $E$  initially activated of the complex and each barrier to reaction path relative to the ground state of the stabilized molecule is divided into  $E/h\langle \nu \rangle$  vibrational quanta. For the total energy variable  $E$ , the symbol  $n$  is used; and for number of quanta to the energy barrier to reaction  $E_0$ , the quantized energy is  $m$  quanta; quantum level and the rate processes are illustrated in Figure 1-a. A very general scheme for unimolecular reaction is as follows:



Here  $M$  stands for the third body and only serves to raise the reacting molecule to its energized state  $A^*$  by collisional activation.

The apparent  $k_{\text{uni}}$ :

$$k_{\text{uni}} = \frac{1}{[A]} \frac{d[\text{Products}]}{dt} \quad (1)$$

then is evaluated by a sum over all energies, assuming pseudo-steady state for each energy level of  $A^*$  and collisional excitation or deexcitation with rate constants  $k_{\text{exc}}$  and  $k_{\text{deexc}}$ :

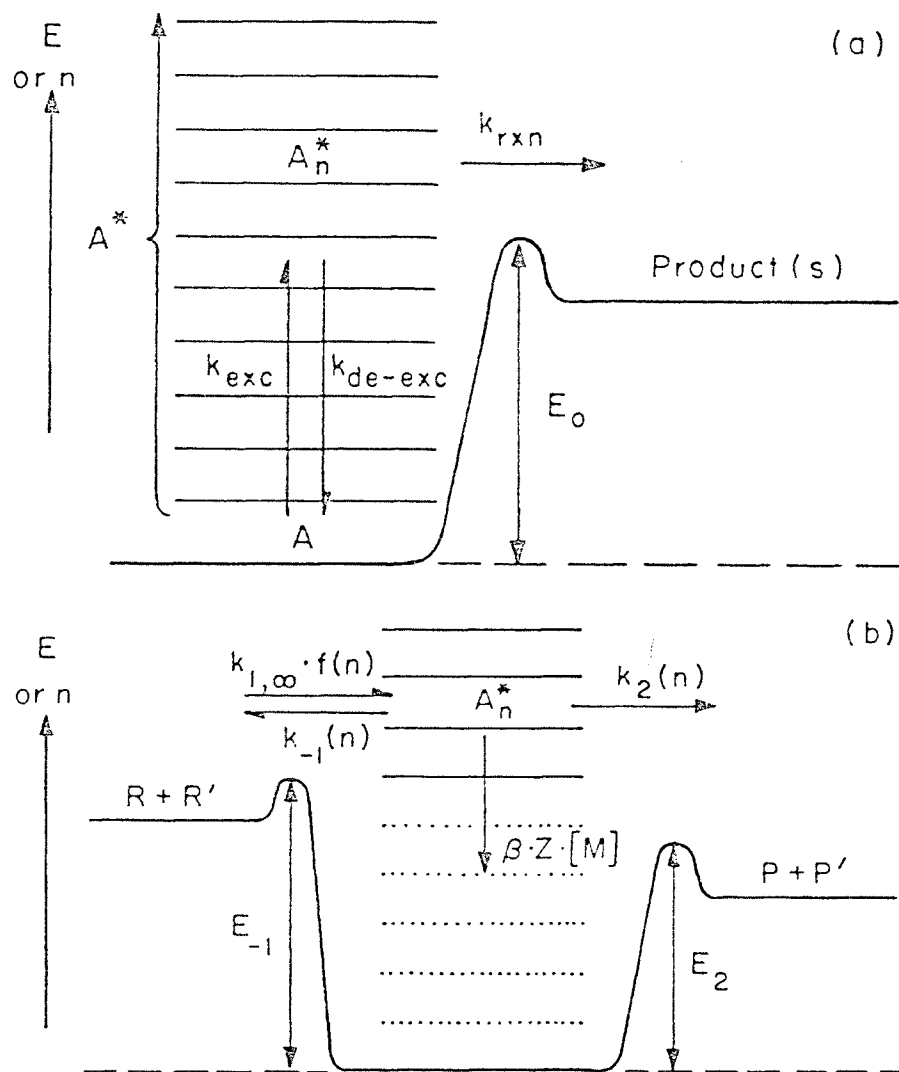


Figure 1. Energy diagrams for pressure-dependent reactions.

- Unimolecular reaction
- Bimolecular reaction with chemically activated pathway

$$\begin{aligned}
 k_{\text{uni}} &= \frac{1}{[A]} k_{\text{rxn}}(E) [A^*(E)] \\
 &= k_{\text{rxn}}(E) \frac{k_{\text{deexc}}[M] K(E,T)}{k_{\text{deexc}}[M] + k_{\text{rxn}}(E)} \quad (2)
 \end{aligned}$$

where  $K(E,T)$  is the thermal-energy distribution function ( $k_{\text{exc}}/k_{\text{deexc}}$ ). Kassel assumed that if a molecule were excited to an energy  $E$ , then  $k_{\text{rxn}}(E)$  would be proportional to the probability that one of the  $s$  oscillators could have energy  $E_0$  or greater (sufficient energy to cause reaction); that is,  $m$  or more of the  $n$  total quanta. The proportionality constant was shown to be  $A$ , the Arrhenius preexponential factor for dissociation of  $A$  in the high pressure limit, so the energy-dependent rate constant is:

$$k_{\text{rxn}}(E) = A \frac{n! (n-m+s-1)!}{(n-m)! (n+s-1)!} \quad (3)$$

Likewise, he derived the quantized thermal energy distribution  $K(E,T)$  to be:

$$K(E,T) = a^n (1-a)^s \frac{(n+s-1)!}{n! (s-1)!} \quad (4)$$

where  $a = e^{(-h\langle v \rangle/kT)}$ .

In the present development, a collisional efficiency  $\beta$  has been applied to modify the traditional but incorrect strong-collision assumption that  $k_{\text{deexc}} = Z [M]$ , where  $Z$  is the collision frequency rate constant. The

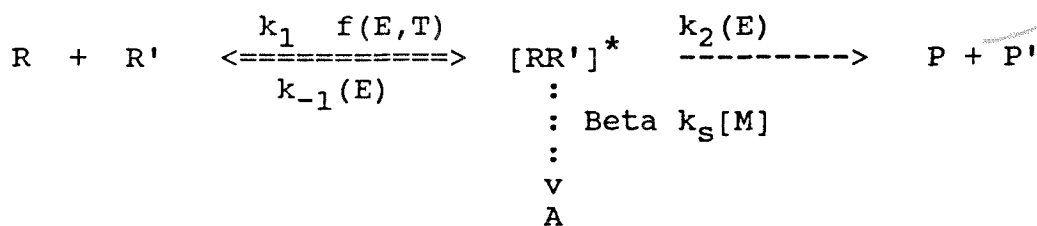
strong-collision assumption implies that any collision between  $A^*$  and  $M$  would have to remove all the excess energy from  $A^*$ . Note that any species included as  $M$  would have to accommodate this energy content, regardless of its capacity for accepting the energy. Analyzing collisional energy transfer for master-equation methods, Troe ( 1977 ) fit most of the temperature dependence of Beta with the equation:

$$\frac{\text{Beta}}{1 - (\text{Beta})^{1/2}} = \frac{-\langle \Delta E_{\text{coll}} \rangle}{F(E) k T} \quad (5)$$

where  $\langle E_{\text{coll}} \rangle$  is the average amount of energy transferred per collision and  $F(E)$  is a factor, weakly dependent on energy, that is related to the number of excited states. Over the temperature range of 300-2500 °K for a series of reactions ( Troe, 1977 );  $F(E) = 1.15$  was observed as a median value. The value of Beta depends on the specific third-body molecule  $M$  through the value of  $\langle \Delta E_{\text{coll}} \rangle$ .

## 2. Bimolecular QRRK Equations

The bimolecular QRRK equations follow ( Dean, 1985 ) from unimolecular QRRK and the definition of the chemical activation distribution function. Consider recombination or addition to occur via the sequence:



Here R is a radical, R' is a radical ( recombination ) or unsaturated molecule ( addition ), A\* is the energized complex which can either dissociate or be collisionally stabilized, Beta is the collisional deactivation efficiency, and ks is the collisional rate constant for stabilization. k<sub>1</sub> is the high-pressure-limit rate constant for forming adduct and f(E,T) is the energy distribution for chemical activation:

$$f(E,T) = \frac{k_{-1}(E) K(E,T)}{k_{-1}(E) K(E,T)} \quad (6)$$

where K(E,T) is the QRRK thermal distribution from Eq. 4. Rate constants k<sub>-1</sub>(E) and k<sub>2</sub>(E) are calculated from the QRRK equation for k<sub>RXN</sub>(E) (Eq.3) using m<sub>-1</sub>(E<sub>-1</sub>/h<v>) and m<sub>2</sub>(E<sub>2</sub>/h<v>), respectively. A typical energy diagram for these reactions is shown in Figure 1-b.

To obtain the bimolecular rate constant for a particular product channel, a pseudosteady-state analysis is made as before. The rate constant for forming the addition/stabilization product [RR'] from R + R' is:

$$k_{stab} = \frac{d[RR']/dt}{[R][R']} = \text{Beta } k_S[M] \frac{k_1 f(E,T)}{\text{Beta } k_S[M] + k_{-1}(E) + k_2(E)} \quad (7)$$

and, for forming the addition/decomposition product P + P':

$$k_{dec} = \frac{d[\text{Prod}]/dt}{[R][R']} = k_2(E) \frac{k_1 f(E,T)}{\text{Beta } k_S[M] + k_{-1}(E) + k_2(E)} \quad (8)$$

If more decomposition channels are available, the  $k_{rxn}(E)$  for each channel is added in the denominator of Eqs.7 and 8, and an equation in the form of Eq.8 is written for each additional channel, substituting the respective  $k_{rxn}(E)$  for  $k_2(E)$  as the multiplier term.

### 3. Low- and High-Pressure Limits

The low-pressure and high-pressure limits for these channels may be derived from Eqs. 7 and 8. As pressure changes, the rate constants change because of the relative magnitudes of terms in the denominator,  $Bk_s[M]$  vs.  $k_{-1}(E)$  and  $k_2(E)$ .

The low-pressure limit for addition/stabilization (or recombination) is derived from Eq.7 to be

$$\lim_{M \rightarrow 0} k_{\theta stab} = [M] \text{ Beta } k_s \frac{k_1 f(E,T)}{k_{-1}(E) + k_2(E)} \quad (9)$$

sometimes written as  $[M]*k_0$  (as a termolecular reaction), and the high-pressure limit reduces properly to  $k_1$ . At a given temperature, the falloff curve for stabilization can be plotted as  $\log(k_{stab})$  vs.  $\log(P)$  or  $\log(M)$ .

Note the presence of  $k_2(E)$  in Eq.9. If chemically activated conversion of  $[RR']^*$  is more rapid than decomposition to reactants [ $k_2(E) \gg k_{-1}(E)$ ], then Eq.9 shows that  $k_{0stab}$  will be divided by  $k_2(E)$  rather than by  $k_{-1}(E)$ . thus, ignoring the chemically activated pathway could

give incorrect rate constants for "simple" addition.

Similar analysis of Eq.8 implies that chemically activated decomposition has a falloff curve that is the opposite of addition/stabilization, with a rate constant that is pressure-independent at low pressure and inversely proportional to pressure at high pressure. From Eq.8, the low-pressure limit for the chemically activated pathway to P and P' will be

$$\lim_{M \rightarrow \infty} k_{dec} = k_1 \frac{k_2(E) f(E,T)}{k_{-1}(E) + k_2(E)} \quad (10)$$

and the high-pressure limit will be

$$\lim_{M \rightarrow \infty} k_{dec} = \frac{1}{[M]} \frac{k_1}{\text{Beta } k_s} k_2(E) f(E,T) \quad (11)$$

with an inverse pressure dependence. While this result goes against past tuition about low- and high- pressure limits, it is a natural consequence of physics when chemically activated reaction are recognized as possibilities. One consequence is that a reaction of the form  $A + B \rightarrow C + D$  with a rate constant measured to be pressure-independent may be proceeding via addition



#### IV. EXPERIMENTAL METHOD

A diagram of the experimental system is shown in Figure 2. A high temperature tubular flow reactor, operated isothermally and atmospheric pressure was used for this study. The tubular flow reactor was made of quartz, which was maintained at a constant temperature by a three - zone oven, each zone controlled separately.

Hydrogen gas, which acted both as reagent and carrier, was passed through separate parallel sets of two saturation bubblers to pick up dichloromethane and 1,1,1-trichloroethane, both kept at 0 °C using an ice bath. Before entering the reactor, the hydrogen, dichloromethane and 1,1,1-trichloroethane were preheated to limit cooling at the reactor entrance. Quartz reactor tubes of 4 mm, 10.5 mm and 16 mm were housed within a three zone Lindberg electric tube furnace. The reactor effluent was monitored using an on - line gas chromatograph ( GC ) equipped with Flame Ionization Detector. The lines between reactor exit and GC analysis were heated to 65 °C to limit condensation.

When the inlet switching valves were properly selected, the mixture (  $\text{CH}_2\text{Cl}_2$  and  $\text{CH}_3\text{CCl}_3$  ) vapor would be transferred directly from the bubbler to GC sample inlet via a reactor by-pass line. This was necessary to determine the GC peak area which corresponded to the input concentration of mixture. The reactor effluent gas passed through heated

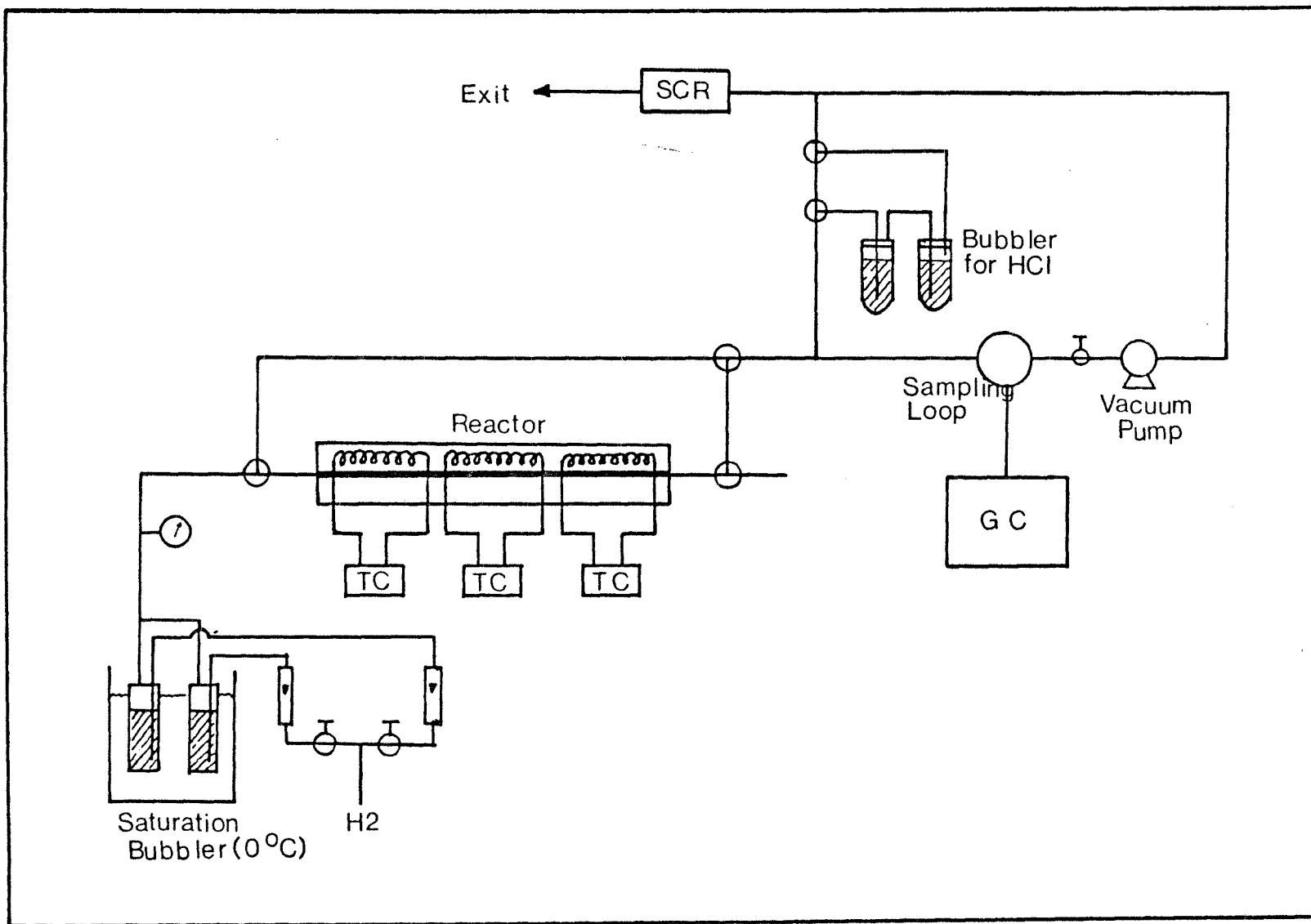


Figure 2. EXPERIMENTAL SET UP

transfer line to the GC sampler and exhaust.

In this study, three different reactor diameters were studied measured 0.4, 1.05 and 1.6 cm as required to vary reactor surface to volume ratio (S/V). This ratio allows one to decouple apparent wall and bulk phase decomposition rates using a plug flow assumption based upon the work of Kaufman<sup><26></sup> for pseudo-first order reaction system.

Outlet gases from the reactor were passed to the GC through a glass tube, loosely packed with glass wool to trap any carbon particles preventing contamination of the GC sampling system. The bulk of the effluent, however, was passed through a sodium - bicarbonate flask before being release to the atmosphere via a fume hood.

#### A. Temperature Control and Measurement

This study was carried out with isothermal reaction at the desired temperature using a three zone furnace equipped with three independent temperature controllers ( Burling Instrument Co. Chatham, NJ ).

The actual temperature profile of the tubular reactor was obtained using type K thermocouple which could be moved coaxially within reactor from one end to the other. The temperature measurements were performed with steady flow rate of Argon gas through reactor. Temperature profiles obtained as shown in Figure 3 were isothermal to within  $\pm 3$  °C for 70 % of reactor length.

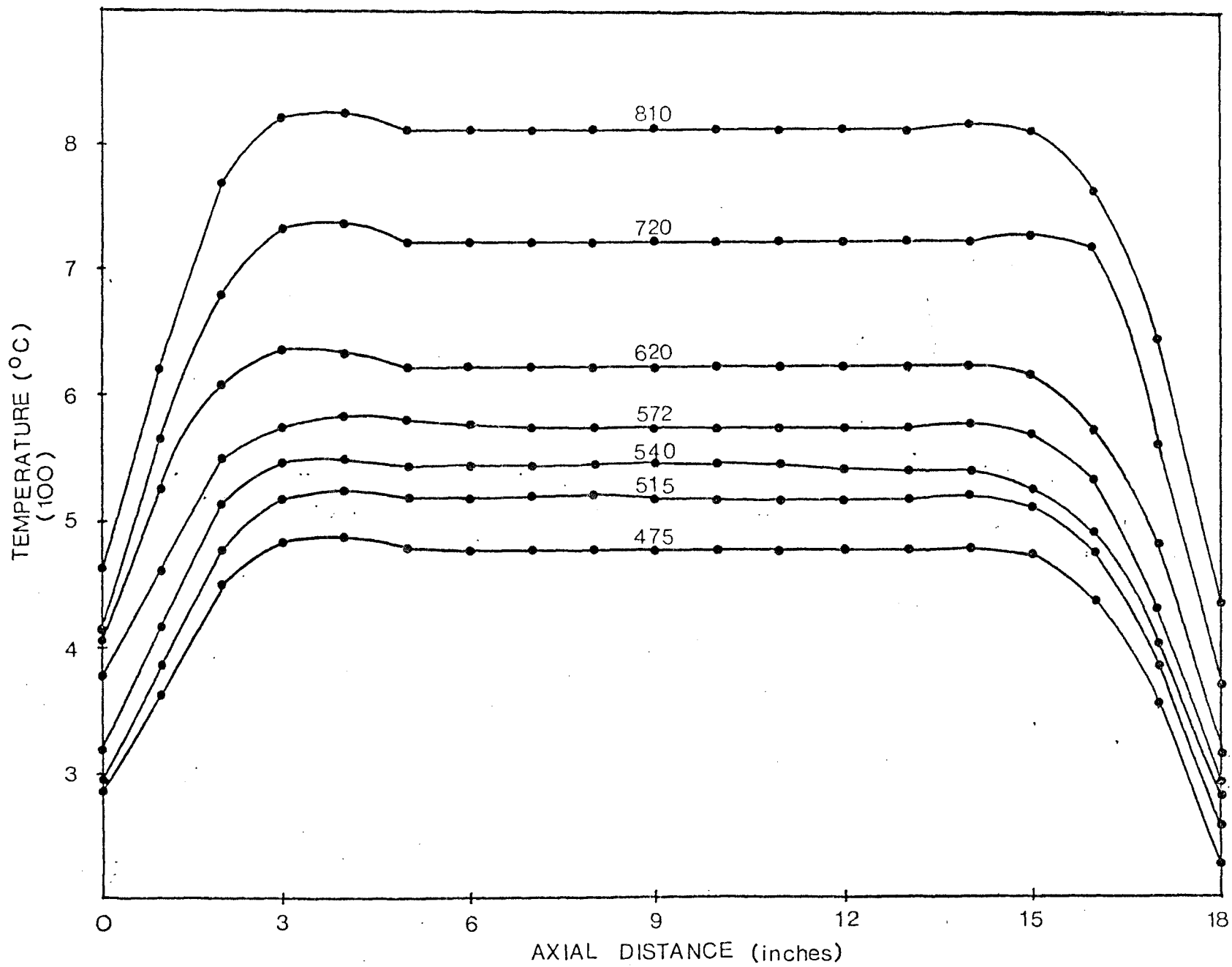


Figure 3. Reactor Temperature Profile (axial)

As illustrated in APPENDIX 2, an energy balance calculation based upon the experimental results and a detailed reaction mechanism is performed. The heat of reaction in this system can change at most 1.5 °C which is less than 50 % of our temperature control error bounds and is insignificant. The reaction condition can be, therefore, controlled by temperature controllers and considered accurate. Thus, the actual temperature profile of the tubular reactor with reaction is occurring indeed that of Figure 3.

#### B. Quantitative Analysis of Reaction Products

A Varian 3700 on-line gas chromatograph with flame ionization detector was used to determine the concentration of the reaction products. The lines between reactor exit and GC analysis were heated to 65 °C to limit condensation. The GC used a 1.5 m long by 1/8 inch o.d. stainless steel column packed with 1 % Alltech AT-1000 on graphpac GB as the column.

A six port gas sample valve ( Valco Instrument Co.) with a 1.0 ml volume loop was maintained at 170 °C and 1 atm pressure. The integration of the chromatogram was performed with Varian 4270 integrator using an attenuation of 2 and a chart speed of 0.5 cm/min. A representative chromatogram is shown Figure 4 and Table 1 with retention times and peak identification.

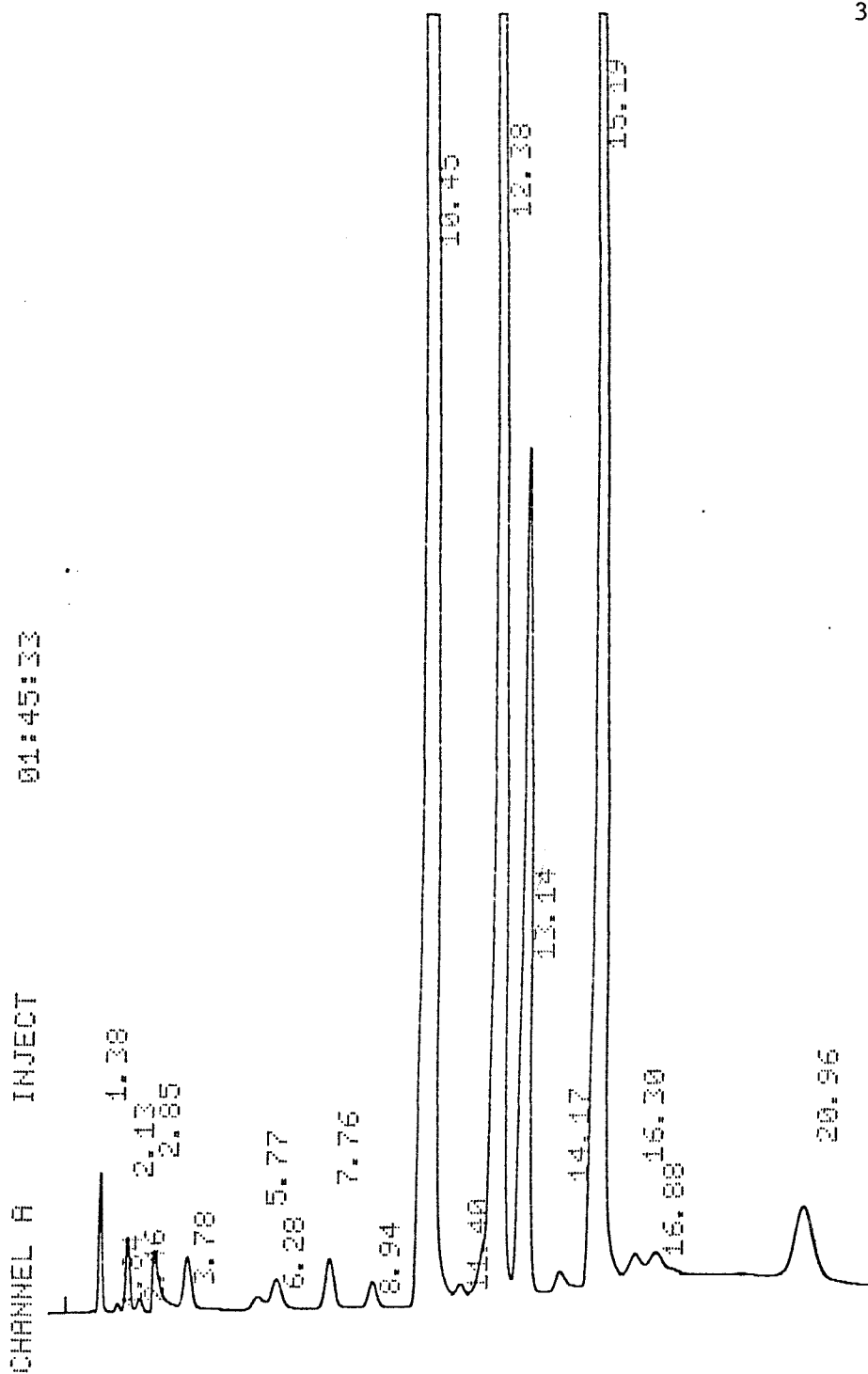


Figure 4-a. Sample Chromatogram CH<sub>2</sub>Cl<sub>2</sub>/CH<sub>3</sub>CCl<sub>3</sub>/H<sub>2</sub> Decomposition

Column: 1.5m x 1/8" ID 1%-AT 1000 on Graphpac GB  
Detector: 270°C (FID)  
Temperature: 45°C(5 min) : 15°C/min to 200°C(final)  
Carrier Gas: He supplied at 100 psig

\* Reaction Conditions: 1 sec. under 515°C

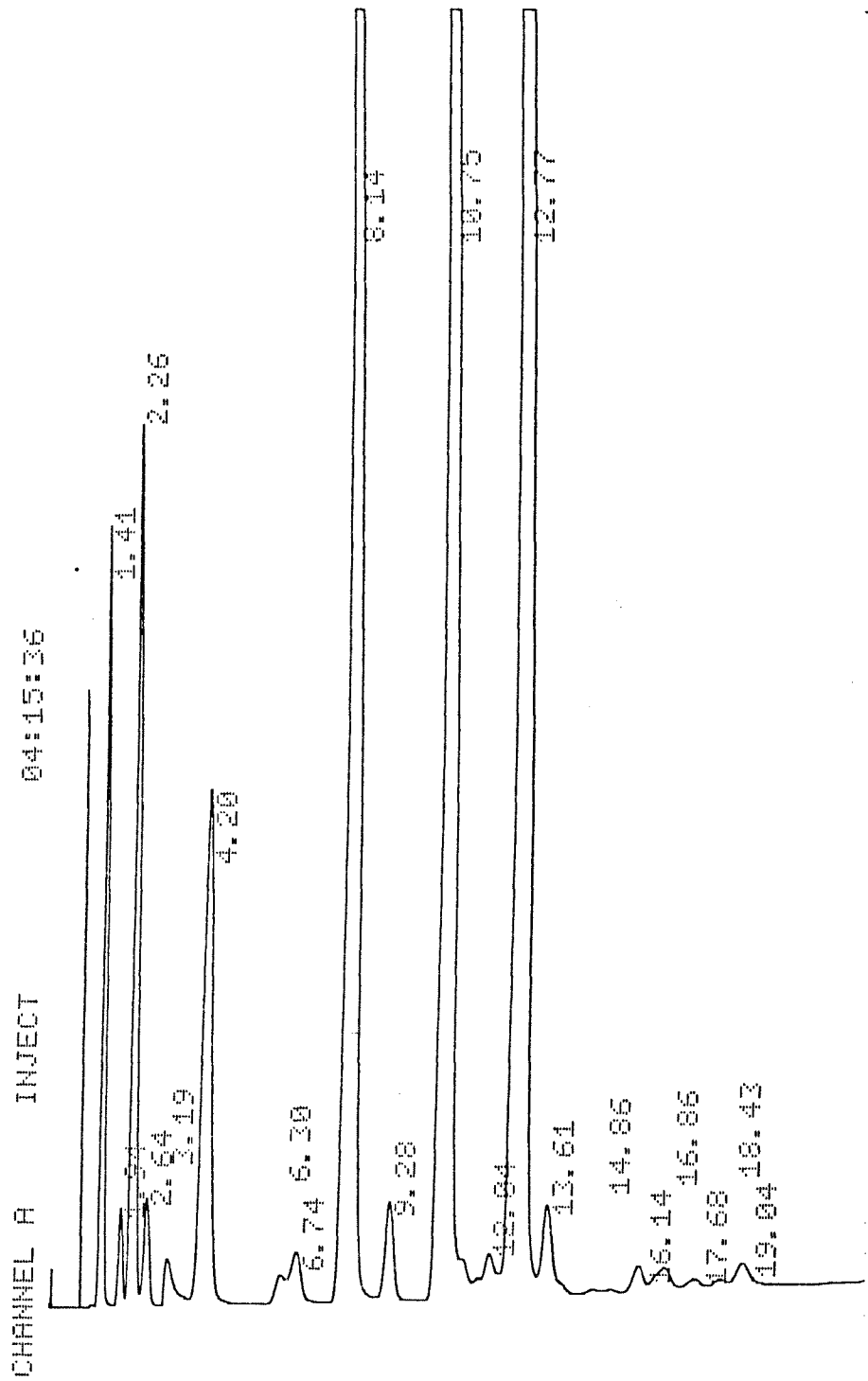


Figure 4-b. Sample Chromatogram CH<sub>2</sub>Cl<sub>2</sub>/CH<sub>3</sub>CCl<sub>3</sub>/H<sub>2</sub> Decomposition

\* Reaction Conditions: 0.3 sec. under 720°C

**Table 1**  
Average Retention Time of Products

Compound	Average Retention Time ( min. )
CH <sub>4</sub>	1.40
CHCH	1.85
CH <sub>2</sub> CH <sub>2</sub>	2.20
CH <sub>3</sub> CH <sub>3</sub>	2.70
CHCCl	3.19
CH <sub>3</sub> Cl	4.00
CHCCH <sub>3</sub>	5.77
C <sub>3</sub> H <sub>6</sub> & C <sub>3</sub> H <sub>8</sub>	6.28
CH <sub>2</sub> CHCl	7.76
CH <sub>3</sub> CH <sub>2</sub> Cl	8.94
CH <sub>2</sub> Cl <sub>2</sub>	10.45
C <sub>4</sub> H <sub>10</sub>	11.40
CH <sub>2</sub> CCl <sub>2</sub>	12.38
CH <sub>3</sub> CHCl <sub>2</sub>	13.14
CHClCHCl	14.17
CH <sub>3</sub> CCl <sub>3</sub>	15.20
CHClCCl <sub>2</sub>	16.88
C <sub>6</sub> H <sub>6</sub>	17.60
CH <sub>2</sub> ClCHCl <sub>2</sub>	20.95



Table 2

## Relative Response Factor of Several Compounds

Compound	Relative Response Factor ( RRF )
Methane	1.07
Acetylene	2.28
Ethylene	2.00
Ethane	1.96
Propyne	3.38
Propene	3.47
propane	3.42
Butane	4.31
Dichloromethane	1.00
1,1,1-Trichloroethane	1.85
1,1-Dichloroethylene	2.10
Chloroform	0.98
Tetrachlorocarbon	1.18
1,1,2-Trichloroethane	2.10

\* corrected area = measured area x RRF

Calibration of the flame ionization detector to obtain appropriate molar response factor was done by injecting a known quantity of the relevant compound such as  $\text{CH}_4$ ,  $\text{C}_2\text{H}_6$ ,  $\text{CH}_2\text{CCl}_2$ ,  $\text{CH}_3\text{CCl}_3$  etc., then measuring the corresponding response area. The relative response factor has been determined for such compounds as shown in Table 2. The response factor for  $\text{C}_1$  compounds are close to each other, and the response factor of  $\text{C}_2$  compounds are near twice the response of  $\text{C}_1$  compounds. These results agree with the general principle of flame ionization detector which is well known as a carbon counter<sup><28></sup>. Thus, the effect of chlorine in the relative response factor can be neglected for this flame ionization detector and the relative response factors being considered as corresponding to the number of carbon in the molecule were found accurate. Based on the experimentally verified relative response factors, the specific component peak area from each set of samples was converted to the equivalent of moles of each component.

### C. Hydrochloric Acid Analysis

Quantitative analysis of HCl product was performed for reactions in each diameter reactor and each residence time. The samples for HCl analysis were collected independent from GC sampling as illustrated as Figure 2. In this analysis, the effluent was bubbled through a two stage bubbler before being exhausted to hood. Each stage contained 15 ml of

standardized 0.01 M NaOH. The gas was passed through the two stage bubbler until the first stage solution reached its phenolphthalein end point. The time required for this to occur was recorded. At this point the bubbling was stopped, the aliquots were combined, and titrated to their end point with standardized 0.01 M HCl.

The HCl produced by reaction was easily calculated; Since the concentration and molar flow rate of chlorine as dichloromethane and 1,1,1 - trichloroethane mixture was known, an estimate of the amount of organic chlorine which remained unaccounted for was available. As we shall show evidence was found that organic chlorine compounds were produced which, for one reason or another, did not lend themselves to GC analysis under the condition of this study.

## V. RESULTS and DISCUSSION

The experimental conditions of the reaction of dichloromethane/1,1,1-trichloroethane mixture with hydrogen are listed below:

.Reactants Ratio ( $\text{CH}_2\text{Cl}_2$ : $\text{CH}_3\text{CCl}_3$ : $\text{H}_2$ )	:	1 : 1 : 24.6
.Reactor Temperature ( $^\circ\text{C}$ )	:	475, 515, 540, 572, 620, 720, 810
.Effective Reactor Length	:	30.5 cm
.Reactor Diameter ( cm )	:	0.40, 1.05, 1.60
.Residence Time Range ( sec.)	:	0.05 - 0.7 ( i.d. = 0.40 ) 0.2 - 2.0 ( i.d. = 1.05 ) 0.5 - 2.0 ( i.d. = 1.60 )
.Operating Pressure	:	1 atm.

Seven temperatures ranging from 475 to 810  $^\circ\text{C}$  were studied within the 1.05 cm i.d. reactor, and each temperature has 7 residence time points from 0.2 to 2.0 sec. When using the 0.4 cm and 1.6 cm i.d. reactor, five temperatures ranging from 540 to 810  $^\circ\text{C}$  were studied. Average residence times within 0.4 cm i.d. ranged from 0.05 sec. to 0.7 sec. and within 1.6 cm i.d. did from 0.5 sec. to 2.0 sec.. Constant molar ratio  $\text{CH}_2\text{Cl}_2:\text{CH}_3\text{CCl}_3:\text{H}_2$  of 1:1:24.6 was maintained through the experiment.

### A. Reaction of Dichloromethane/1,1,1-trichloroethane Mixture with Hydrogen

Experimental results on decomposition of

dichloromethane( $\text{CH}_2\text{Cl}_2$ ) and 1,1,1-trichloroethane( $\text{CH}_3\text{CCl}_3$ ), are in Figure 5, shows the normalized each compound concentration ( $C / C_0$ ) for each chlorocarbon reagent as a function of the average residence time for several temperatures studied and each different i.d. reactor.

The dichloromethane and 1,1,1-trichloroethane concentration consistently decrease with increasing reaction time for all temperature shown; and for a constant residence times increases in temperature result in lower reactant concentrations.

It is observed that dissociation of the  $\text{CH}_3\text{CCl}_3$  is favored over that of  $\text{CH}_2\text{Cl}_2$ , since the dissociation activation energy of the  $\text{CH}_3\text{CCl}_3$  is only 47.6 cal/mol for products  $\text{CH}_2\text{CCl}_2 + \text{HCl}$ <sup><29></sup> and the bond dissociation energy of  $\text{CH}_3\text{CCl}_2\text{-Cl}$  is lower than that of  $\text{CH}_2\text{Cl-Cl}$  [ BE ( $\text{CH}_3\text{CCl}_2\text{-Cl}$ ) = 73.2 Kcal/mol as opposed to BE ( $\text{CH}_2\text{Cl-Cl}$ ) = 82.8 Kcal/mol]. Dissociation of the C-Cl bonds are favored compared with 10 Kcal/mol stronger C-H bond<sup><30,31></sup>.

Conversion of  $\text{CH}_3\text{CCl}_3$  was 85 %, while that of  $\text{CH}_2\text{Cl}_2$  was only 16 % in 0.5 sec. reaction time, 540 °C and 1.05 cm i.d. reaction conditions. Complete decay (99%) of parent compounds took place at about 810 °C for  $\text{CH}_2\text{Cl}_2$  and around 570 °C for  $\text{CH}_3\text{CCl}_3$  in 1 sec. residence time of 1.05 i.d.cm reactor. This indicates that  $\text{CH}_2\text{Cl}_2$  is more stable than  $\text{CH}_3\text{CCl}_3$  under our conditions.

The large excess of hydrogen allowed simplification to

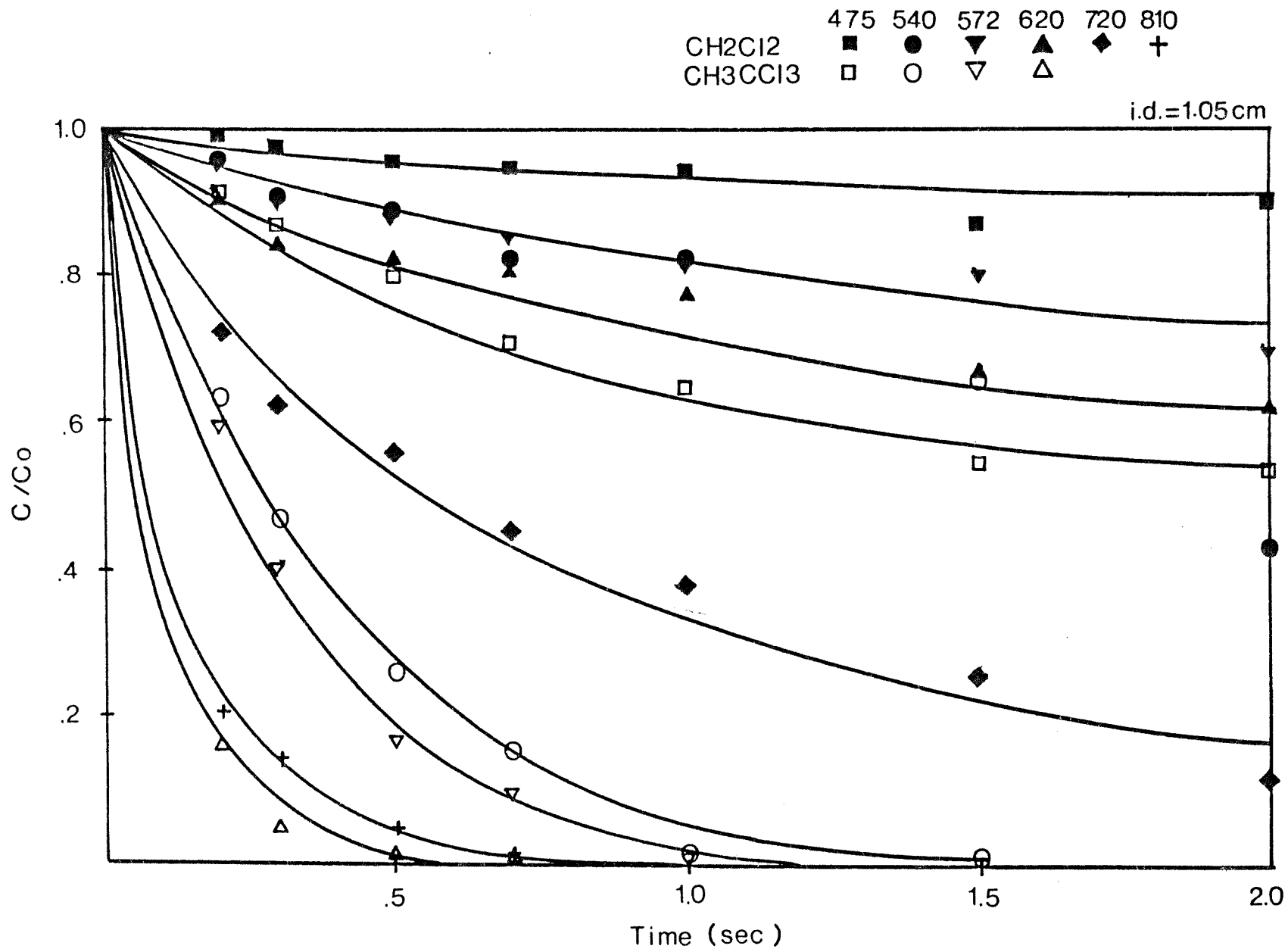
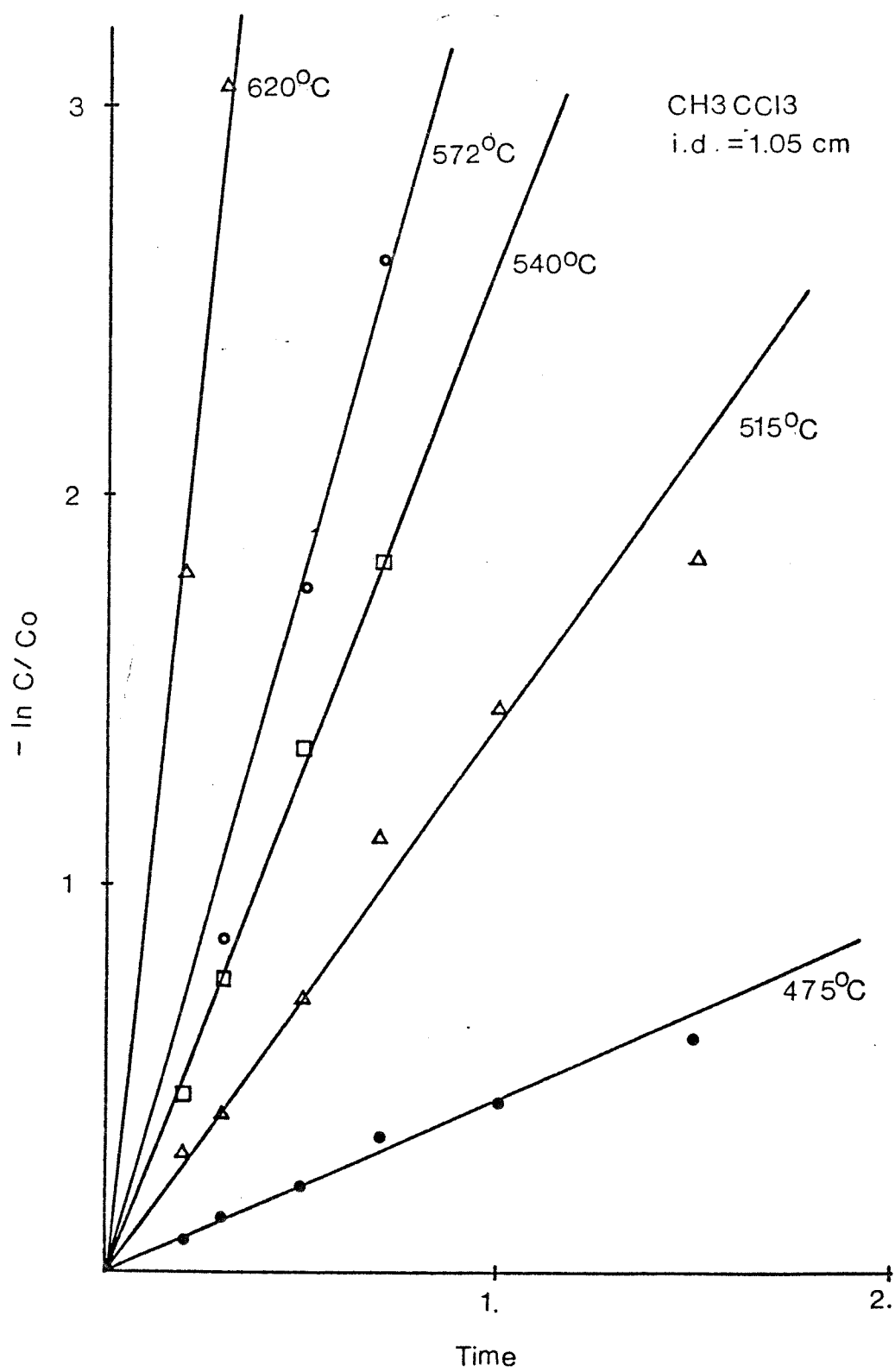


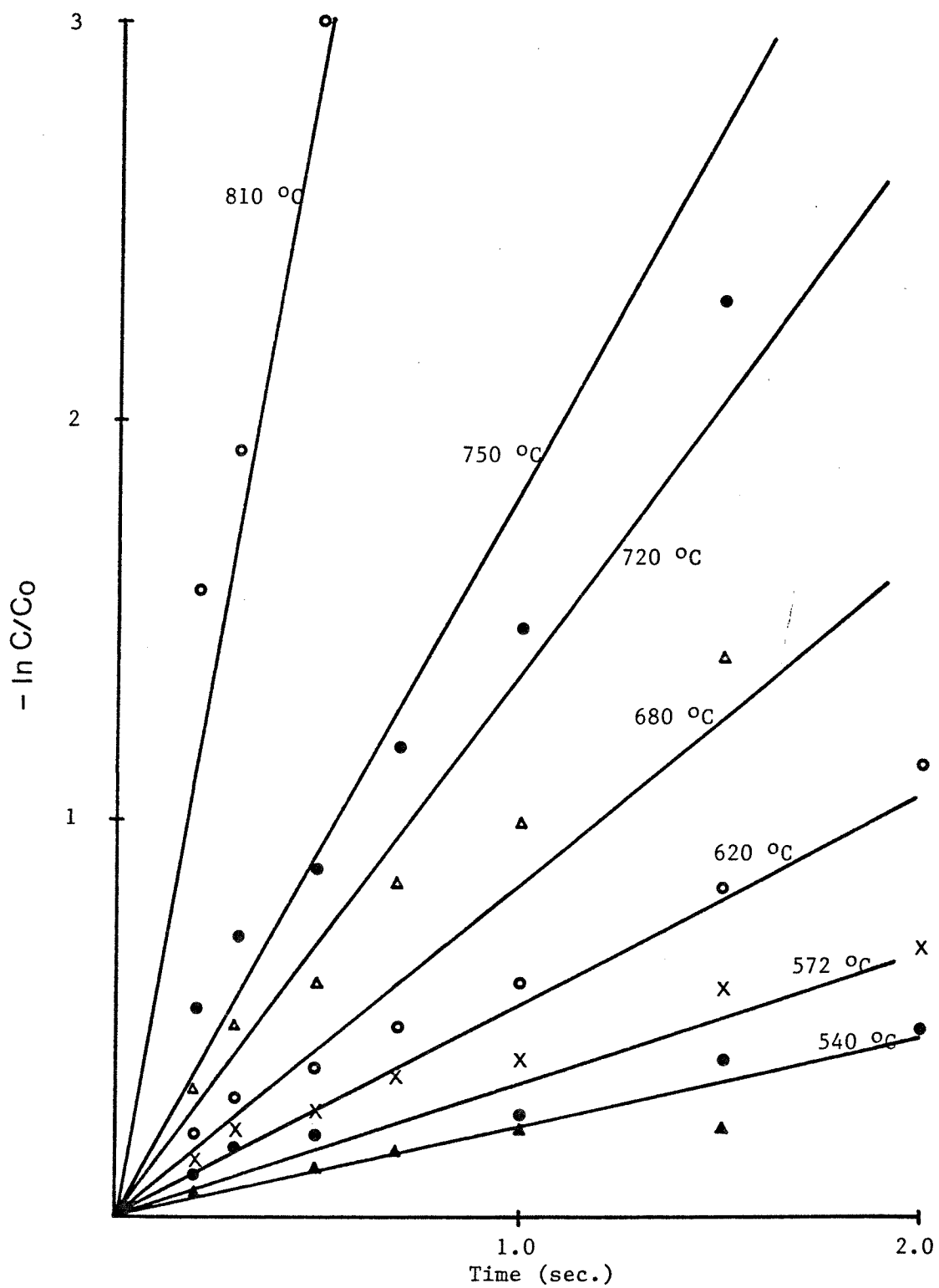
Figure 5 Decay of CH<sub>2</sub>Cl<sub>2</sub> and CH<sub>3</sub>CCl<sub>3</sub> vs Time

pseudo-1st order kinetics for each reactants of mixture. Integrated rate equation plots for the each conversion of  $\text{CH}_2\text{Cl}_2$  and  $\text{CH}_3\text{CCl}_3$  in mixture reaction to fit the first order rate equation are shown in Figure 6 and 7. A 1st order rate plot for decay of  $\text{CH}_3\text{CCl}_3$  shows excellent linearity for all temperature but similar  $\text{CH}_2\text{Cl}_2$  plots are not linear from the lower temperature mixed reagent experiments. This implies that there is a strong interaction of decay products from  $\text{CH}_3\text{CCl}_3$  which react with parent  $\text{CH}_2\text{Cl}_2$ .

It is seen that for different values of temperature and diameter, the data fit the integrated first order rate equation well for each reagent. Decomposition was most rapid with the 4mm i.d. and slowest with the 16mm i.d. reactor as shown in Figure 8. This trend is expected since observed reagent loss may be the result of two reaction paths, both contributing under our conditions. The homogeneous reaction occurs in the bulk of the gas mixture and a heterogeneous reaction occurs on the surface of the flow tube wall. Clearly the relative importance of the wall reaction is greater when the surface to volume (S/V) ratio or relative extent of the wall surface is greater. The activation energies and Arrhenius frequency factor for each reagent in the mixture are found from Arrhenius plot such as Figure 9 and 10. The equations for each compounds and diameters in mixture reaction are listed below:

Figure 6. 1st-order Kinetics Fit of CH<sub>3</sub>CCl<sub>3</sub> Decomposition



Figure 7. 1st Order Kinetics Fit of  $\text{CH}_2\text{Cl}_2$  Decomposition

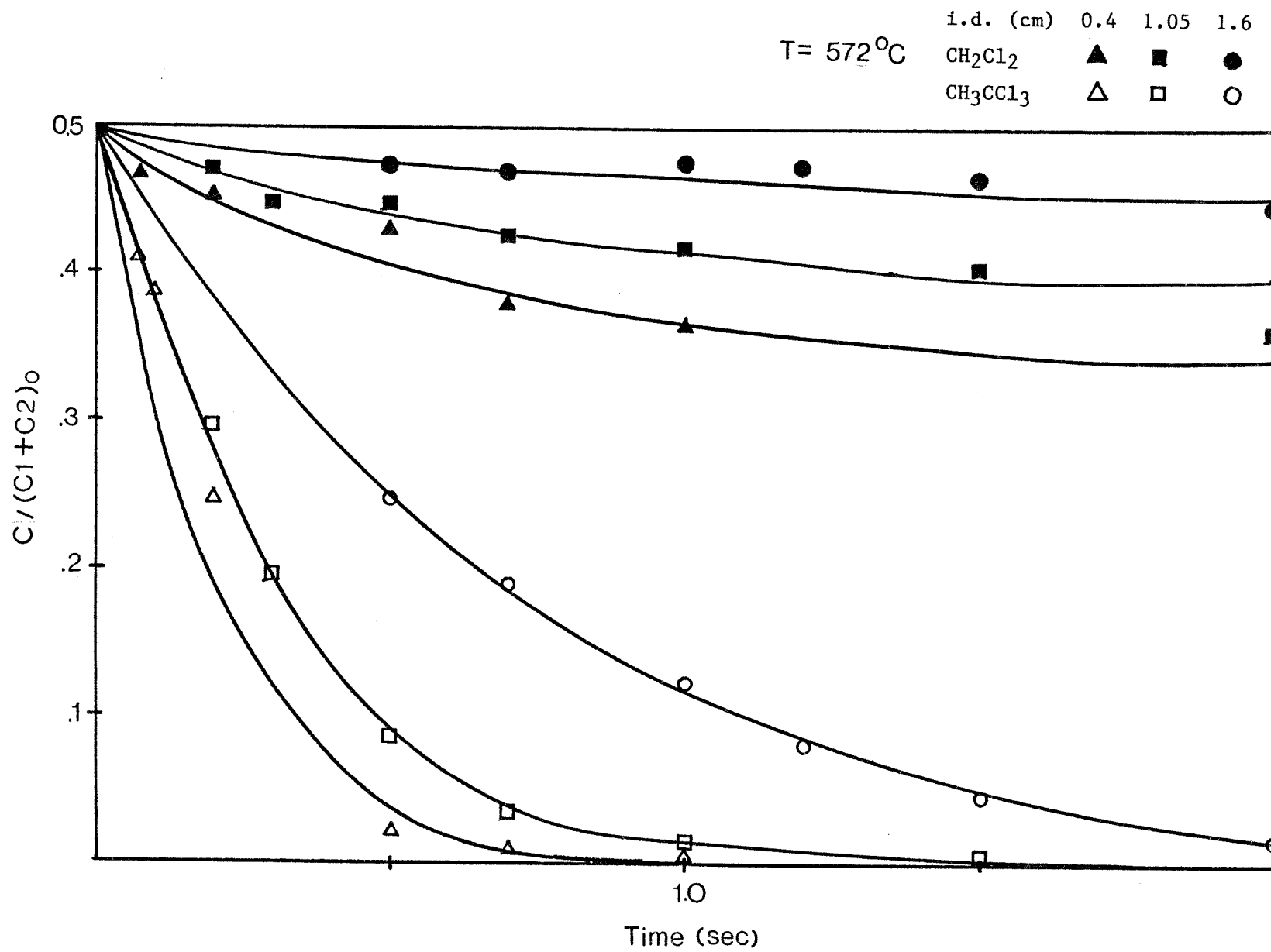


Figure 8. Reagent Decay vs Reaction Time: Comparison of Different Tube Diameters

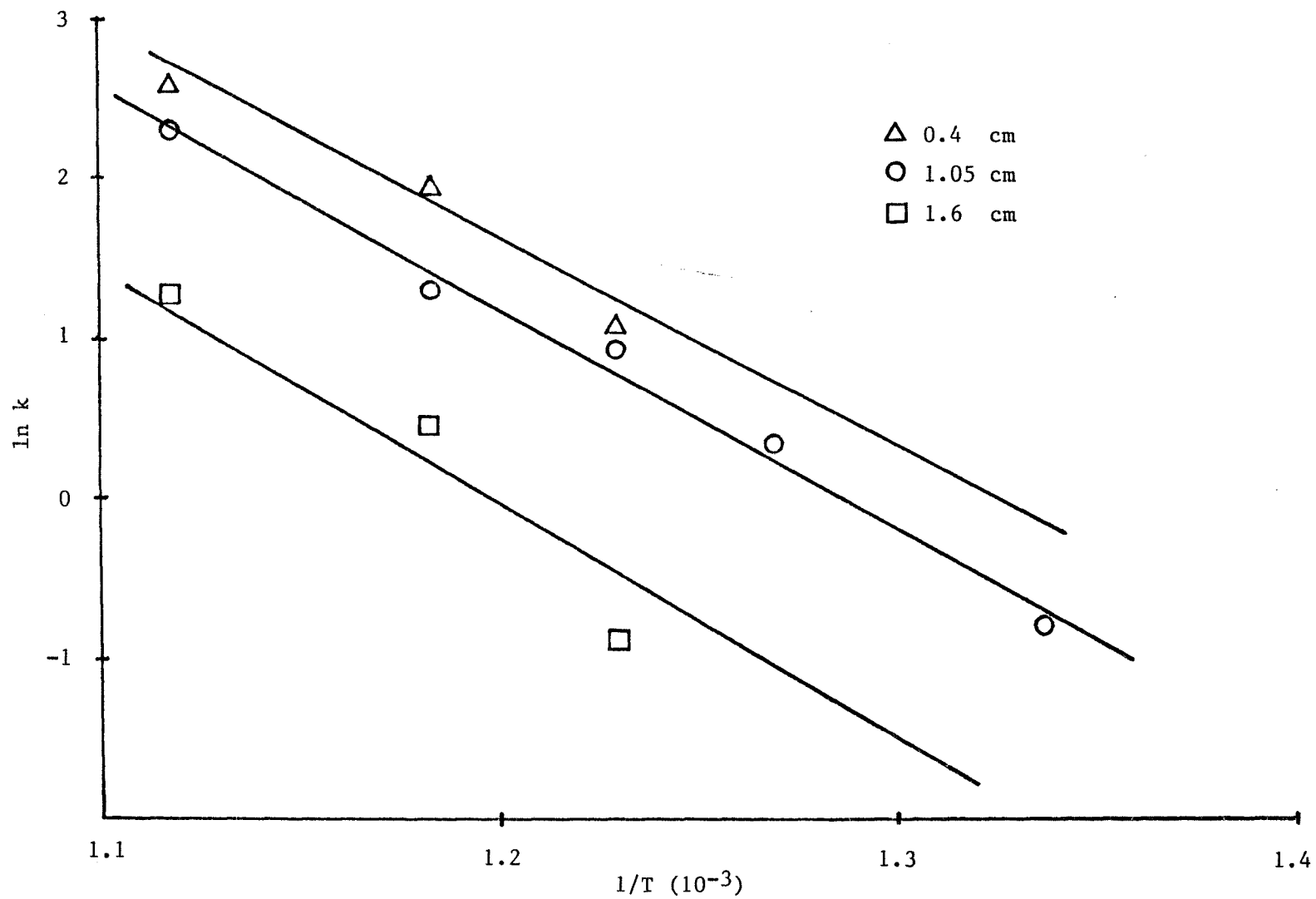


Figure 9. Arrhenius Behavior of  $k_{\text{exp}}$  for  $\text{CH}_3\text{CCl}_3$

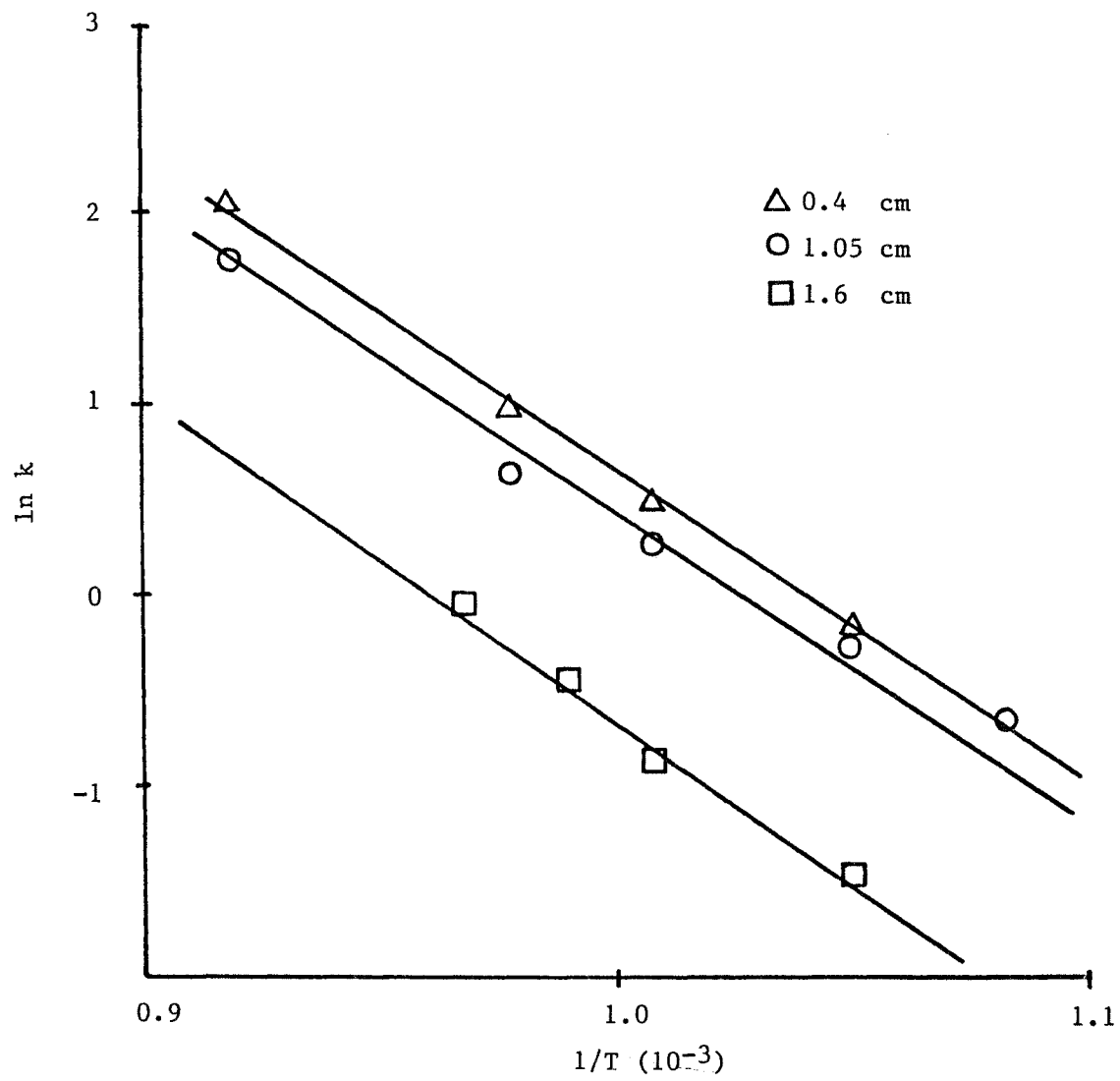
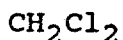


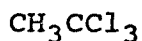
Figure 10. Arrhenius Behavior of  $k_{exp}$  for  $CH_2Cl_2$



$$\text{for } 0.40 \text{ cm} \quad k = 6.27 * 10^{16} \quad e^{(-31,800/RT)} \quad (1/\text{sec.})$$

$$\text{for } 1.05 \text{ cm} \quad k = 6.03 * 10^{16} \quad e^{(-32,500/RT)} \quad (1/\text{sec.})$$

$$\text{for } 1.60 \text{ cm} \quad k = 2.56 * 10^{16} \quad e^{(-33,900/RT)} \quad (1/\text{sec.})$$

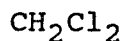


$$\text{for } 0.40 \text{ cm} \quad k = 2.50 * 10^{17} \quad e^{(-26,100/RT)} \quad (1/\text{sec.})$$

$$\text{for } 1.05 \text{ cm} \quad k = 5.80 * 10^{17} \quad e^{(-27,400/RT)} \quad (1/\text{sec.})$$

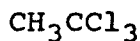
$$\text{for } 1.60 \text{ cm} \quad k = 2.50 * 10^{17} \quad e^{(-28,800/RT)} \quad (1/\text{sec.})$$

This is done by plotting  $k$  against  $2/R$ , where  $R$  is the radius of reactor in centimeter. The slope is  $k_w$  and the intercept is  $k_b$ . Activation energies for the wall and homogeneous rate constants as well as for global rate constants are found by Arrhenius plots as shown in Figure 11 and 12. The values found for all the parameters are discussed and are listed .



$$k_b = 3.24 * 10^{15} \quad e^{(-35,600/RT)} \quad (1/\text{sec.})$$

$$k_w = 9.49 * 10^{10} \quad e^{(-24,500/RT)} \quad (\text{cm}/\text{sec.})$$



$$k_b = 6.40 * 10^8 \quad e^{(-32,000/RT)} \quad (1/\text{sec.})$$

$$k_w = 1.24 * 10^7 \quad e^{(-27,600/RT)} \quad (\text{cm}/\text{sec.})$$

As can be seen in Figure 11 and 12, there is poor linear regression relationship for determining of bulk and wall reaction rate constant comparing with each pure

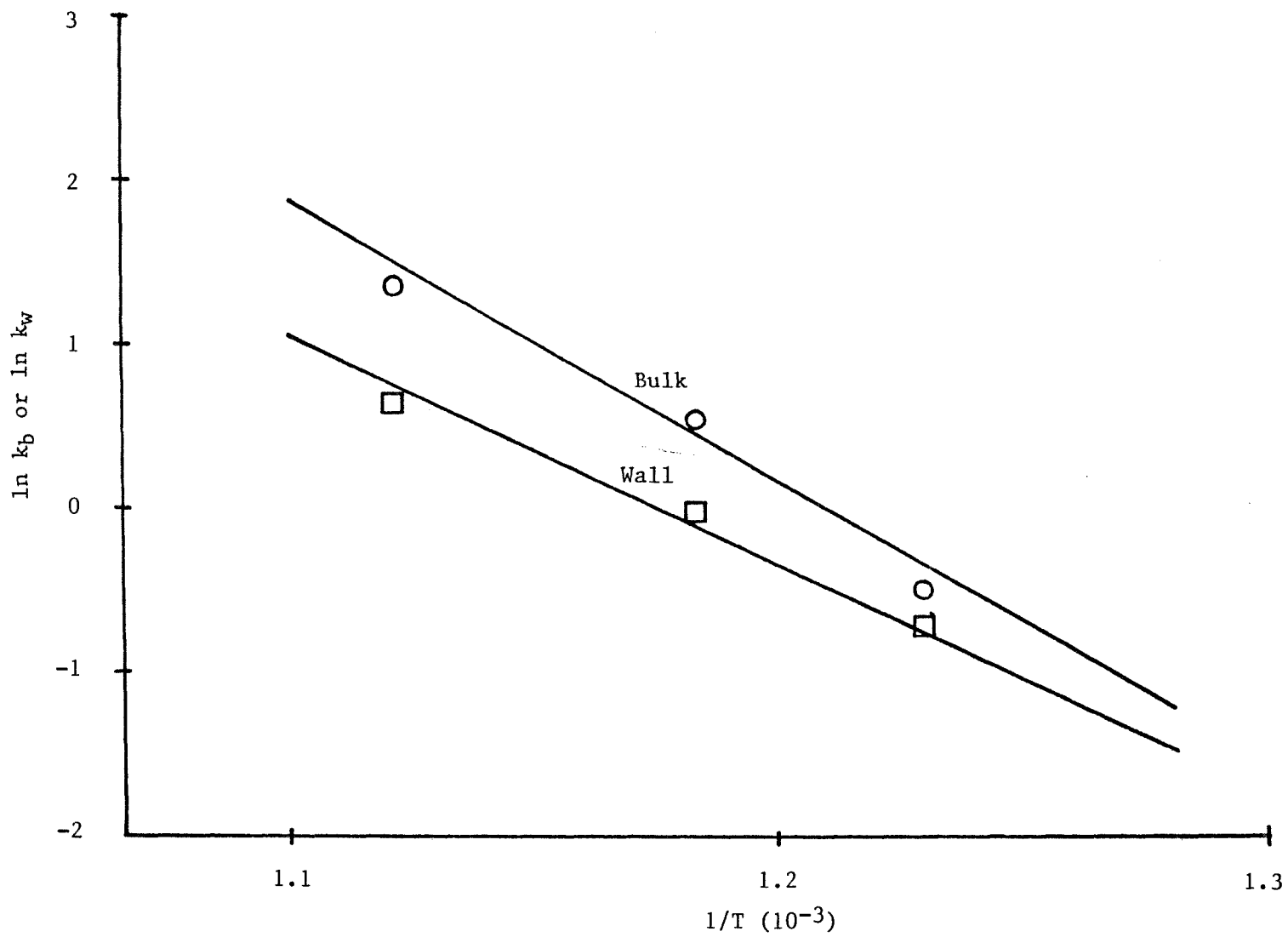


Figure 11. Arrhenius Behavior of  $k_b$  and  $k_w$  for  $\text{CH}_3\text{CCl}_3$

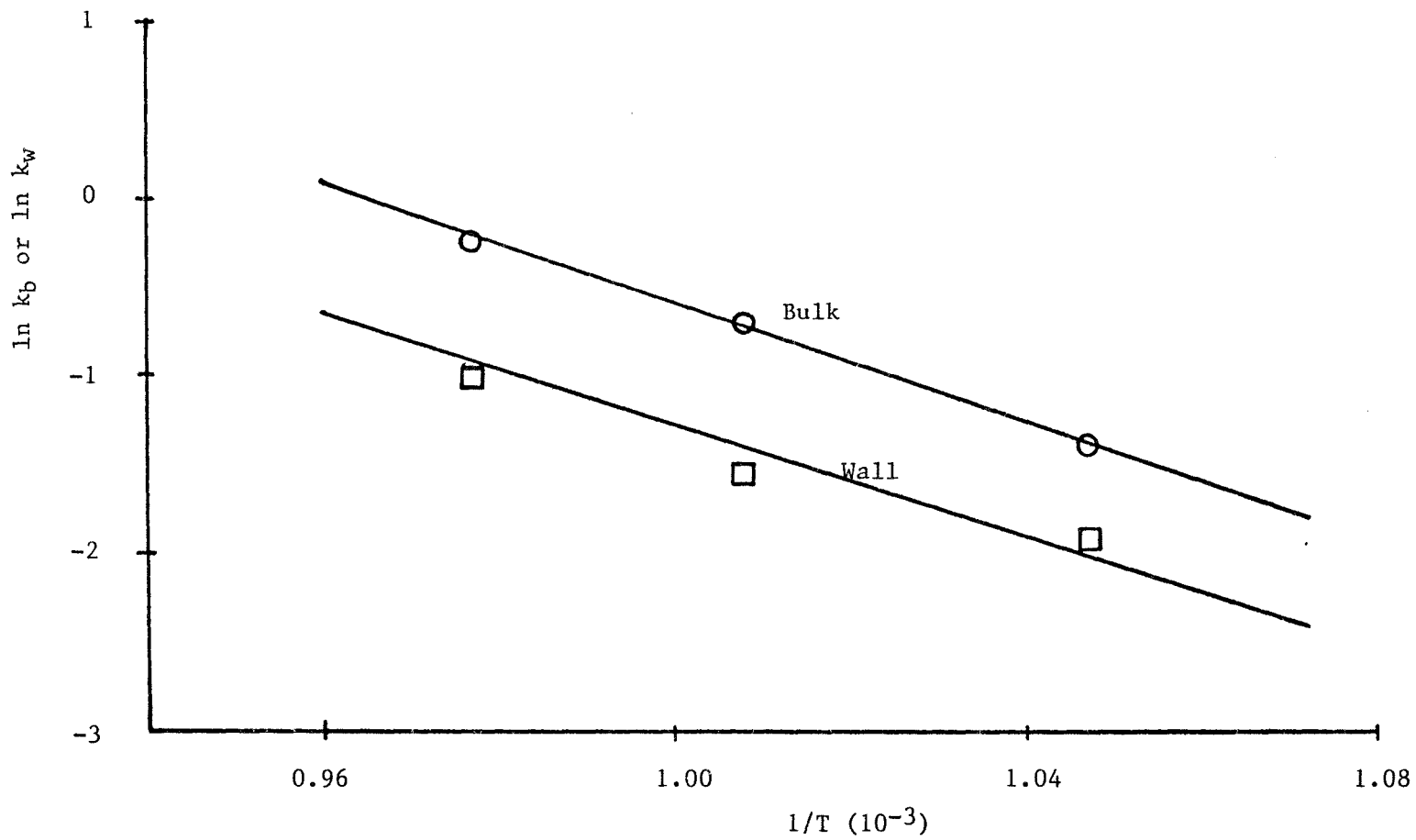


Figure 12. Arrhenius Behavior of  $k_b$  and  $k_w$  for  $\text{CH}_2\text{Cl}_2$

compound reactions<sup><11,15></sup> because of synergistic effects of mixture reaction which will be discussed in next sections and reaction acceleration or self catalysis at higher temperatures due to reactions of chlorine radical.

#### B. Reagent Conversion and Product Distribution

Appreciable conversions (50%) of dichloromethane and 1,1,1-trichloroethane were observed at reaction temperature above 720 °C and 515 °C for the respective reagents at 0.5 sec. residence time as shown in Figure 5. Figure 5 shows that the conversion of each reagent consistently increases with increasing temperature and mean residence time. The major product distributions are shown in Figure 13 and 14 for varying temperature and reaction conditions. 1,1-dichloroethylene ( $\text{CH}_2\text{CCl}_2$ ), 1,1-dichloroethane ( $\text{CH}_3\text{CHCl}_2$ ), vinyl chloride ( $\text{CH}_2\text{CHCl}$ ), methyl chloride ( $\text{CH}_3\text{Cl}$ ) and HCl were the major product at 570 °C, where up to 95 % conversion of  $\text{CH}_3\text{CCl}_3$  and 13 % conversion of  $\text{CH}_2\text{Cl}_2$  were observed as shown in Figure 5 and 13. Minor products at this temperature of methane, ethylene and ethane ( whereas these are major products at temperatures above 720 °C ). Monochloroethane ( $\text{CH}_3\text{CH}_2\text{Cl}$ ) and 1,1,2-trichloroethane ( $\text{CHCl}_2\text{CH}_2\text{Cl}$ ) are also found at this temperature; As shown in semi-quantitative product distribution Table 6 and 7 the trace quantities of trichloroethylene ( $\text{CCl}_2\text{CHCl}$ ), 1,2-dichloroethylene ( $\text{CHClCHCl}$ ) and  $\text{C}_3$  hydrocarbon were also



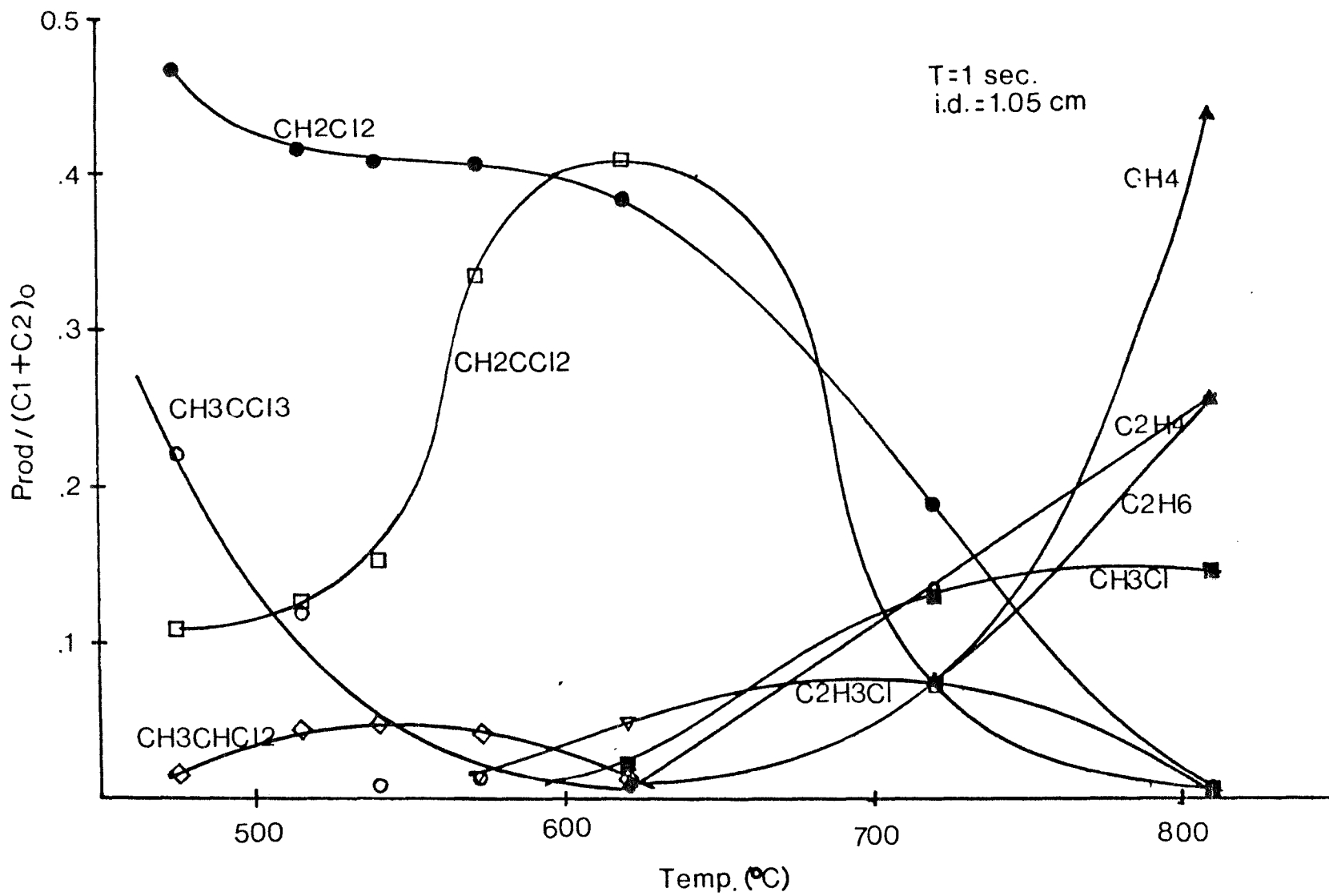


Figure 13. Product Distribution vs Temp. in CH<sub>2</sub>Cl<sub>2</sub>/CH<sub>3</sub>CCl<sub>3</sub>/H<sub>2</sub>

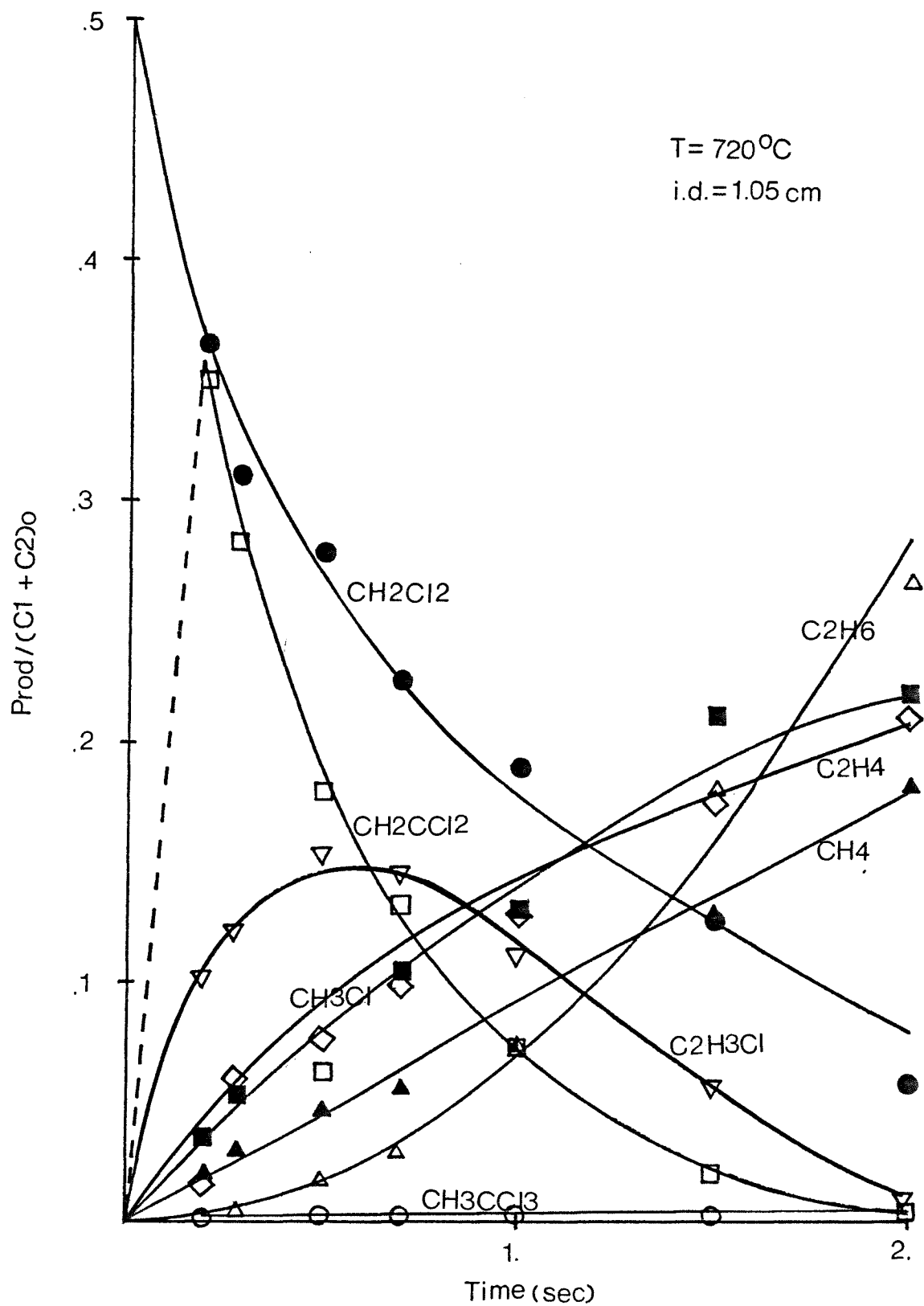


Figure 14. Product Distribution vs Time in CH<sub>2</sub>Cl<sub>2</sub>/CH<sub>3</sub>CCl<sub>3</sub>/H<sub>2</sub>

observed at temperatures below 720 °C . As illustrated in Figure 15, formation of non-chlorinated hydrocarbon is shown to increase with increasing temperature. The number of chlorine containing hydrocarbon products decreases with increasing temperature and residence time and HCl formation increases as shown in the chlorine material balance Table 3. The number and quantity of chlorinated hydrocarbon products drops quickly at about 720 °C, where only CH<sub>3</sub>Cl was observed at 810 °C and 1 sec. reaction conditions. This indicates that CH<sub>3</sub>Cl is the most stable chlorocarbon in this reacting system. It is consistent with the bond strengths C-Cl bonds on chlorocarbons which increases with decreasing chlorination.

The conversion of CH<sub>2</sub>Cl<sub>2</sub> increases slowly or reaches an apparent steady state value of about 13 % at temperature below 515 and 620 °C as illustrated in Figure 13. However, conversion for CH<sub>2</sub>Cl<sub>2</sub> rises quickly as the temperature increase from 620 °C where CH<sub>3</sub>Cl and CH<sub>4</sub> as the C<sub>1</sub> products rapidly increase. This occurs because CH<sub>2</sub>Cl<sub>2</sub> by itself does not react to significant degree below 620 °C but radicals which are produced from CH<sub>3</sub>CCl<sub>3</sub> can attack the CH<sub>2</sub>Cl<sub>2</sub>. However, as the temperature increases from about 620 °C, CH<sub>2</sub>Cl<sub>2</sub> decomposition reaction sets in. Formation of CH<sub>3</sub>Cl and CH<sub>4</sub> increases proportionally to decrease in CH<sub>2</sub>Cl<sub>2</sub> from 620 to 720 °C and further reaction of these species will be discussed with CH<sub>3</sub>CCl<sub>3</sub> by-product reaction.

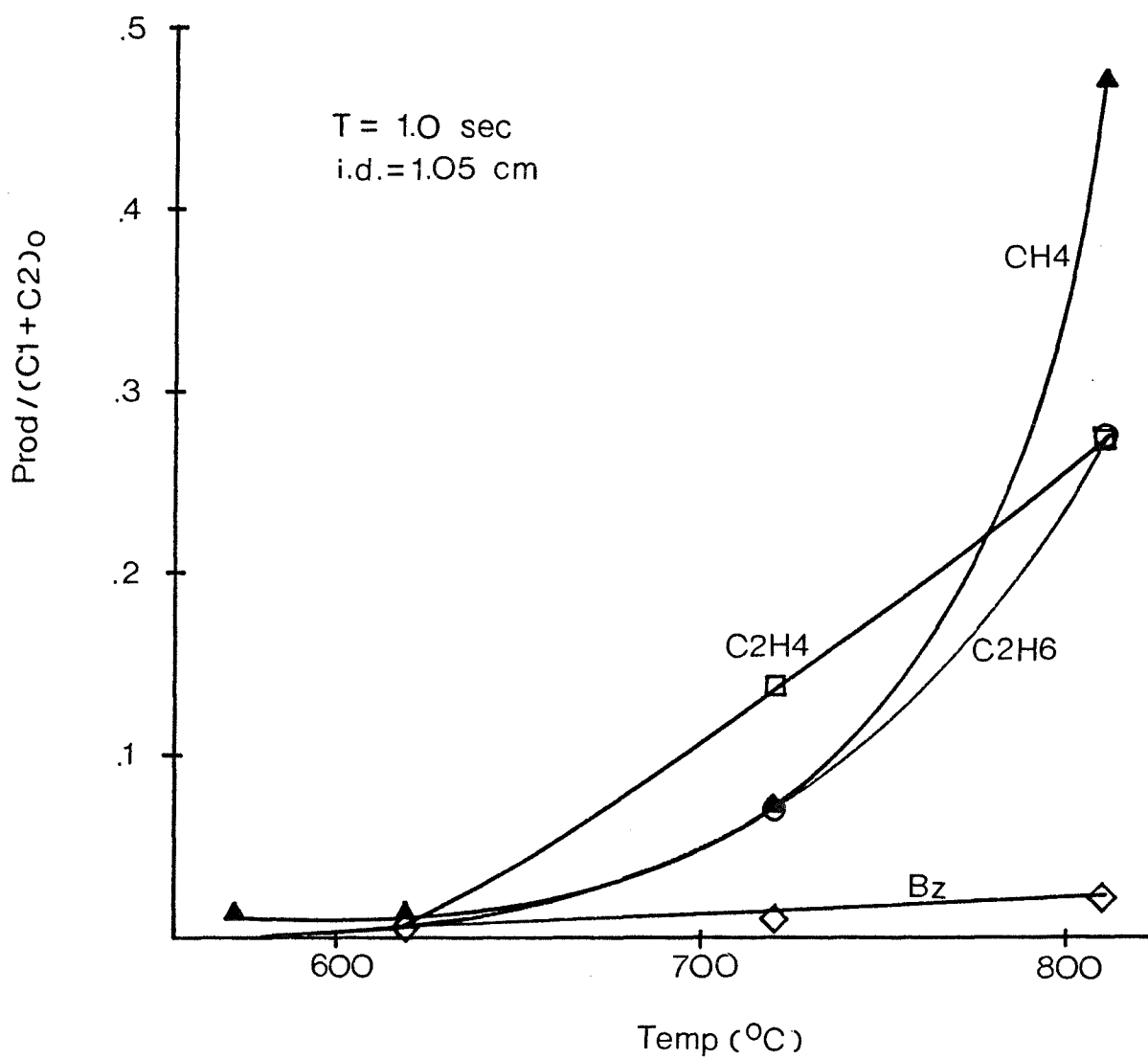
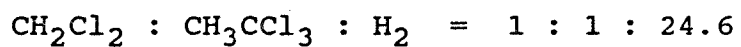


Figure 15. Dechlorinated Hydrocarbon Product Distribution versus Temperature

Table 3

## Material Balance for 100 Moles Chlorine



Reactor Diameter : 1.05 cm  
Residence Time : 1.0 sec.

Species ( % )	Temperature ( °C )				
	475	572	620	720	810
CHCCl	ND	0.28	0.12	1.0	2.3
CH <sub>3</sub> Cl	0.12	0.84	1.1	6.3	3.8
CH <sub>2</sub> CHCl	0.03	0.75	1.92	4.8	ND
CH <sub>3</sub> CH <sub>2</sub> Cl	ND	0.15	0.15	0.5	ND
CH <sub>2</sub> Cl <sub>2</sub>	35.7	33.4	30.9	16.2	0.4
CH <sub>2</sub> CCl <sub>2</sub>	8.8	27.0	33.0	8.1	0.2
CH <sub>3</sub> CHCl <sub>2</sub>	ND	3.7	1.0	0.3	ND
CHClCHCl	0.12	0.12	0.1	ND	ND
CH <sub>3</sub> CCl <sub>3</sub>	38.9	0.3	0.1	0.54	0.5
CHClCCl <sub>2</sub>	ND	0.1	0.1	ND	ND
CHCl <sub>2</sub> CH <sub>2</sub> Cl	0.3	0.5	0.2	1.4	ND
HCl	12.5	35.6	37.5	56.7	92.7
Total	98.3	102.7	106.5	95.8	99.9

Table 4

Material Balance for 100 Moles Carbon

 $\text{CH}_2\text{Cl}_2 : \text{CH}_3\text{CCl}_3 : \text{H}_2 = 1 : 1 : 24.6$ Reactor Diameter : 1.05 cm  
Residence Time : 1.0 sec.

Species ( % )	Temperature ( °C )				
	475	572	620	720	810
$\text{CH}_4$	0.1	0.5	1.0	4.7	29.4
CHCH	ND	0.15	0.5	0.8	ND
$\text{CH}_2\text{CH}_2$	ND	0.3	0.2	19.2	28.4
$\text{CH}_3\text{CH}_3$	ND	0.15	0.2	9.5	28.4
CHCCL	ND	0.2	0.3	1.5	3.8
$\text{CH}_3\text{Cl}$	0.2	1.4	1.8	10.5	6.3
CHCCH <sub>3</sub>	ND	0.3	0.2	0.3	ND
$\text{C}_3\text{H}_6$ & $\text{C}_3\text{H}_8$	ND	0.3	0.4	1.3	0.15
$\text{CH}_2\text{CHCl}$	0.1	2.5	6.5	16.0	ND
$\text{CH}_3\text{CH}_2\text{Cl}$	ND	0.5	0.5	1.6	ND
$\text{CH}_2\text{Cl}_2$	31.2	27.8	25.7	13.5	0.3
$\text{CH}_2\text{CCl}_2$	14.6	45.0	55.0	9.8	ND
$\text{CH}_3\text{CHCl}_2$	ND	6.1	1.6	0.5	ND
CHClCHCl	0.2	0.2	0.15	ND	ND
$\text{CH}_3\text{CCl}_3$	43.2	0.3	0.1	0.2	0.3
CHClCCl <sub>2</sub>	ND	0.1	0.1	ND	ND
$\text{C}_6\text{H}_6$	ND	ND	0.1	1.4	2.6
$\text{CHCl}_2\text{CH}_2\text{Cl}$	0.3	0.5	0.2	1.5	ND
Total	89.9	86.3	94.5	92.4	99.75

Formation of  $\text{CH}_2\text{CCl}_2$  as one of major product from  $\text{CH}_3\text{CCl}_3$  increases with increasing temperature to a maximum near  $620^\circ\text{C}$  with 1.0 sec. residence time and then drops quickly with increasing temperature; strongly indicating that  $\text{CH}_2\text{CCl}_2$  is the initial stable product in unimolecular reaction of this mixture diluted in hydrogen. Figure 16 also specifically illustrates  $\text{CH}_2\text{CCl}_2$  normalized concentration versus residence time for seven different temperature, and demonstrates that  $\text{CH}_2\text{CCl}_2$  concentration increases with increasing residence time under  $572^\circ\text{C}$  while it increases and then decreasing with residence time over  $620^\circ\text{C}$ . The increase in  $\text{CH}_2\text{CCl}_2$  with residence time suggests that its rate of formation is faster than its destruction of this  $572^\circ\text{C}$  temperature and is another indication that the  $\text{CH}_2\text{CCl}_2$  is a stable intermediate product in overall reaction. Formation of  $\text{CH}_3\text{CHCl}_2$ ,  $\text{CH}_2\text{CHCl}$  (vinyl chloride) and  $\text{CH}_3\text{Cl}$  also show a similar trend; These trends may be due to a high formation rate of precursor products (  $\text{CH}_2\text{CCl}_2$ ,  $\text{CH}_3\text{CHCl}_2$  and  $\text{CH}_3\text{Cl}$  ) from the chlorinated parent compounds. These products are also dechlorinated to  $\text{CH}_2\text{CHCl}$ ,  $\text{CH}_2\text{CH}_2$ ,  $\text{CH}_3\text{CH}_3$  and  $\text{CH}_4$  in further reaction steps with increasing temperature.

Formation of  $\text{CH}_2\text{CHCl}$  and  $\text{CH}_2\text{CH}_2$  increases from  $620$  to  $720^\circ\text{C}$  as the temperature increases. This indicates that the more stable compound,  $\text{CH}_2\text{CHCl}$  is apparently formed from overall reaction of  $\text{CH}_2\text{CCl}_2$  and  $\text{CH}_3\text{CHCl}_2$  with hydrogen, and

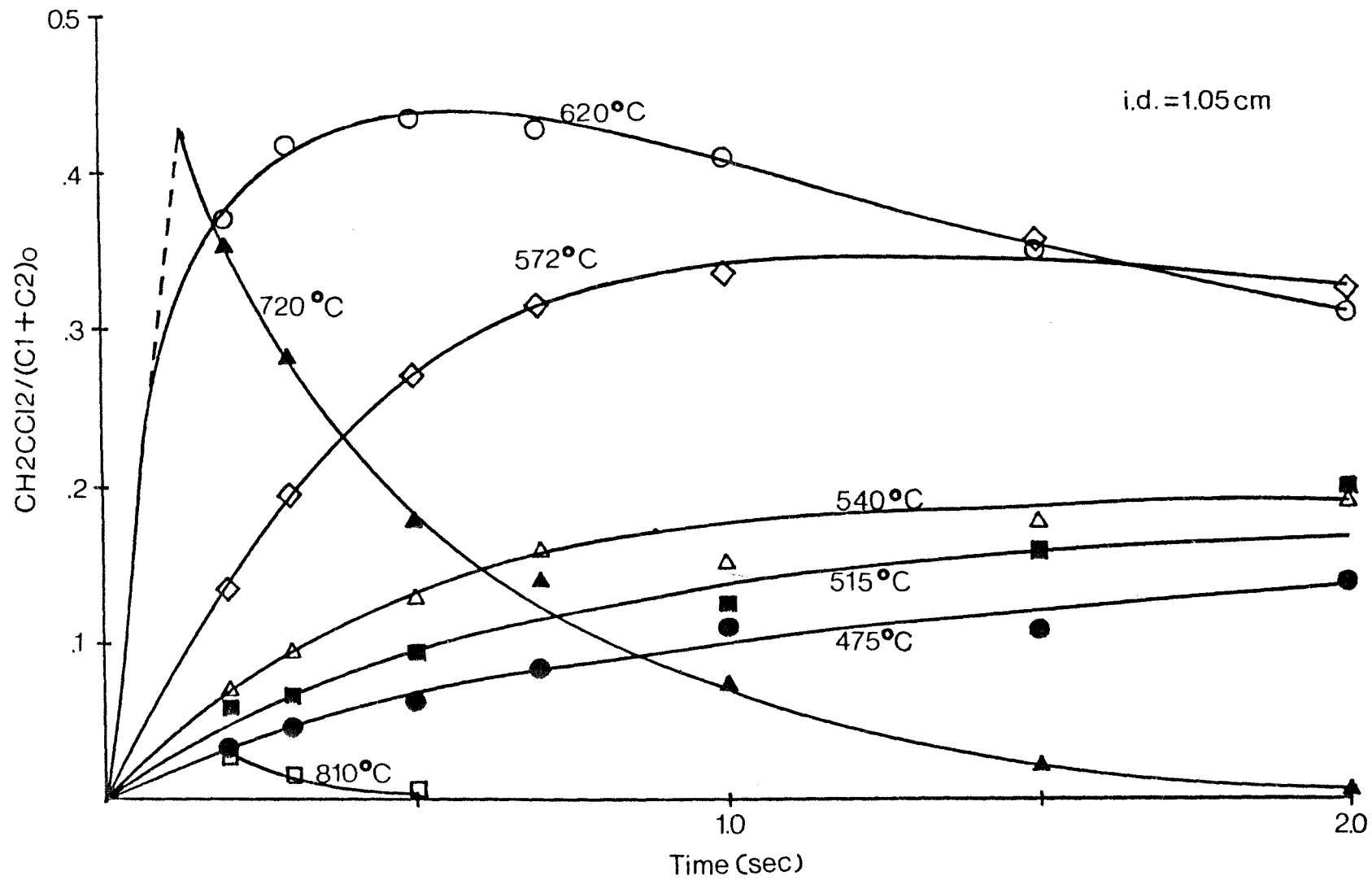


Figure 16.  $\text{CH}_2\text{CCl}_2$  Formed per mole of feed



then  $\text{CH}_2\text{CH}_2$  or  $\text{CH}_3\text{CH}_3$  is produced from further reaction of  $\text{CH}_2\text{CHCl}$  with hydrogen in this temperature reaction region. The 720 - 810 °C temperature range reaction of  $\text{CH}_2\text{CHCl}$  appears very similar to 620 - 720 °C that of  $\text{CH}_2\text{CCl}_2$ .

Formation of  $\text{CH}_4$ ,  $\text{CH}_2\text{CH}_2$  and  $\text{CH}_3\text{CH}_3$  increases with increasing temperature to 810 °C. This indicates the less chlorinated hydrocarbon is more stable in the reacting system. As shown in Table 5, the greater the bond energy between carbon and chloride, the higher temperature required to observe reaction of the chlorocarbon.

TABLE. 5

Product Maxima Formation Temperatures and Bond Energies  
between Carbon and Chlorine in This Reaction System

Species	Max. Form. Temp. ( °C )	Bond Energy ( Kcal/mol )
$\text{CH}_3\text{CHCl}_2$	540	78.15
$\text{CH}_2\text{CCl}_2$	620	88.59
$\text{CH}_2\text{CHCl}$	720	90.90
$\text{CH}_3\text{CCl}_3$	< 570	73.20

\* Reaction residence time 0.5 sec. with 1.05 cm id tube

The  $\text{C}_2$  trace products from pure  $\text{CH}_2\text{Cl}_2$  reaction could be observed by Tsao<sup><15></sup>, but those quantities cannot be

Table 6

Thermal Reaction Products Distribution with Temperature

$\text{CH}_2\text{Cl}_2 : \text{CH}_3\text{CCl}_3 : \text{H}_2 = 1 : 1 : 24.6$   
 Reactor Diameter : 1.05 cm  
 Residence Time : 1.0 sec.

Species	Temperature ( °C )				
	515	572	620	720	810
CH <sub>4</sub>	x	x	xx	xxx	****
CHCH		x	x	x	
CH <sub>2</sub> CH <sub>2</sub>	x	x	x	*	**
CH <sub>3</sub> CH <sub>3</sub>		x	x	xxx	**
CHCCl	x	x	x	x	xx
CH <sub>3</sub> Cl	x	xx	xx	*	xxx
CHCCH <sub>3</sub>	x	x	x	x	
C <sub>3</sub> H <sub>6</sub> & C <sub>3</sub> H <sub>8</sub>	x	x	x	xx	x
CH <sub>2</sub> CHCl	x	xx	xx	*	
CH <sub>3</sub> CH <sub>2</sub> Cl	x	x	x	xx	
CH <sub>2</sub> CCl <sub>2</sub>	*	***	****	xxx	
CH <sub>3</sub> CHCl <sub>2</sub>	xx	xx	xx	x	
CHClCHCl	x	x	x		
CHClCCl <sub>2</sub>		x	x		
C <sub>6</sub> H <sub>6</sub>			x	x	xx
CHCl <sub>2</sub> CH <sub>2</sub> Cl	x	x	x	x	

0.1 % < x < 1.0 % < xx < 5.0 % < xxx < 10 %

10 % < \* < 20 % < \*\* < 30 % < \*\*\* < 40 % < \*\*\*\*

Percent = ( Product Mol Conc. ) / ( C<sub>1</sub> + C<sub>2</sub> )<sub>o</sub>

Table 7

Thermal Reaction Products Distribution  
with Residence Time

$\text{CH}_2\text{Cl}_2 : \text{CH}_3\text{CCl}_3 : \text{H}_2 = 1 : 1 : 24.6$   
 Reactor Diameter : 1.05 cm  
 Reaction Temperature : 720 °C

Species	Residence Time ( sec. )				
	0.2	0.5	1.0	1.5	2.0
$\text{CH}_4$	xx	xx	xxx	*	*
CHCH	x	x	x	x	x
$\text{CH}_2\text{CH}_2$	xx	xxx	*	*	**
$\text{CH}_3\text{CH}_3$	x	xx	xxx	*	**
CHCCl	x	x	x	xx	xx
$\text{CH}_3\text{Cl}$	xx	xxx	*	**	**
CHCCH <sub>3</sub>			x		
$\text{C}_3\text{H}_6$ & $\text{C}_3\text{H}_8$	x	x	x	x	x
$\text{CH}_2\text{CHCl}$	*	*	*	xxx	xx
$\text{CH}_3\text{CH}_2\text{Cl}$	x	x	xx	xx	x
$\text{CH}_2\text{CCl}_2$	***	*	xxx	xx	x
$\text{CH}_3\text{CHCl}_2$	x	x	x	x	x
CHClCHCl	x	x			
CHClCCl <sub>2</sub>		x		x	
$\text{C}_6\text{H}_6$	x	x	x	x	xx
$\text{CHCl}_2\text{CH}_2\text{Cl}$	x	x	x		

0.1 % < x < 1.0 % < xx < 5.0 % < xxx < 10 %

10 % < \* < 20 % < \*\* < 30 % < \*\*\* < 40 % < \*\*\*\*

Percent = ( Product Mol Conc. ) / (  $C_1 + C_2$  )

separated from  $\text{CH}_3\text{CCl}_3$  by product. And these results will be discussed further detail in the reaction mechanism. No observation of  $\text{C}_1$  products from pyrolysis of  $\text{CH}_3\text{CCl}_3$  in hydrogen occurred in this study even though it overlapped the compounds whose bonds are relatively stable. Chuang's study<sup><10></sup> show that very tiny amount of  $\text{C}_1$  products from 1,1,2-trichloroethane reaction was seen at above 850 °C.

The overall reaction scheme based on analysis of major concentration products and thermochemical kinetics estimation will be discussed in the detailed mechanism section.

As shown in the semi-quantitative product distribution Table 6, benzene formation is observed above 620 °C and the non-chlorinated  $\text{C}_3$  products are also seen above 515 °C and over a wide temperature range.  $\text{C}_2\text{H}_2$  concentration increases slightly and then decreases as more benzene is formed. The formations of benzene and non-chlorinated  $\text{C}_3$  hydrocarbon may be due to pyrolysis of methane and  $\text{C}_2$  hydrocarbons, followed by ring closure mechanism with olefinic and acetylenic species as intermediates. A general commercial pathway to synthesis of benzene is pyrolysis and hydrogasification of paraffinic hydrocarbons<sup><32></sup>.

#### C. Comparison of Dichloromethane/1,1,1-Trichloroethane mixture Reaction with Each Pure Compound Reactions of Previous Studies

It worth comparing the two reagents in the mixture with

each pure reagent reaction in hydrogen to find effects of mixed system. Tsao<sup><15></sup>( 1987 ) studied thermal decomposition of pure dichloromethane in hydrogen under similar experimental conditions within the temperature range of 700 to 950 °C and residence time of 0.3 to 3.1 sec.. Dichloromethane feed concentration was 20 %. While, as shown in Figure 17, conversion trends are similar in both cases; here are, however, conversion differences present between the two results. Figure illustrates that conversion difference decreases with temperature rise. For both cases, however, the complete decay (99%) temperature for dichloromethane is the same, about 810 °C. The conversion of pure dichloromethane reaction increases slowly between 515 and 620 °C and it appears to reach an apparent steady state value of 13 % in the above temperature range as illustrated in Figure 17. This occurs because dichloromethane by itself does not react to significant degree below 620 °C but the radicals which are produced from 1,1,1-trichloroethane reaction on subsequent reaction with hydrogen can attack dichloromethane. The pure dichloromethane reaction, however does not follow this kind of behavior ( pure CH<sub>2</sub>Cl<sub>2</sub> conversion is near 0 % for temperature ( 515 - 620 °C ) range ). As the temperature increases above 700 °C, the conversion difference decreases. This indicates that unimolecular decomposition reaction of dichloromethane starts and becomes dominant, eventually to

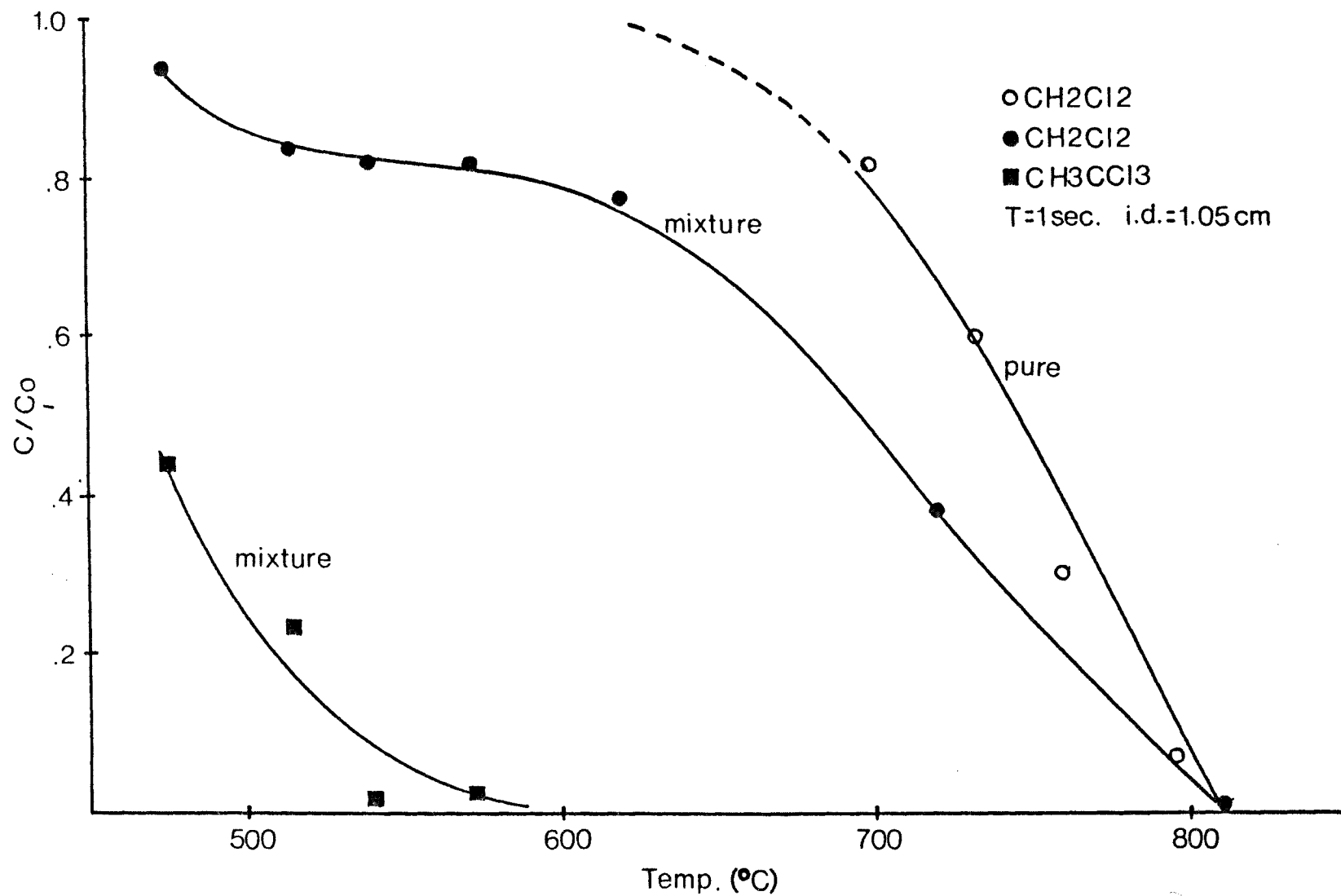


Figure 17. Comparison of Pure and Mixed System of CH<sub>2</sub>Cl<sub>2</sub>

overcome the earlier radical initiated reaction.

It is valuable to analyze excess hydrogen concentration difference effect on rate constant for each two experimental sets. The difference in the concentration of excess hydrogen may explain the change the rate constant. The reactant to hydrogen ratios are 1:12.3 and 1:4 respectively for mixture and neat studies of dichloromethane. The reactant concentration of two studies change by a factor of three; but the hydrogen concentration does not change significantly. Attempts to explain the effect of change in hydrogen concentration fail to provide reliable results due to the close proximity of the two hydrogen concentration and complicated mixture reaction effects.

Major products from the pure  $\text{CH}_2\text{Cl}_2$  by Tsao' study<sup><15></sup> reaction are  $\text{CH}_4$ ,  $\text{CH}_3\text{Cl}$  and traces of  $\text{CHCH}$ ,  $\text{CH}_2\text{CH}_2$ ,  $\text{CH}_3\text{CH}_3$  and  $\text{CH}_2\text{CHCl}$ . Methane and methyl chloride normalized concentration the mixture, on the other hand, are slightly higher than that of pure dichloromethane/hydrogen reaction. This occurs because the conversion of mixture reaction is higher than that of pure  $\text{CH}_2\text{Cl}_2$  reaction. Above  $800^\circ\text{C}$ , the methane normalized concentration difference is indicates  $\text{CH}_3\text{CCl}_3$  dissociates to  $\text{CH}_3$  and  $\text{CCl}_3$ , and then converts to  $\text{CH}_4$ .

Chang<sup><11></sup>(1985) had studied the thermal decomposition of pure 1,1,1-trichloroethane in hydrogen using similar experimental system at the temperature range of 555 to 681

$^{\circ}\text{C}$  and short residence times between 0.04 to 1.0 sec. for 5.89 % of 1,1,1-trichloroethane present in feed concentration.

Figure 18 shows that both conversion trends are similar with small difference present. The major products from 1,1,1-trichloroethane reaction were observed to be 1,1-dichloroethylene, chloroform, 1,1-dichloroethane, trichloroethylene, methylene chloride and HCl. Propane, proylene and propyne as minor products were seen at all reaction temperature ranges, when a mixture of chlorocarbons were used. These products however, were not identified in each pure compound reaction systems.

In order to simplify the kinetic analysis and obtain global rate parameters, pseudo-first order reaction conditions were utilized by having a large excess of  $\text{H}_2$ . Decoupling of the wall and bulk reaction constant was achieved by the assuming plug flow reactor conditions (Kaufman<sup><26></sup>) and pseudo first order reaction condition prevail. Apparent bulk activation energies were estimated to be 32 Kcal/mol for  $\text{CH}_3\text{CCl}_3$  and 36 Kcal/mol for  $\text{CH}_2\text{Cl}_2$  with  $\text{H}_2$  in the mixture reaction system.  $\text{CH}_3\text{CCl}_3$  apparent bulk activation energy is close to that of pure compound reaction of  $\text{CH}_3\text{CCl}_3$  ( 26 Kcal/mol ) reported in the literature<sup><18></sup>. But  $\text{CH}_2\text{Cl}_2$  apparent bulk activation energy is 39 % smaller than that of pure  $\text{CH}_2\text{Cl}_2$  ( 50 Kcal/mol ) reported in the literature<sup><15></sup>. This is because radicals which are more



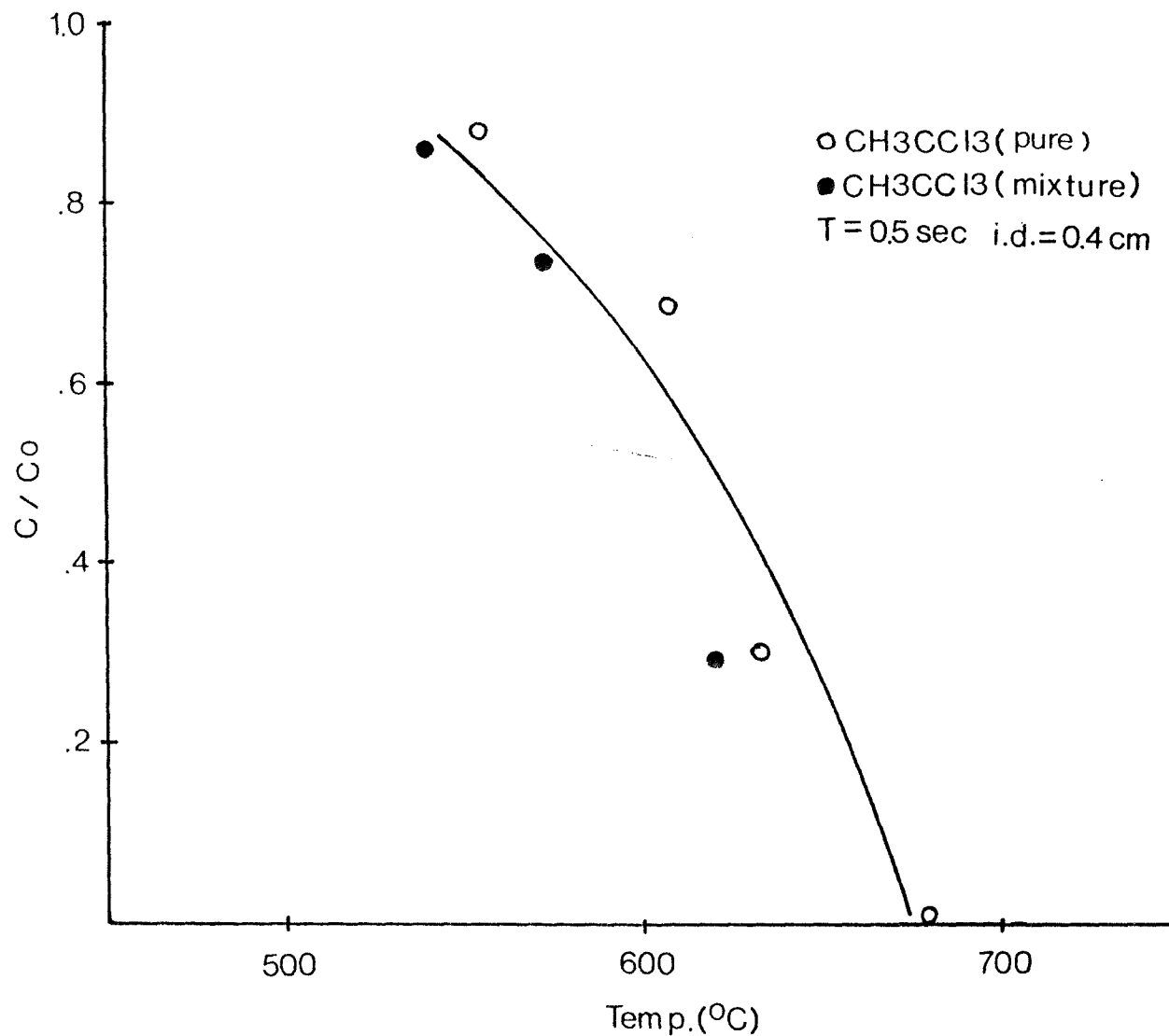


Figure 18. Comparison of Pure and Mixed System for CH<sub>3</sub>CCl<sub>3</sub>

easily produced from  $\text{CH}_3\text{CCl}_3$  decomposition initiate  $\text{CH}_2\text{Cl}_2$  decomposition. These radical reactions decrease the  $\text{CH}_2\text{Cl}_2$  activation energy similar to the role of a catalyst.

#### D. Quantum RRK

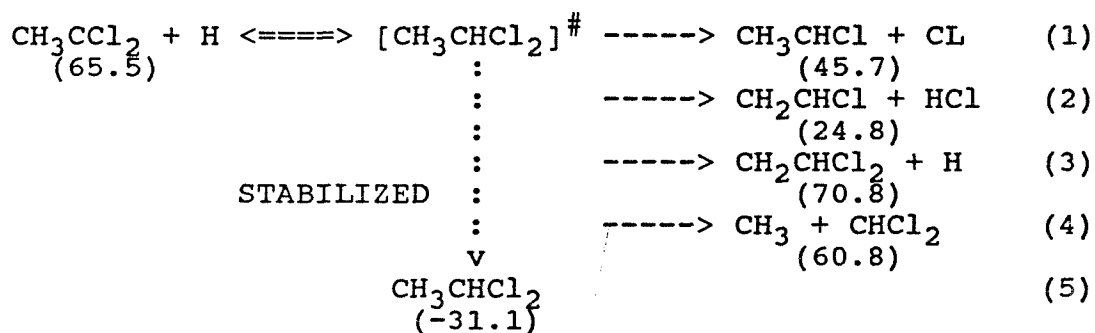
The decomposition/stabilization of the energized radical and molecule complexes was modeled using the QRRK calculation. The details of the bimolecular QRRK method in theory section and its application to a number of chemically activated reaction systems have been discussed<sup><27,33></sup>.

Energized Complex/QRRK theory as presented by Westmoreland and Dean<sup><33></sup> is used for modelling of radical addition and combination reactions. This has been modified by Ritter and Bozzelli<sup><34></sup> to use gamma function. The QRRK computer code was used to determine the energy dependent rate constants for all channels. The program incorporates QRRK theory to calculate rate constants as function of temperature and pressure. It is important in determination of the mechanism and choice of the paths (accurate product prediction from the activated complex).

A QRRK analysis of the chemically activated system, using generic estimates or literature values for high pressure rate constants and species thermodynamic properties for the enthalpies of reaction, yields apparent rate constants as will be shown in Figure 20 & 22 and APPENDIX 1. And the results from the calculations input rate parameters

used in these calculations are summarized in APPENDIX Table 1 - 12. The calculations were performed for each of six pressures between 0.76 torr and 7600 torr.

The combination reaction of primary radicals,  $\text{CH}_3\text{CCl}_2$  ( another source : Cl transfer metathetical reaction of H with  $\text{CH}_3\text{CCl}_3$  ) and H, is similar but will produce different end-products as shown in all possible reactions which will explain formation procedure of other products



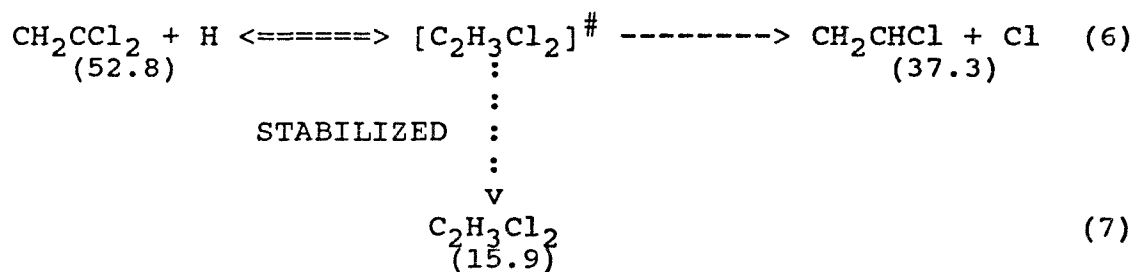
where the energized complex (# denotes energized) further decomposes as shown in reaction (1) to (4). The energy diagram for the above reaction channels(1) to (5) is illustrated in Figure 19. Reactions (3) and (4) do not occur due to thermo limitation (high energy barrier). They are endothermic, while reactions (1), (2) and (5) are thermodynamically favorable channels ( low energy barrier) relative to initial energy of the reactants. It must be noted that reaction (2) corresponds to the composite behavior of four-center 1,2 and three-center 1,1 HCl elimination processes, because the  $\text{CH}_3\text{CCl}$ : formed in the latter case rapidly isomerized to  $\text{CH}_2\text{CHCl}$ . Both 1,2 and 1,1

HCl elimination processes are expected to have similar A factors<sup><35></sup> and slightly higher activated energies for 1,1 HCl elimination processes<sup><36></sup>.

The calculation results, pressure dependent rate constants and an energy diagram for H atom addition to CH<sub>2</sub>CCl<sub>2</sub> are shown in Figure 19 and 20. The QRRK calculations for temperature 773 to 1273 °K and pressure range of 0.001 - 10 atm. show that the rate constant for the CH<sub>2</sub>CHCl+HCl channel and CH<sub>3</sub>CHCl + Cl channel are dominant below 0.1 atm. whereas at pressures above 1 atm. stabilization of activated complex is dominant. The CH<sub>3</sub>CHCl radical, from reaction (1) can undergo beta scission to CH<sub>2</sub>CHCl+ H or CH<sub>3</sub>CH +Cl and stabilized CH<sub>3</sub>CH<sub>2</sub>Cl can also react splitting out HCl forming C<sub>2</sub>H<sub>4</sub>.

The QRRK calculation results show for this reaction system that the rate constant for CH<sub>2</sub>CHCl+HCl channel is close to CH<sub>3</sub>CHCl+Cl and three times greater than CH<sub>3</sub>CHCl<sub>2</sub> (stabilization) at temperature range 773 -873 °K and 1 atm..

For the CH<sub>2</sub>CCl<sub>2</sub> + H system, the energy diagram is shown in Figure 21, where the following major reactions are expected to be important:



E (Kcal/mol)

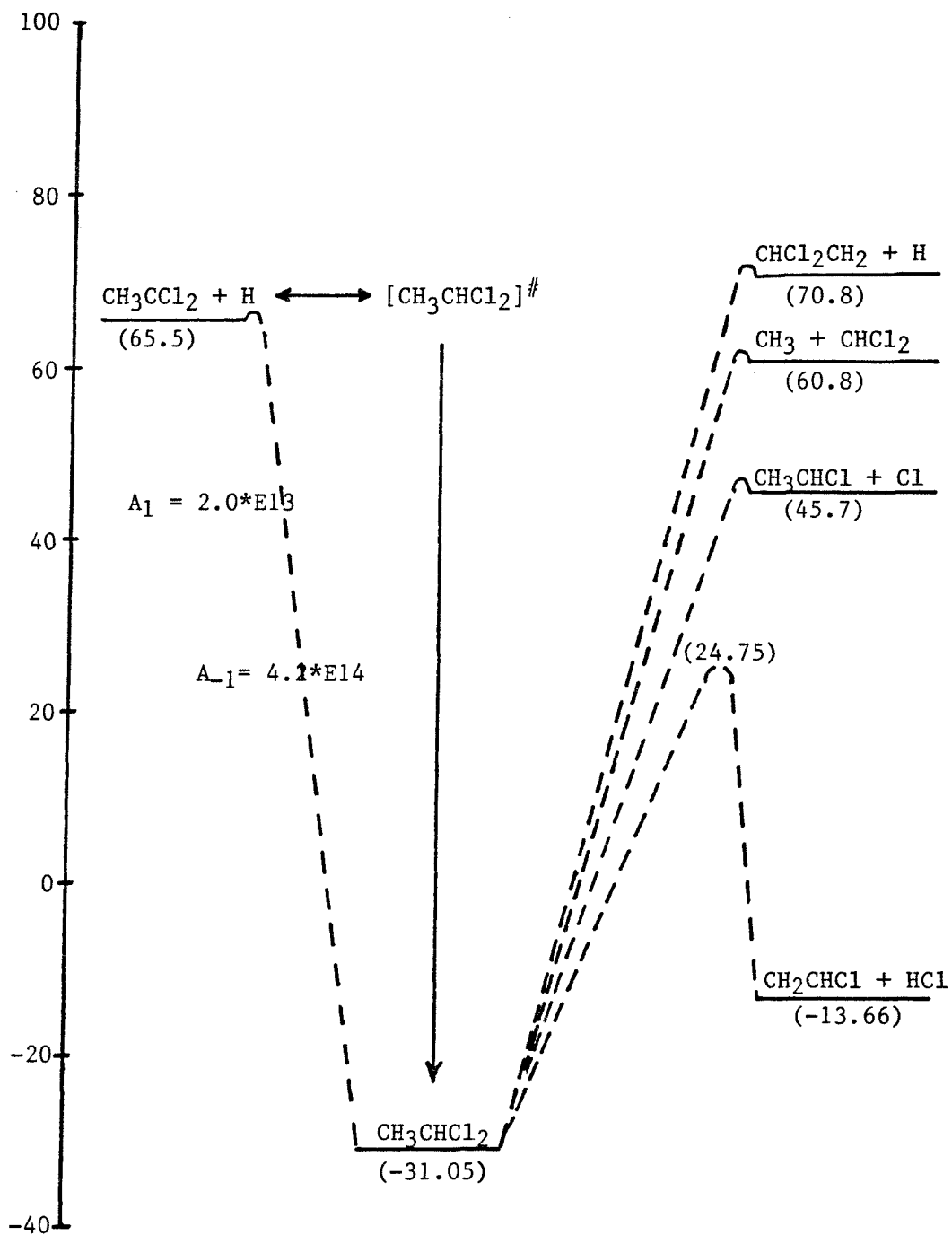


Figure 19. Energies of Activation Complex Theory Calculation for Reaction CH<sub>3</sub>CCl<sub>2</sub> + H

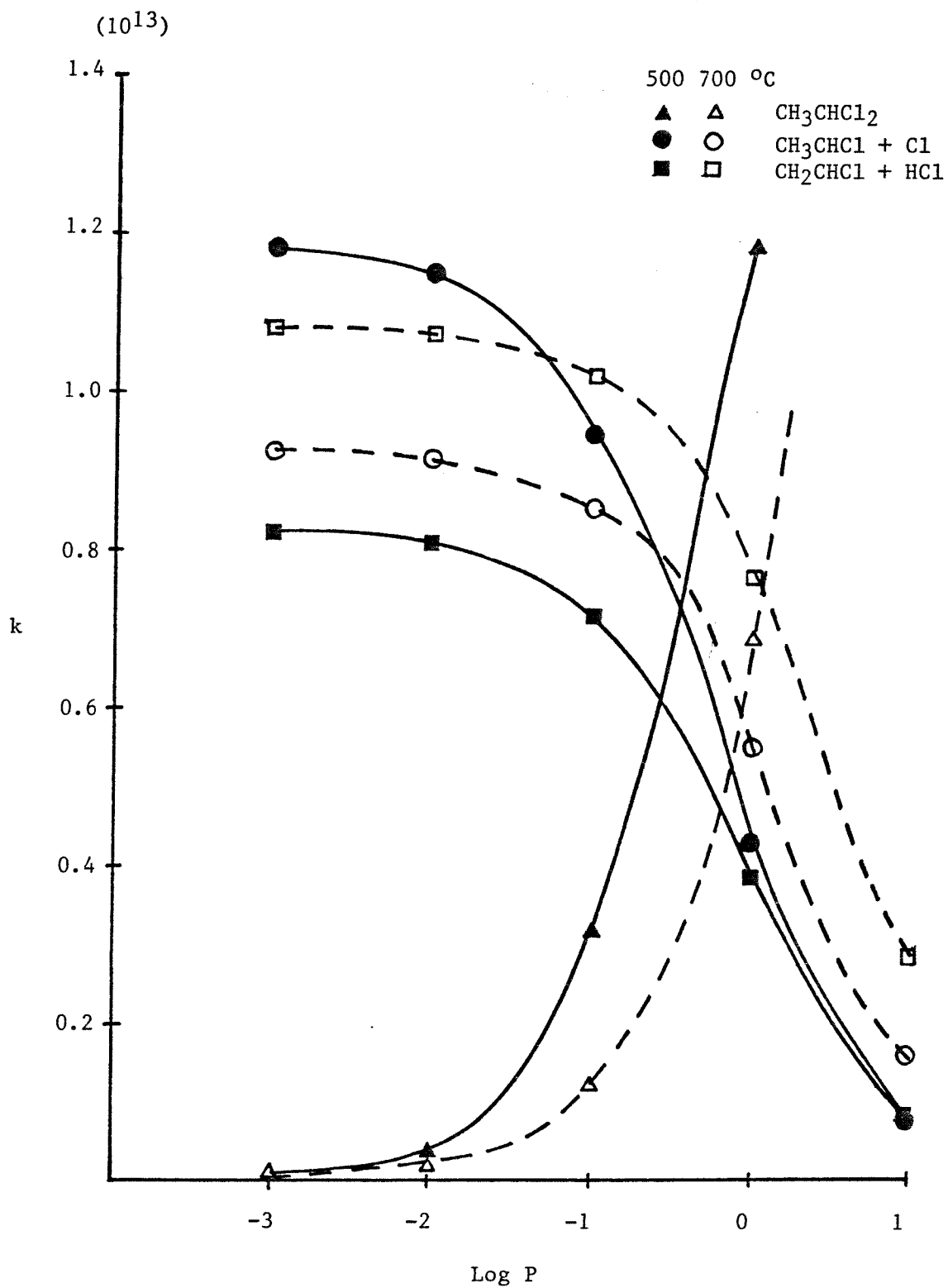
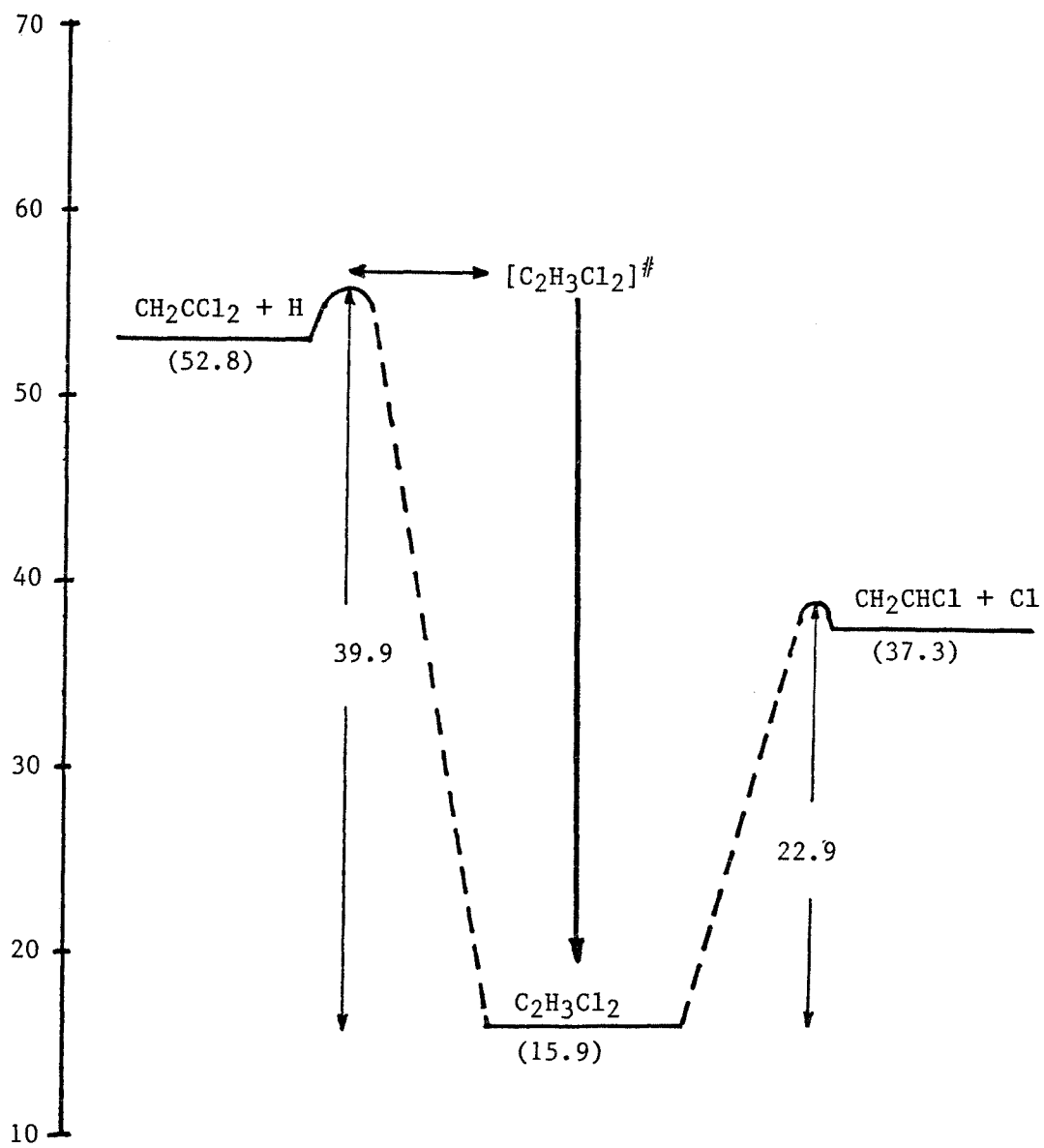


Figure 20. Results of Activated Complex Theory Calculation for Reaction CH<sub>3</sub>CCl<sub>2</sub> + H

E (Kcal/mol)

Figure 21. Energy Diagram for  $\text{CH}_2\text{CCl}_2 + \text{H}$

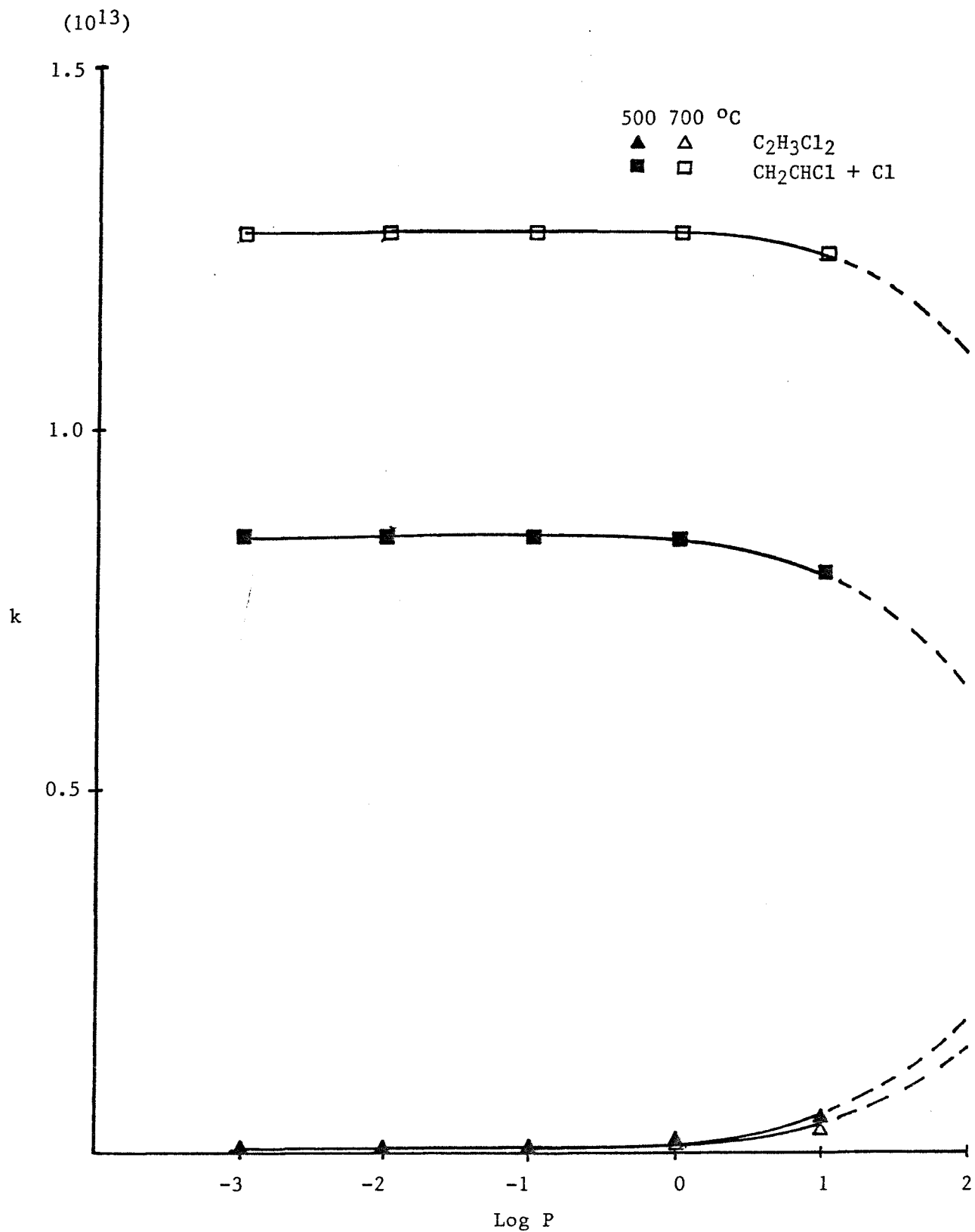


Figure 22. Results of Activated Complex Theory Calculation for Reaction CH<sub>2</sub>CCl<sub>2</sub> + H



Atomic H produced from  $\text{Cl} + \text{H}_2 = \text{HCl} + \text{H}$  will add to  $\text{CH}_2\text{CCl}_2$  to form  $\text{CHCl}_2\text{CH}_2$  radicals as shown above reactions. The energy diagram of the reaction (6) and (7) is illustrated in Figure 21 and the calculation results are shown in Figure 22.

The  $\text{CHCl}_2\text{CH}_2$  complex is initially "hot" since, in addition to the thermal energy, it contains energy resulting from formation of the new chemical bond. Prior to stabilization it may unimolecularly isomerize. It can undergo a hydrogen shift, become a stabilized radical or beta scission to  $\text{CH}_2\text{CHCl} + \text{Cl}$ .

#### E. Detailed Kinetic Mechanism and Modeling

The reaction mechanism and decomposition kinetics for  $\text{CH}_2\text{Cl}_2/\text{CH}_3\text{CCl}_3$  mixture in  $\text{H}_2$  are developed.

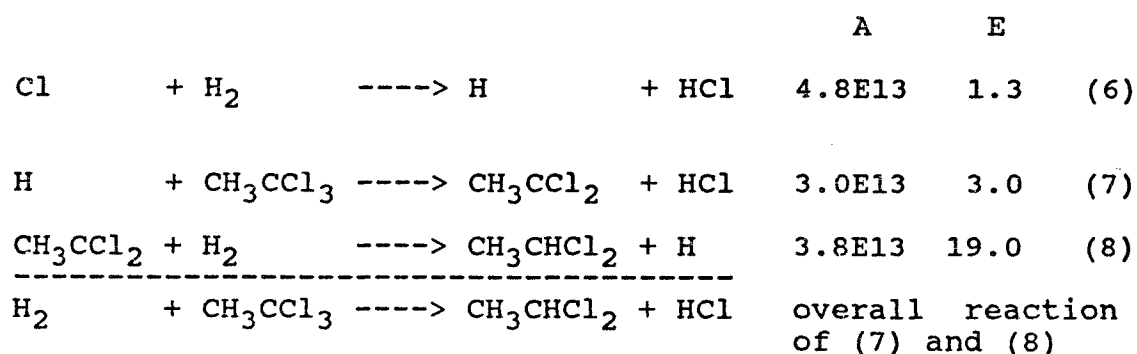
The possible initial reactions are unimolecular decomposition of  $\text{CH}_2\text{Cl}_2$  and  $\text{CH}_3\text{CCl}_3$  as follows:

		A (1/s)	E (Kcal/mol)	
$\text{CH}_2\text{Cl}_2$	$\text{---> CH}_2\text{Cl} + \text{Cl}$	1.1E16	82.8	( $\Delta\text{Hr}$ ) (1)
$\text{CH}_2\text{Cl}_2$	$\text{---> CHCl} + \text{HCl}$	1.2E14	105.0	( $\Delta\text{Hr}+40$ ) (2)
$\text{CH}_3\text{CCl}_3$	$\text{---> CH}_3\text{CCl}_2 + \text{Cl}$	2.4E16	73.2	( $\Delta\text{Hr}$ ) (3)
$\text{CH}_3\text{CCl}_3$	$\text{---> CH}_2\text{CCl}_2 + \text{HCl}$	3.8E13	47.9	( $\Delta\text{Hr}+38$ ) (4)
$\text{CH}_3\text{CCl}_3$	$\text{---> CH}_3 + \text{CCl}_3$	9.1E15	84.7	( $\Delta\text{Hr}$ ) (5)

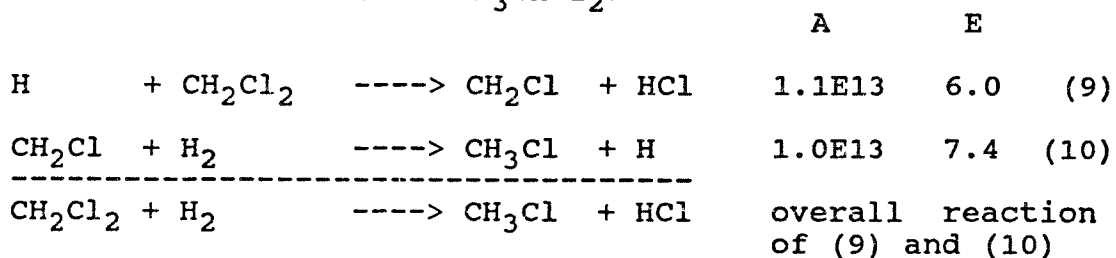
( kinetic data source refer to source part of Table 8 )

It is observed from the above kinetic listing that reaction (4) dominates the other pathways by more than three

orders of magnitude at temperatures below 600 °C. This is consistent with our experimental results.  $\text{CH}_2\text{CCl}_2$  and  $\text{HCl}$  are the major products detected below 600 °C. The formation of  $\text{CH}_3\text{CHCl}_2$  as one of the main products at low temperature results from reaction of  $\text{CH}_3\text{CCl}_2$  radical with  $\text{H}_2$ .  $\text{CH}_3\text{CCl}_2$  results from metathetical reaction (abstraction reaction (7)) of  $\text{H}$  with  $\text{CH}_3\text{CCl}_3$  combined with reaction (3).  $\text{H}$  is produced from reaction of  $\text{Cl}$  with  $\text{H}_2$  as follows:



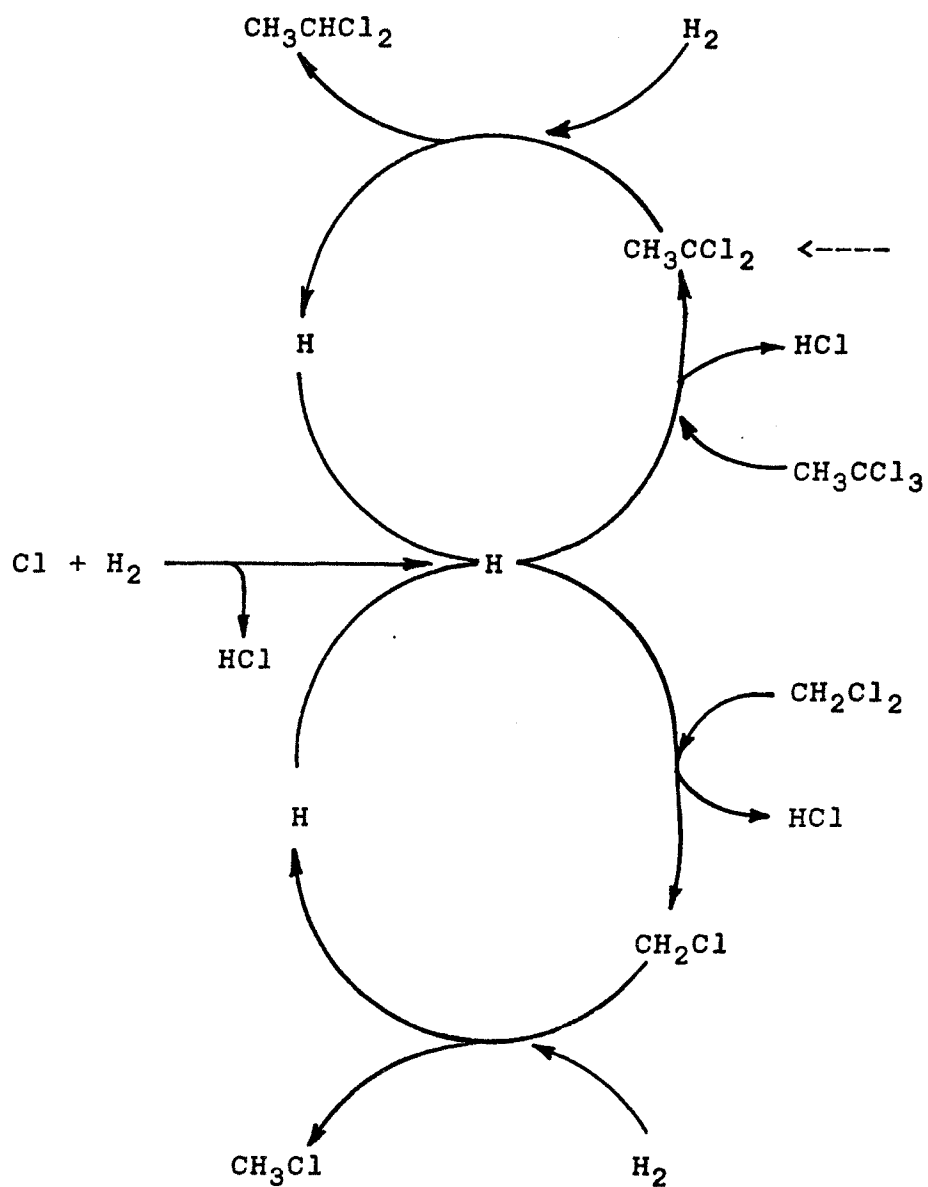
The above three reactions are fast and one sees that  $\text{H}$  radical plays a catalytic role in formation of  $\text{CH}_3\text{CHCl}_2$ .  $\text{CH}_3\text{CHCl}_2$  is one of the major products even though reaction (3) only accounts for ca. 0.1 % of the total  $\text{CH}_3\text{CCl}_3$  decomposition in our low temperature range. In addition,  $\text{CH}_2\text{Cl}_2$  decay below 620 °C is explained by a mechanism similar to formation of  $\text{CH}_3\text{CHCl}_2$ .



The reactions (7 to 10) can be represented in a sort of

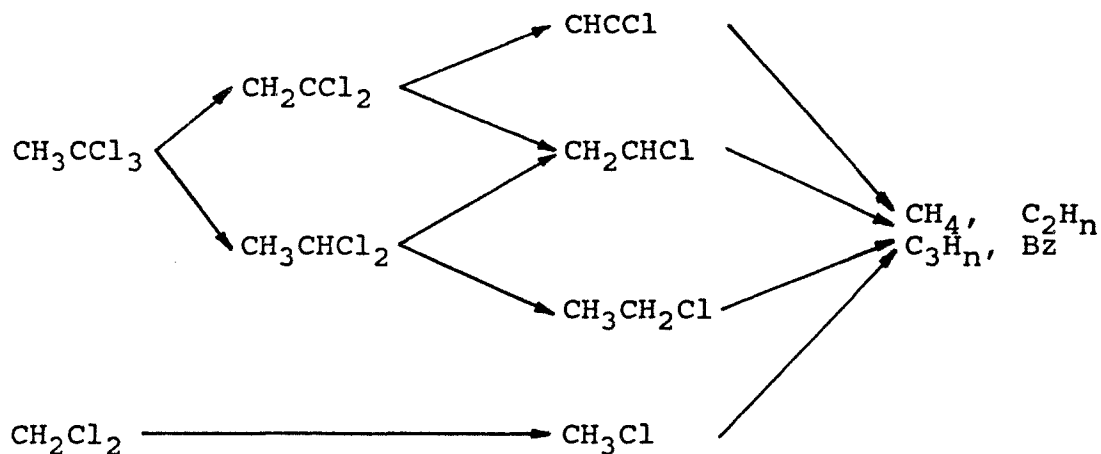
cyclic pathway, Figure 23, driven by unimolecular decomposition reaction (3). Figure 23 illustrated that H atoms react with both reagents  $\text{CH}_3\text{CCl}_3$  and  $\text{CH}_2\text{Cl}_2$  and rapidly form HCl and chlorocarbon radicals. The chlorocarbon radicals then react, rapidly at our temperature with  $\text{H}_2$  bath gas to regenerate H atoms and to produce a chlorocarbon molecule with one less Cl than the parent. This process will continue on both the parent and product chlorocarbons until organic hydrocarbons (and HCl) remain.

Distributions of major products vs temperature are shown in Figure 13. Formation of  $\text{CH}_2\text{CCl}_2$  increases with increasing temperature to a maximum near  $620^\circ\text{C}$  and then drops quickly. Formations of  $\text{CH}_2\text{CHCl}$  and  $\text{CH}_3\text{Cl}$  also shows the same trend, but with maximum around  $720^\circ\text{C}$  and  $810^\circ\text{C}$  respectively. This is consistent with the bond strengths of C-Cl bonds on chlorocarbons which increases with decreasing chlorination<sup><7,37></sup>. The formation of  $\text{CH}_2\text{CCl}_2$  increases proportionally to decrease in  $\text{CH}_3\text{CCl}_3$  in temperature range  $475 - 620^\circ\text{C}$ , strongly demonstrating that  $\text{CH}_2\text{CCl}_2$  is the initial stable product in the thermal unimolecular decomposition of  $\text{CH}_3\text{CCl}_3$  in  $\text{H}_2$ .  $\text{CH}_2\text{CHCl}$  is then produced from further reaction of primary products  $\text{CH}_2\text{CCl}_2$  and  $\text{CH}_3\text{CHCl}_2$  with hydrogen. The overall reaction scheme based on analysis of the major concentration products and thermochemical kinetic estimation can be illustrated as follow:



<----- : addition of CH<sub>3</sub>CCl<sub>2</sub> from CH<sub>3</sub>CCl<sub>3</sub> unimolecular reaction

Figure 23. CH<sub>3</sub>CHCl<sub>2</sub> and CH<sub>3</sub>Cl Formation cycle with H Radical



(plus one HCl from each step). It should be pointed out that this reaction scheme is not a complete detailed mechanism, with the actual mechanism obviously including a significant number of free radical reactions.

#### Mechanism Modeling by CHEMKIN Program

The CHEMKIN computer program package is used in interpreting and integrating the detailed reaction mechanisms (models) of the systems studied. The CHEMKIN program<sup><38></sup>, Figure 24, reads the user's symbolic description of the reaction mechanism. The thermodynamic data base, which has the appropriate thermodynamic information and mass for all species present in mechanism with a format similar to the one used by the NASA complex chemical equilibrium code. The information on the elements, species, and reactions in the mechanism; and finally the CHEMKIN gas phase subroutines, which can be called to return

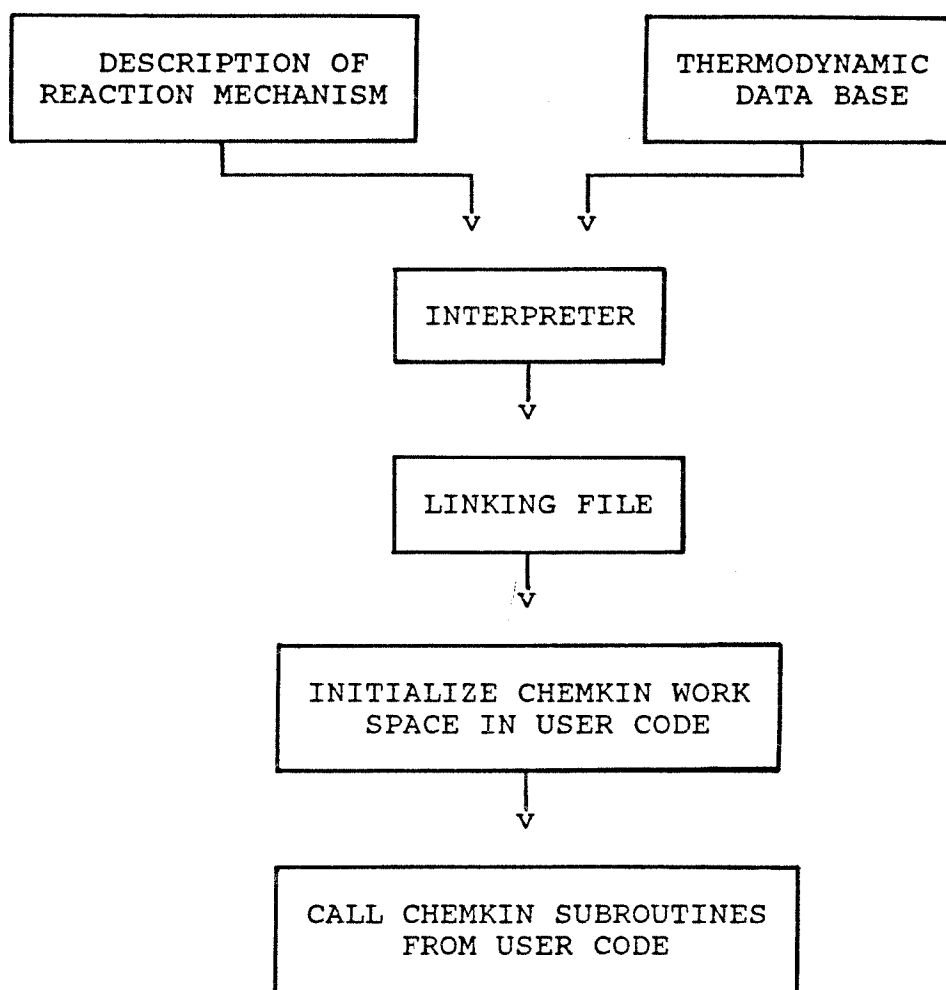


Figure 24. Structure of the CHEMKIN package

information on the elements, species, reactions, equation of state, thermodynamic properties, chemical production rates, and derivatives of thermodynamic properties relative to any time in the integration. Generally the input to these subroutines are the state variables of gas pressure or density, temperature and species composition. All routines can be called with the species composition defined in terms of mass fractions or molar concentrations. Numerical calculations were carried out using the CHEMKIN computer code.

The input data requirement to run CHEMKIN program Include:

- . Detailed reaction mechanism
- . Mole fraction of all gases present in the reaction system
- . Pressure and temperature at which the reaction system being studied
- . Time increment at which the concentration of species present in the system be reported

A thermodynamic data base for species with C/H/Cl elements is developed at NJIT and used for modeling of the kinetic scheme of reaction system investigated. For those species that thermodynamic information were not available in the data base, a thermo data was generated utilizing JANAFIT program. This program requires heat capacities in the temperature range of interest, as input. Heat of formations and entropies, as well as heat capacities, were

calculated by group additivity method of Benson<sup><35></sup> when not available in literature.

This computer work was executed at Digital VAX/VMS 11/785 computer of NJIT.

Detailed reaction kinetic mechanism were developed to describe the systems of reactions studied. A mechanism composed of 94 elementary reactions, which appears in Table 8, were found to fit experimental results.

These kinetic schemes were formulated considering all reaction products detected by GC. Elementary reaction rate parameters for abstraction reactions are based upon literature comparison, thermodynamic estimations and Transition State Theory methods of Benson<sup><35></sup>. QRRK calculations<sup><33,34></sup>, as described in previous section, were used to estimate apparent rate parameters for addition and dissociation reactions (1 atm).

Experimental pyrolysis data are compared with model predictions in Figure 25 for reagent decomposition and product distribution between 475 and 810 °C. Predictions for loss of the two reagents and product distribution match experiment well. Figure 27 demonstrates calculated concentration of parent reactants and products versus reaction time at temperature of 720 °C and shows quite good agreement with the experimentally observed data for decay of reactants and formation of products.

Figure 25 and 27 show the small difference seen between



calculated and experimental values for various species ( reagents and products ). The important reasons for this difference can be explained as following; First, the kinetic scheme does not include all possible products, specifically polyaromatic compound and carbon (solid) production. Second, the detailed mechanism only considers gaseous phase reaction; heterogeneous reaction effects are not included. Finally, the kinetic parameters estimated for several number of elementary reactions incorporated in detailed mechanism, are estimated based on best available thermodynamic and kinetic collision frequency data in literature or for similar reactions. This may produce error when used for our actual reaction conditions.

Table 8

Detailed Mechanism for  $\text{CH}_2\text{Cl}_2/\text{CH}_3\text{CCl}_3/\text{H}_2$  Reaction System

REACTION	A	Ea(Kcal/mol)	source
1. $\text{CH}_3\text{CCl}_3 = \text{CH}_2\text{CCl}_2 + \text{HCl}$	$3.80\text{E}+13^{\#}$ $3.23\text{E}+13^*$	47.9 47.8	a DISSOC
2. $\text{CH}_3\text{CCl}_3 = \text{CH}_3\text{CCl}_2 + \text{Cl}$	$2.40\text{E}+16^{\#}$ $2.80\text{E}+15^*$	73.2 71.0	b DISSOC
3. $\text{CH}_3\text{CCl}_3 = \text{CH}_3 + \text{CCl}_3$	$9.10\text{E}+16^{\#}$ $4.23\text{E}+16^*$	84.7 82.9	c,k DISSOC
4. $\text{CH}_3\text{CHCl}_2 = \text{CH}_2\text{CHCl} + \text{HCl}$	$2.60\text{E}+13^{\#}$ $2.45\text{E}+13^*$	55.8 54.6	d DISSOC
5. $\text{CH}_3\text{CHCl}_2 = \text{CH}_3\text{CHCl} + \text{Cl}$	$7.85\text{E}+15^{\#}$ $3.09\text{E}+15^*$	76.8 76.1	e,k DISSOC
6. $\text{CH}_3\text{CHCl}_2 = \text{CH}_3 + \text{CHCl}_2$	$1.31\text{E}+17^{\#}$ $6.77\text{E}+16^*$	91.6 90.1	c DISSOC
7. $\text{CH}_3\text{CH}_2\text{Cl} = \text{CH}_2\text{CH}_2 + \text{HCl}$	$3.24\text{E}+13^{\#}$ $3.03\text{E}+13^*$	56.6 57.4	f DISSOC
8. $\text{CH}_3\text{CH}_2\text{Cl} = \text{CH}_3\text{CH}_2 + \text{Cl}$	$2.18\text{E}+15^{\#}$ $7.11\text{E}+14^*$	81.5 81.0	g,k DISSOC
9. $\text{CH}_3\text{CH}_2\text{Cl} = \text{CH}_3 + \text{CH}_2\text{Cl}$	$6.84\text{E}+15^{\#}$ $5.81\text{E}+15^*$	89.0 89.5	h DISSOC
10. $\text{CH}_3\text{CH}_3 = \text{CH}_3\text{CH}_2 + \text{H}$	$1.26\text{E}+16^{\#}$ $1.15\text{E}+15^*$	98.0 95.9	i DISSOC
11. $\text{CH}_3\text{CH}_3 = \text{CH}_3 + \text{CH}_3$	$7.94\text{E}+16^{\#}$ $1.59\text{E}+17^*$	89.4 93.5	i DISSOC
12. $\text{CH}_3\text{CCl}_2 = \text{CH}_2\text{CCl}_2 + \text{H}$	$2.60\text{E}+13$	41.4	j
13. $\text{CH}_3\text{CHCl} = \text{CH}_2\text{CHCl} + \text{H}$	$2.76\text{E}+13$	47.3	j
14. $\text{CH}_3\text{CH}_2 = \text{CH}_2\text{CH}_2 + \text{H}$	$5.01\text{E}+13$	40.9	i
15. $\text{CH}_2\text{CH}_2 = \text{CH}_2\text{CH} + \text{H}$	$2.00\text{E}+16$	110.0	i
16. $\text{CH}_2\text{CH} = \text{CHCH} + \text{H}$	$3.16\text{E}+12$	38.3	i

17.	$\text{CH}_3\text{CHCl} + \text{H}_2 = \text{CH}_3\text{CH}_2\text{Cl} + \text{H}$	5.00E+12	17.2	l,k
18.	$\text{CH}_3\text{CCl}_2 + \text{H}_2 = \text{CH}_3\text{CHCl}_2 + \text{H}$	6.26E+12	16.5	m,w
19.	$\text{CH}_3\text{CCl}_3 + \text{H} = \text{CH}_3\text{CCl}_2 + \text{HCl}$	3.00E+13	1.5	n,w
20.	$\text{CH}_3\text{CHCl}_2 + \text{H} = \text{CH}_3\text{CHCl} + \text{HCl}$	2.00E+13	4.0	o,w
21.	$\text{CH}_3\text{CH}_2\text{Cl} + \text{H} = \text{CH}_3\text{CH}_2 + \text{HCl}$	1.50E+13	8.0	p,w
22.	$\text{CH}_2\text{CCl}_2 = \text{CHCCl} + \text{HCl}$	7.10E+13 <sup>#</sup> 2.90E+15 <sup>*</sup>	69.1 80.3	q DISSOC
23.	$\text{CH}_2\text{CCl}_2 = \text{CH}_2\text{CCl} + \text{Cl}$	9.34E+15 <sup>#</sup> 7.85E+14 <sup>*</sup>	88.6 85.9	r,k DISSOC
24.	$\text{CH}_2\text{CHCl} = \text{CHCH} + \text{HCl}$	3.55E+13 <sup>#</sup> 1.76E+15 <sup>*</sup>	68.73 82.9	s DISSOC
25.	$\text{CH}_2\text{CHCl} = \text{CH}_2\text{CH} + \text{Cl}$	4.08E+15 <sup>#</sup> 5.34E+14 <sup>*</sup>	87.6 85.7	t,k DISSOC
26.	$\text{CH}_2\text{CHCl} + \text{H} = \text{CH}_2\text{CH} + \text{HCl}$	1.00E+13	6.5	l
27.	$\text{CH}_2\text{CCl}_2 + \text{H} = \text{CH}_2\text{CCl} + \text{HCl}$	1.20E+13	5.5	u
28.	$\text{CH}_2\text{CCl} + \text{H}_2 = \text{CH}_2\text{CHCl} + \text{H}$	6.16E+11	6.0	v
29.	$\text{CH}_3\text{CH}_3 + \text{H} = \text{CH}_3\text{CH}_2 + \text{H}_2$	6.61E+13	9.7	w
30.	$\text{CH}_2\text{CH}_2 + \text{H} = \text{CH}_2\text{CH} + \text{H}_2$	1.91E+13	10.3	w
31.	$\text{CHCH} + \text{H} = \text{CHC} + \text{H}_2$	2.00E+14	19.0	w
32.	$\text{CH}_2\text{Cl}_2 = \text{CHCl} + \text{HCl}$	1.20E+14	105.0	x
33.	$\text{CH}_2\text{Cl}_2 = \text{CH}_2\text{Cl} + \text{Cl}$	1.06E+16 <sup>#</sup> 2.39E+14 <sup>*</sup>	82.8 78.2	y,k DISSOC
34.	$\text{CH}_3\text{Cl} = \text{CH}_2 + \text{HCl}$	9.30E+13	130.9	z
35.	$\text{CH}_3\text{Cl} = \text{CH}_3 + \text{Cl}$	2.63E+15 <sup>#</sup> 1.27E+14 <sup>*</sup>	83.3 79.7	1,k DISSOC
36.	$\text{CH}_4 = \text{CH}_3 + \text{H}$	1.00E+16 <sup>#</sup> 2.48E+14 <sup>*</sup>	105.0 102.0	i DISSOC
37.	$\text{CH}_2\text{Cl}_2 + \text{H} = \text{CH}_2\text{Cl} + \text{HCl}$	1.10E+13	6.1	w
38.	$\text{CH}_3\text{Cl} + \text{H} = \text{CH}_3 + \text{HCl}$	3.72E+13	9.3	w
39.	$\text{CH}_4 + \text{H} = \text{CH}_3 + \text{H}_2$	5.00E+12	11.0	w

40.	$\text{CH}_2\text{Cl} + \text{H}_2 = \text{CH}_3\text{Cl} + \text{H}$	2.86E+12	14.0	2,w
41.	$\text{CHCH} + \text{H} = \text{CHC} + \text{H}_2$	3.10E+13	3.7	w
42.	$\text{CH}_3\text{CCl}_3 + \text{Cl} = \text{CH}_2\text{CCl}_3 + \text{HCl}$	2.51E+12	3.6	w
43.	$\text{CH}_2\text{CCl}_3 = \text{CH}_2\text{CCl}_2 + \text{Cl}$	1.35E+14	19.0	3,w
44.	$\text{CH}_2\text{Cl}_2 + \text{Cl} = \text{CHCl}_2 + \text{HCl}$	5.03E+13	2.9	w
45.	$\text{CH}_3\text{Cl} + \text{Cl} = \text{CH}_2\text{Cl} + \text{HCl}$	1.29E+14	3.6	w
46.	$\text{CH}_3 + \text{CH}_2\text{Cl}_2 = \text{CH}_4 + \text{CHCl}_2$	6.76E+10	7.2	w
47.	$\text{CH}_3 + \text{CH}_2\text{Cl}_2 = \text{CH}_3\text{Cl} + \text{CH}_2\text{Cl}$	1.40E+11	4.9	w
48.	$\text{CH}_3 + \text{CH}_3\text{Cl} = \text{CH}_4 + \text{CH}_2\text{Cl}$	3.30E+11	9.4	w
49.	$\text{CCl}_3 + \text{H}_2 = \text{CHCl}_3 + \text{H}$	5.37E+12	14.3	w
50.	$\text{CHCl}_3 = \text{CHCl}_2 + \text{Cl}$	2.52E+16 <sup>#</sup> 2.21E+14 <sup>*</sup>	78.8 72.2	4,k DISSOC
51.	$\text{CHCl}_2 + \text{H}_2 = \text{CH}_2\text{Cl}_2 + \text{H}$	4.12E+12	3.5	2,w
52.	$\text{C}_2\text{H}_5 + \text{CH}_2\text{Cl}_2 = \text{C}_2\text{H}_5\text{Cl} + \text{CH}_2\text{Cl}$	2.80E+11	7.0	5
53.	$\text{CH}_3\text{CH}_2\text{CH}_2 = \text{CH}_3 + \text{CH}_2\text{CH}_2$	1.00E+13	32.9	i
54.	$\text{CH}_3\text{CH}_2\text{CH}_2 = \text{CH}_3\text{CHCH}_2 + \text{H}$	1.26E+13	38.5	i
55.	$\text{CH}_2\text{CHCH}_2 = \text{CH}_2\text{CCH}_2 + \text{H}$	1.26E+13	61.3	i
56.	$\text{CH}_3\text{CH}_2\text{CH}_2\text{CH}_3 = 2\text{CH}_3\text{CH}_2$	8.00E+16	81.9	i
57.	$\text{CH}_2\text{CCl}_2 + \text{H} = \text{CH}_2\text{CHCl}_2$	2.67E+09 <sup>*</sup>	-4.7	QRRK 1
58.	$\text{CH}_2\text{CCl}_2 + \text{H} = \text{CH}_2\text{CHCl} + \text{Cl}$	6.02E+13 <sup>*</sup>	3.0	QRRK 1
59.	$\text{CH}_2\text{CCl} + \text{H} = \text{CH}_2\text{CHCl}$	1.80E+10 <sup>*</sup>	-7.0	QRRK 2
60.	$\text{CH}_2\text{CCl} + \text{H} = \text{CH}_2\text{CH} + \text{Cl}$	1.02E+14 <sup>*</sup>	0.1	QRRK 2
61.	$\text{CH}_2\text{CCl} + \text{H} = \text{CHCH} + \text{HCl}$	8.31E+11 <sup>*</sup>	-2.1	QRRK 2
62.	$\text{CH}_2\text{CHCl} + \text{H} = \text{CH}_2\text{CH}_2\text{Cl}$	1.39E+10 <sup>*</sup>	-2.4	QRRK 3
63.	$\text{CH}_2\text{CHCl} + \text{H} = \text{CH}_2\text{CH}_2 + \text{Cl}$	8.51E+12 <sup>*</sup>	3.5	QRRK 3
64.	$\text{CH}_3 + \text{CH}_3\text{CH}_2 = \text{C}_3\text{H}_8$	6.52E+12 <sup>*</sup>	-0.7	QRRK 4

65.	$\text{CH}_3 + \text{CH}_3\text{CH}_2 = \text{CH}_3\text{CH}_2\text{CH}_2 + \text{H}$	$1.16\text{E}+14^*$	25.2	QRRK 4
66.	$\text{CH}_3 + \text{CHCH}_2 = \text{C}_3\text{H}_6$	$1.15\text{E}+13^*$	-0.7	QRRK 5
67.	$\text{CH}_3 + \text{CHCH}_2 = \text{CH}_2\text{CHCH}_2 + \text{H}$	$9.80\text{E}+13^*$	13.7	QRRK 5
68.	$\text{CH}_3 + \text{CCH} = \text{CH}_3\text{CCH}$	$2.11\text{E}+11^*$	-3.9	QRRK 6
69.	$\text{CH}_3 + \text{CCH} = \text{CH}_2\text{CCH} + \text{H}$	$1.24\text{E}+13^*$	4.2	QRRK 6
70.	$\text{CH}_3\text{CCl}_2 + \text{H} = \text{CH}_3\text{CHCl}_2$	$2.54\text{E}+11^*$	-6.1	QRRK 7
71.	$\text{CH}_3\text{CCl}_2 + \text{H} = \text{CH}_2\text{CHCl} + \text{HCl}$	$7.50\text{E}+12^*$	0.7	QRRK 7
72.	$\text{CH}_3\text{CCl}_2 + \text{H} = \text{CH}_3\text{CHCl} + \text{Cl}$	$7.92\text{E}+13^*$	4.6	QRRK 7
73.	$\text{CH}_3\text{CHCl} + \text{H} = \text{CH}_3\text{CH}_2\text{Cl}$	$1.30\text{E}+12^*$	-4.2	QRRK 8
74.	$\text{CH}_3\text{CHCl} + \text{H} = \text{CH}_2\text{CH}_2 + \text{HCl}$	$5.12\text{E}+13^*$	2.7	QRRK 8
75.	$\text{CH}_3\text{CHCl} + \text{H} = \text{CH}_3\text{CH}_2 + \text{Cl}$	$7.64\text{E}+14^*$	7.8	QRRK 8
76.	$\text{CH}_3\text{CH}_2 + \text{H} = \text{CH}_3 + \text{CH}_3$	$7.65\text{E}+14^*$	4.1	QRRK 9
77.	$\text{CH}_2\text{Cl} + \text{CH}_2\text{Cl} = \text{CH}_2\text{ClCH}_2\text{Cl}$	$1.34\text{E}+11^*$	-5.0	QRRK 10
78.	$\text{CH}_2\text{Cl} + \text{CH}_2\text{Cl} = \text{CH}_2\text{CHCl} + \text{HCl}$	$2.51\text{E}+12^*$	1.6	QRRK 10
79.	$\text{CH}_2\text{Cl} + \text{CH}_2\text{Cl} = \text{CH}_2\text{ClCH}_2 + \text{Cl}$	$7.37\text{E}+12^*$	6.5	QRRK 10
80.	$\text{CH}_2\text{Cl} + \text{CH}_3 = \text{CH}_2\text{CH}_2 + \text{HCl}$	$1.67\text{E}+13^*$	2.5	QRRK 11
81.	$\text{CH}_2\text{Cl} + \text{CH}_3 = \text{CH}_3\text{CH}_2 + \text{Cl}$	$1.76\text{E}+12^*$	7.9	QRRK 11
82.	$\text{CH}_2\text{Cl} + \text{CHCl}_2 = \text{CH}_2\text{ClCHCl}_2$	$4.88\text{E}+11^*$	-4.4	QRRK 12
83.	$\text{CH}_2\text{Cl} + \text{CHCl}_2 = \text{CH}_2\text{CCl}_2 + \text{HCl}$	$4.81\text{E}+10^*$	4.1	QRRK 12
84.	$\text{CH}_2\text{Cl} + \text{CHCl}_2 = \text{CHClCHCl} + \text{HCl}$	$1.84\text{E}+11^*$	4.1	QRRK 12
85.	$\text{CH}_2\text{ClCH}_2 + \text{H}_2 = \text{CH}_3\text{CH}_2\text{Cl} + \text{H}$	$4.00\text{E}+12$	15.7	6,1
86.	$\text{CHCl}_2\text{CH}_2 + \text{H}_2 = \text{CH}_3\text{CHCl}_2 + \text{H}$	$5.26\text{E}+12$	15.0	7
87.	$\text{CH}_3\text{CH}_2\text{CH}_2 + \text{H}_2 = \text{C}_3\text{H}_8 + \text{H}$	$2.63\text{E}+12$	14.8	w
88.	$\text{C}_3\text{H}_6 + \text{H} = \text{CH}_2\text{CHCH}_2 + \text{H}_2$	$2.80\text{E}+12$	1.1	w
89.	$\text{C}_4\text{H}_{10} = \text{C}_3\text{H}_7 + \text{CH}_3$	$1.00\text{E}+17$	84.7	i
90.	$\text{H}_2 = \text{H} + \text{H}$	$5.26\text{E}+08$	105.0	8

91.	$\text{Cl}_2 = \text{Cl} + \text{Cl}$	7.69E+08	55.6	8
92.	$\text{HCl} = \text{H} + \text{Cl}$	6.09E+08	97.3	8
93.	$\text{Cl} + \text{H}_2 = \text{HCl} + \text{H}$	4.80E+13	1.3	w,8
94.	$\text{H} + \text{Cl}_2 = \text{HCl} + \text{Cl}$	4.57E+12	1.4	w,8

# High pressure limit value

\* Pressure dependent : rate expression given for 760 torr  
Temperature range : 773 - 1273 ° K

DISSOC : apparent rate constant by DISSOCIATION computer code analysis

QRRK : apparent rate constant by QRRK computer code analysis

#### SOURCES

- $A = 10^{13.55} * 10^{(-4/4.6)} * 9$   
 $E_a = 47.9 (\Delta H_r + 38)$  (ref: Bamford, D.H. and Tipper, C.F., Comprehensive Chemical Kinetics, Vol.5 1972)
- A factor based upon entropy change for reverse.  
 $A_{-1}$  taken as that for  $\text{CH}_3\text{CCl}_2 + \text{Cl} = \text{CH}_3\text{CCl}_3$  ( $A = 3.0 \text{ E}+13$ )  
 $E_a = \Delta H_r$
- A factor based upon entropy change for reverse.  
 $A_{-1}$  taken as that for  $\text{CH}_3 + 1\text{-C}_4\text{H}_9$  ( $A = 2.0 \text{ E}+13$ )  
 $E_a = \Delta H_r$
- $A = 10^{13.55} * 10^{(-4/4.6)} * 6$   
 $E_a = \Delta H_r + 38.5$
- A factor based upon entropy change for reverse.  
 $A_{-1}$  taken as that for  $1\text{-C}_3\text{H}_7 + \text{CH}_3$  ( $A = 2.0\text{E}+13$ )  
 $E_a = \Delta H_r$
- $E_a = \Delta H_r + 39.4$   
Benson, S.W., "Thermochemical Kinetics", 2nd ed., John Wiley & Son, (1976)
- A factor based upon  $\Delta S$  for reverse  
 $A_{-1}$  taken as that for  $\text{C}_2\text{H}_5 + \text{CH}_3$  ( $A = 2.0 \text{ E}+13$ )  
 $E_a = \Delta H_r$

- h. A factor based upon entropy change for reverse.  
 $A_{-1}$  taken as that for  $\text{CH}_3 + \text{CH}_3\text{CH}_2$  ( $A = 2.0\text{E}+13$  and  $E_a = 0$ )  
 $E_a = \Delta H_r$
- i. Dean, A.M., J. Phys. Chem., 89, 4600, 1985
- j. A factor based upon entropy change for reverse.  
 $A_{-1}$  taken as that for  $\text{CH}_3\text{CCl}_2 = \text{CH}_2\text{CCl}_2 + \text{H}$  ( $A = 1.6\text{E}+13$ )  
 $E_a = \Delta H_r + 2.0$
- k. Allara, D.L. and Shaw, R., J. Phys. Chem. Ref. Data, 9, 523, 1980
- l. Barat, R.B. and Bozzelli, J.W., "Reaction of Atomic Hydrogen with Vinyl Chloride", submitted to J. Phys. Chem. (1988)  
 (A factor taken that for  $2\text{-C}_4\text{H}_9 + \text{H}_2$ )
- m.  $A = A_{17} + \Delta A$        $\Delta A = A_{\text{CHCl}_2+\text{H}_2} - A_{\text{CH}_2\text{Cl}+\text{H}_2}$   
 ( $A_{\text{CHCl}_2+\text{H}_2}$  and  $A_{\text{CH}_2\text{Cl}+\text{H}_2}$  from source No.2)  
 $E_a$  from "Evans-Polanyi" plot  
 ("Evans-Polanyi" plot for a set of abstraction reaction.  
 This is a plot of  $E_a$  versus  $\Delta H_r$  from similar reactions using data of w. After completing the plot obtain the best slope and put into form of general equation for determination of  $E_a$  knowing only  $\Delta H_r$ .)
- n. A factor taken as that for  $\text{CH}_3\text{Cl} + \text{H} = \text{CH}_3 + \text{HCl}$   
 $E_a$  from "Evans-Polanyi" plot
- o. A factor taken as 2/3 that for  $\text{CH}_3\text{Cl} + \text{H} = \text{CH}_3 + \text{HCl}$   
 $E_a$  from "Evans-Polanyi" plot
- p. A factor taken as 1/2 that for  $\text{CH}_3\text{Cl} + \text{H} = \text{CH}_3 + \text{HCl}$   
 $E_a$  from "Evans-Polanyi" plot
- q.  $A = 10^{13.55} * 2$   
 $E_a = \Delta H_r + 45$  (ref: Skinner)
- r. A factor based upon entropy change for reverse.  
 $A_{-1}$  taken as that for  $2\text{-C}_4\text{H}_9 + \text{CH}_3$  ( $A = 1.6 \text{E}+13$ )  
 $E_a = \Delta H_r$
- s.  $A = 10^{13.55} * 1$   
 $E_a = \Delta H_r + 45$  (ref: Zabel, F., Int. J. Chem. Kinetics, 9, 651, 1977)
- t. A factor based upon  $\Delta S$  for reverse.  
 $A_{-1}$  taken as that for  $\text{C}_2\text{H}_5 + \text{CH}_3$  ( $A = 2.0 \text{E}+13$ )  
 $E_a = \Delta H_r$
- u. A factor taken as 1.2 that for reaction (26)

- v. A factor taken as 1.5 that for reverse reaction (30) with  
 $A = 4.1 \text{ E}+11$
- w. Kerr, J.A. and Moss, S.J., "Handbook of Bimolecular and Termolecular Gas Reaction, Vol.I & II", CRC Press Inc., 1981
- x.  $A = 10^{13.55} * 4$ ,  $E_a = \Delta H_r + 40$  (ref: Setser, D.W. and Lee, T., Am. Chem. Soc., 89, 5799, 1985)
- y. A based upon  $\Delta S$  for reverse.  
 $A_{-1}$  taken as that for  $C_2H_5 + CH_3$  ( $A = 2.0 \text{ E}+13$ )  
 $E_a = \Delta H_r$
- z.  $A = 10^{13.55} * 3$   
 $E_a = \Delta H_r + 40$  (ref: same with x)
1. A based upon  $\Delta S$  for reverse.  
 $A_{-1}$  taken as that for  $CH_3 + CH_3$  ( $A = 2.5 \text{ E}+13$ )  
 $E_a = \Delta H_r$
2. A factor taken as that for interpolation between  $CH_3+H_2$  ( $1.6 \text{ E}+12$ ) and  $CCl_3 + H_2$  ( $5.37 \text{ E}+12$ ) with chlorine number  
 $E_a$  from "Evans-Polanyi" plot
3. A factor based upon entropy change for reverse.  
 $A_{-1}$  taken as that for  $C_2H_3Cl + Cl$  ( $A = 2.0 \text{ E}+13$ )  
 $E_a = \Delta H_r + 1.5$
4. A factor based upon entropy change for reverse.  
 $A_{-1}$  taken as that for  $2-C_3H_7 + CH_3$  ( $A = 1.6 \text{ E}+13$ )
5. A factor taken as 2 that for reaction (47)
6. A factor taken as that for reaction  $1-C_4H_9 + H_2$
7.  $A = A_{85} + \Delta A$      $\Delta A = A_{CHCl_2+H_2} - A_{CH_2Cl+H_2}$
8. Ritter, E., Bozzelli, J.W. and Dean, A.M.'s paper accepted in J. Phys. Chem. (1988)

#### References of Thermochemical Properties

- <1> JANAF Thermochemical Tables issued as supplement No.1, Vol.14, (1985) J. Phys. Chem. Ref. Data
- <2> Wagman, D.D. and Evans, W.H., The NBS Tables of Chemical Thermodynamic Properties, J. Phys. Chem. Ref. Data, Vol.11 (1982)



- <3> Pedley, J.B., Naylor, R.D. and Kirby, S.P., "Thermochemical Data of Organic Compounds", 2nd ed., Chapman and Hall, NY (1986)
- <4> Stull, D.R., Westrum, E.F. and Sinke, G.C., "The Chemical Thermodynamic of Organic Compounds", Robert Krieger Publishing Co. FL (1987)
- <5> Benson, S.W., "Thermochemical Kinetics", 2nd ed. John Wiley & Son, NY (1976)
- <6> Allara, D.L. and Shaw, R., J. Phys. Chem. Ref. Data, Vol.9, 523 (1980)
- <7> Ritter, E. and Bozzelli, J.W., "Thermochemical Estimation of Molecule and Radical", computer code submitted to J. Phys. Chem. Ref. Data for publication

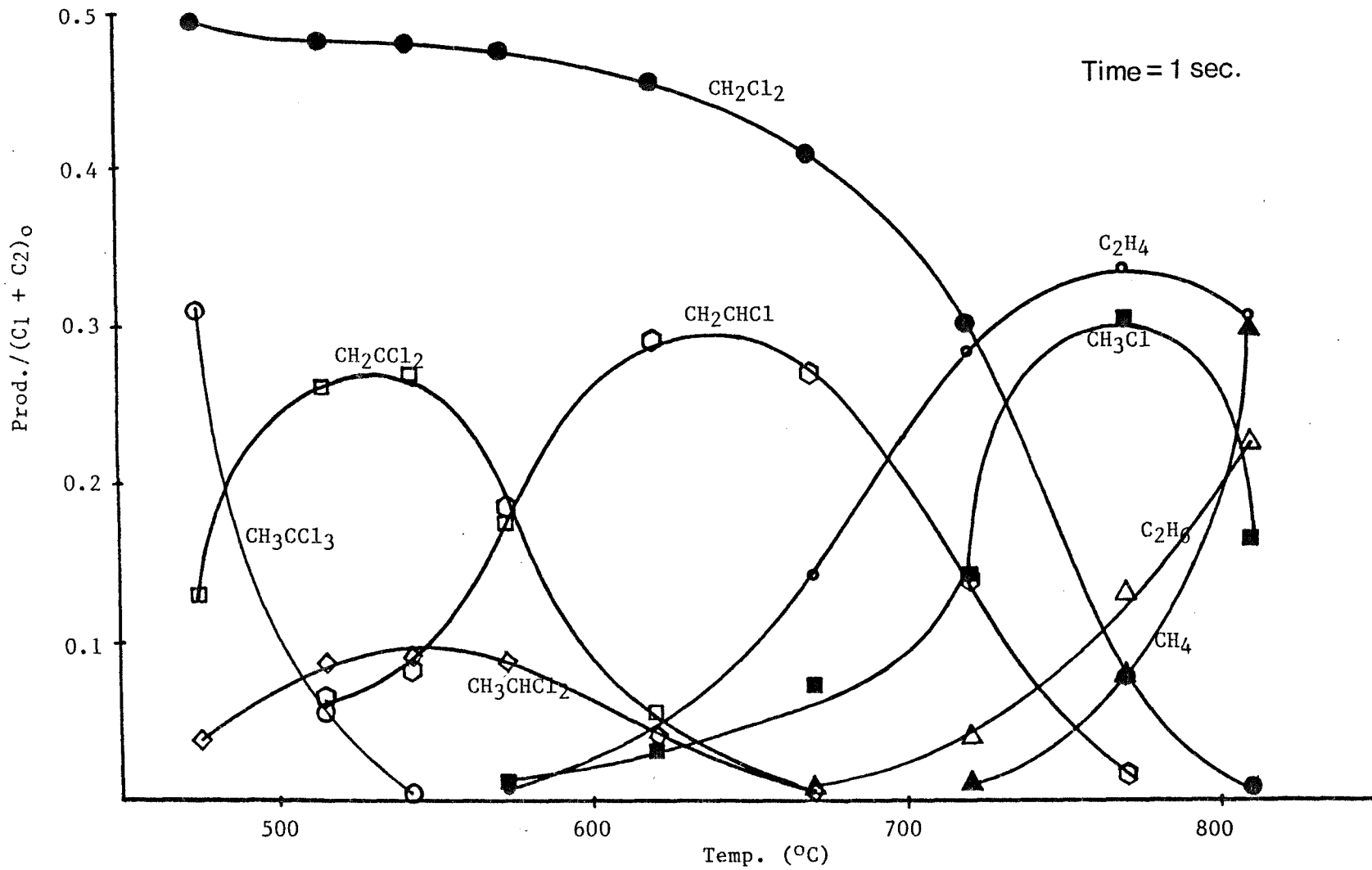


Figure 25. Model Prediction: Product Distribution vs Temperature

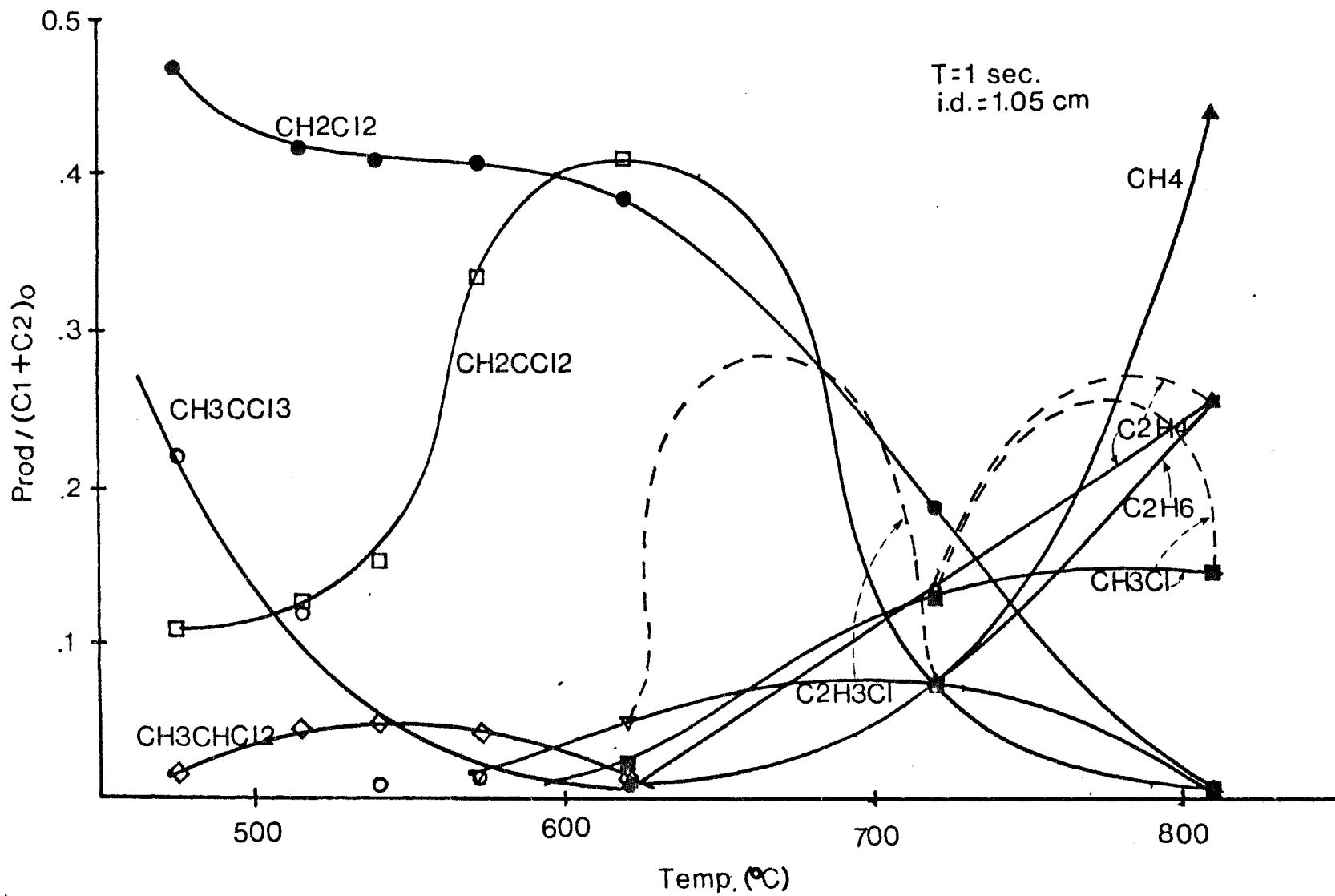


Figure 26. Modified Experimental Product Distribution vs. Temp.  
 (dash lines based on the model prediction results)

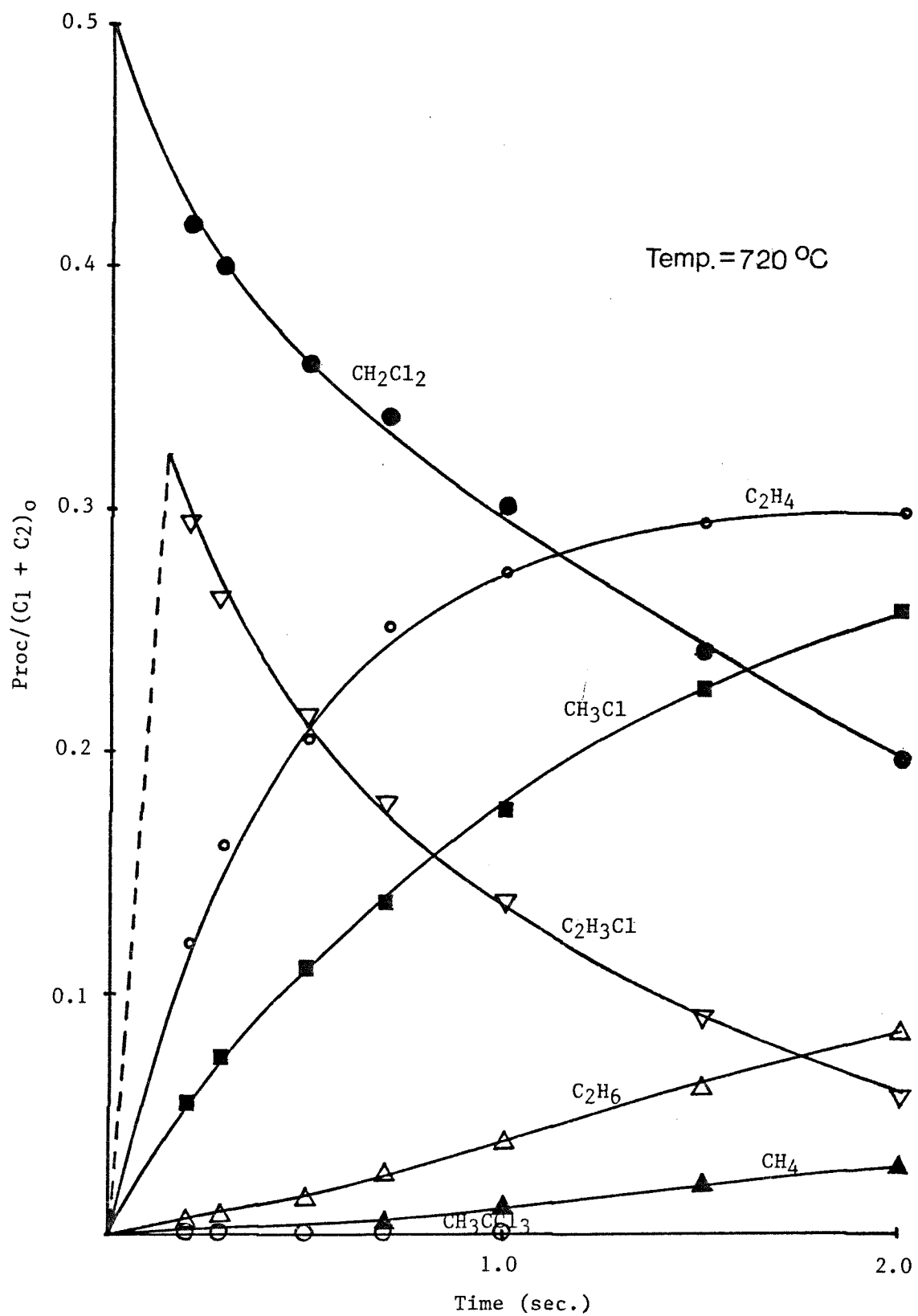


Figure 27. Model Prediction: Product Distribution vs Time

## VI. CONCLUSION

The decomposition of dichloromethane/1,1,1-trichloroethane mixture in a hydrogen bath gas was carried out at 1 atmosphere total pressure in a tubular flow reactor. Temperature ranged from 475 - 810 °C; and residence times studied were in the range from 0.02 - 2.0 seconds.

Complete decay ( 99 % ) occurs at about 810 oC for dichloromethane and around 572 °C for 1,1,1-trichloroethane at 1 second residence time. The number and quantity of chlorinated products decrease with increasing temperature and residence time, with HCl formation decreasing. The major products at our high temperature ranges (above 720 °C) were HCl and non-chlorinated hydrocarbons: methane, ethylene and ethane. The most thermodynamically stable ( resistant to reaction ) chlorocarbon product observed in this system was methyl chloride with excess hydrocarbon.

An increase in surface to volume ratio of reactor tube was observed to accelerate the decomposition process in hydrogen bath, but it had no effect on distribution of principal products.

This study demonstrated that selective formation of HCl can result from thermal reaction of chlorocarbon mixture and showed that synergistic effects of 1,1,1-trichloroethane decomposition accelerate the rate of dichloromethane

decomposition. There is strong interaction of decay products from 1,1,1-trichloroethane with parent dichloromethane.

Decoupling of the wall and bulk reaction constant was achieved by the assuming plug flow reactor condition (Kaufman) and pseudo 1st order reactions prevail. Apparent bulk activation energies were estimated to be 32 Kcal/mol for 1,1,1-trichloroethane and 36 Kcal/mol for dichloromethane with hydrogen in the mixture reaction system. 1,1,1-trichloroethane apparent bulk activation energy is close to that of pure compound reaction. But dichloromethane apparent bulk activation energy is 39 % smaller than that of pure dichloromethane. This suggests that radicals which are more easily produced from 1,1,1-trichloroethane decomposition initiate dichloromethane decomposition. These radical reactions decrease the dichloromethane activation energy similar to the role of a catalyst.

A detailed kinetic reaction mechanism was developed and used to model result obtained from the experimental reaction system. The kinetic reaction mechanism includes 94 elementary reaction steps involving stable compounds and free radical species with the addition, beta scission and recombination type reactions all analyzed by Quantum RRK theory.

## VII. REFERENCES

- <1> Gerber, C.R., J. Air Pollut. Cont. Assoc., 35, 749 (1985)
- <2> Mason, L. and Unget, S., U.S. EPA 600/2.79.198, NTIS 80-131964 (1979)
- <3> Chuang, S.C. and Bozzelli, J.W., Environ. Sci. Tech., 20, 568 (1986)
- <4> Graham, J.L., Hall, D.L. and Dellinger, B., Environ. Sci. Tech., 20, 703 (1986)
- <5> Barton, D.H.R. and Onyon, P.F., J. Am. Chem. Soc. 72, 988 (1950)
- <6> Manion, J.A., Mulder, P. and Louw, R., Environ. Sci. Tech., 19, 280 (1969)
- <7> Chuang, S.C. and Bozzelli, J.W., Ind. Eng. Chem. Pro. Des. Dev., 25, 317 (1986)
- <8> Tavakoli, J. and Bozzelli J.W., Paper presented at the Central States Technology Meeting, The combustion Institute, Argonne, IL, May 11 - 12 (1987)
- <9> C & EN, 26, Aug. 17 (1987)
- <10> Chuang, S.C., M.Sc. Thesis, New Jersey Institute of Technology (1982)
- <11> Chang, S.H., Doctoral Dissertation, New Jersey Institute of Technology (1985)
- <12> Mahmood, M., M.Sc. Thesis, NJIT (1985)
- <13> Lee, W.L., M.Sc. Thesis, NJIT (1986)
- <14> Ritter, E.R., M.Sc. Thesis, NJIT (1986)

- <15> Tsao, H., M.Sc. Thesis, NJIT (1987)
- <16> Hung, M., M.Sc. Thesis, NJIT (1987)
- <17> Huang, S.H., M.Sc. Thesis. NJIT (1987)
- <18> Chang, S.H. and Bozzelli, J.W., *AIChE J.*, 33, 1207 (1987)
- <19> Benson, S.W. and Spokes, G.N., *Symp. Comb.*, 11, 95 (1966)
- <20> Smith, J.M., *Chemical Engineering Kinetics*, 3rd ed., Mc Graw Hill, NY (1981)
- <21> Levenspiel, O., *Chemical Reaction Engineering*, 2nd ed., John Wiley & Son Inc., NY (1962)
- <22> Reman, G.H., *Chem. & Ind.*, 46 (1955)
- <23> Cremer, H.W. and Watkins, S.B., *Chemical Engineering Practice*, Vol. 8, Butterworth, London (1965)
- <24> Butt, J.B., *Reaction kinetics and Reactor Design*, Prentice Hall (1980)
- <25> Poirier, R.V. and Carr, R.W., *J. Phys. Chem.*, 74, 1593, (1971)
- <26> Kaufman, F. ,*Progress in Reaction Kinetics*, Vol.VI, Pergamon Press, NY (1961)
- <27> Dean, A.M. ,*J. Phys. Chem.*, 89, 4600 (1985)
- <28> Leathard, D.A. and Shwrlock ,*Indentification Techniques in Gas Chromatography*, Wiley, NY (1970)
- <29> Bamford, D.H. and Tipper, C.F. ,*Comprehesive Chemical Kinetics*, Vol.5, Elsevier Publishing Co. (1972)
- <30>McMillen, D.and Golden, D., *Annual Review Physical*



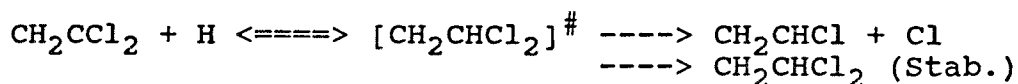
- Chemistry, 33, 493 (1982)
- <31> Tschuikow, R.E. and Paddison, S., Int. J. Chem. Kin.,  
19, 15 (1987)
- <32> Viek, P.S., Chember, L.E. and Wosbcke, H.N., Advances  
in Chemical Series 131
- <33> Westmoreland, P.R. and Dean, A.M., AIChE J., 32, 171  
(1986)
- <34> Ritter, E, and Bozzelli, J.W. and Dean, A.M.'s paper  
Accepted in J. Phys. Chem. (1988)
- <35> Benson, S.W., Thermochemical Kinetics, 2nd ed. Wiley, NY  
(1976)
- <36> Setser, D.W. and Lee, T., Am. Chem. Soc., 89, 5799  
(1985)
- <37> Darwent, B. deB., U.S. Department of commerce, NBS  
NSRDS-31 (1971)
- <38> Kee, R.J., Miller, T.H. and Jefferson, T.H., CHEMKIN: A  
General-Purpose, Problem-Independent, Transportable,  
Fortran Chemical Kinetics Code Package, SANDIA (1980)

## APPENDIX

1. GISOQRRK INPUT DATA and CALCULATION RESULTS
2. ENERGY BALANCE CALCULATION

## APPENDIX 1. GISOQRRK INPUT DATA and CALCULATION RESULTS

Table 1-a



k	A	Ea	source
1	6.0 E+13	3.0	a
-1	1.1 E+14	39.9	a
2	4.0 E+14	22.9	b
<v> = 736/cm			c
Lennard-Jones Parameters :			d
sigma = 5.103 °A		e/k = 435.91 cal	

a

A factor taken as that for C<sub>2</sub>H<sub>4</sub> + H (A=6.0 E+13)  
(ref: Kerr, J.A. and Moss, S.J., "Handbook of Bimolecular  
and Termolecular Gas Reaction Vol.I & II", CRC Press inc.,  
1981)

b

based upon (del S) for CH<sub>2</sub>CH<sub>2</sub> + Cl = CH<sub>2</sub>CH<sub>2</sub>Cl  
with A<sub>-2</sub> = 1.8 E+13 cc/mol sec ( Ref: Kerr )

c

Shimanouchi, T., Tables of Molecular Vibration Frequencies  
Consolidated Vol.I, Natl. Stand. Ref. Data Ser. (U.S. Natl.  
Bur. Stand.) 1972, NSRDS-NBS 39. (refer to CH<sub>2</sub>ClCHCl)

d

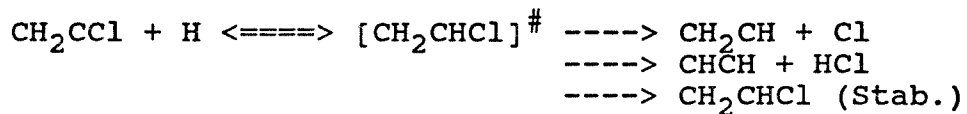
Activated complex L-J parameters are estimated using  
critical property data tabulated in Reid, Prausnitz and  
Sherwood (The Properties and Gases and Liquids, 3rd ed.)

Table 1-b

APPARENT REACTION RATE CONSTANTS PREDICTED  
 USING BIMOLECULAR QRRK ANALYSIS

P (torr)	Reaction	A (cc/mol s)	Ea (Kcal/mol)
7.6	$\text{CH}_2\text{CCl}_2 + \text{H} = \text{CH}_2\text{CHCl}_2$	2.64 E+07	-4.71
76.0		2.64 E+08	-4.70
760.0		2.67 E+09	-4.68
7.6	$\text{CH}_2\text{CCl}_2 + \text{H} = \text{CH}_2\text{CHCl} + \text{Cl}$	5.97 E+13	2.99
76.0		5.98 E+13	2.99
760.0		6.02 E+13	3.01

Table 2-a



k	A	Ea	source
1	1.0 E+14	0.0	a
-1	3.0 E+15	104.1	a
2	7.9 E+16	87.6	b
3	3.6 E+13	68.7	c
$\langle v \rangle = 1344.3/\text{cm}$			d
LJ Parameters :			e
$\text{sigma} = 4.644 \text{ \AA}^\circ$		$e/k = 349 \text{ cal}$	

a

A factor taken as that for  $\text{H} + 2\text{-C}_4\text{H}_9$   
 $A_{-1}$  based upon entropy change for reverse.  
 (ref: Allara, D.L. and Shaw, R., J. Phys. Chem. Ref. Data,  
 9, 523, 1980)

b

A factor based upon entropy change for reverse.  
 $\text{CH}_2\text{CH} + \text{CH}_3 = \text{CH}_2\text{CHCH}_3$  with  $A = 1.8 \text{ E}+13$  and  $E_a = 0.0$   
 (ref: Dean, A.M., J. Phys. Chem., 89, 4600, 1985)

c

$A = 10^{13.55} * 1$   
 $E_a = \Delta H_r + 45$  (ref: Zabel, F., Int. Che. Kineticb, 9, 651,  
 1977)

d

see note (c) Table 1-a.  
 Geometric mean frequency estimated as follows:  
 $\langle v \rangle_{\text{CH}_2\text{CHCl}} = \langle v \rangle_{\text{CH}_2\text{CH}_2} - \frac{\Delta \langle v \rangle}{2}$   
 $\Delta \langle v \rangle = \langle v \rangle_{\text{CH}_3\text{CH}_3} - \langle v \rangle_{\text{CH}_3\text{CH}_2\text{Cl}}$

e

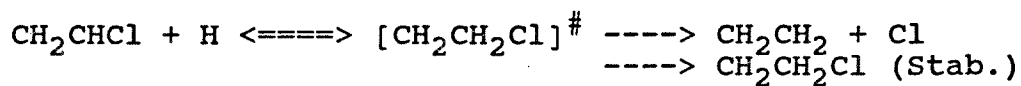
see note (d) Table 1-a

Table 2-b

APPARENT REACTION RATE CONSTANTS PREDICTED  
USING BIMOLECULAR QRRK ANALYSIS

P (torr)	Reaction	A (cc/mol s)	Ea (Kcal/mol)
7.6	$\text{CH}_2\text{CCl} + \text{H} = \text{CH}_2\text{CHCl}$	1.78 E+08	-7.09
76.0		1.77 E+09	-7.08
760.0		1.80 E+10	-7.03
7.6	$\text{CH}_2\text{CCl} + = \text{CH}_2\text{CH} + \text{Cl}$	1.00 E+14	0.05
76.0		1.00 E+14	0.06
760.0		1.02 E+14	0.11
7.6	$\text{CH}_2\text{CCl} + \text{H} = \text{CHCH} + \text{HCl}$	8.15 E+11	-2.16
76.0		8.16 E+11	-2.16
760.0		8.31 E+11	-2.11

Table 3-a



k	A	Ea	source
1	8.0 E+12	3.3	a
-1	7.7 E+12	45.1	a
2	1.0 E+13	22.7	b
$\langle v \rangle = 1265.3/\text{cm}$			c
LJ Parameters :			d
$\text{sigma} = 4.898 \text{ \AA}^\circ$		$e/k = 300 \text{ cal}$	

a

A factor taken as that for  $\text{CH}_3\text{CHCH}_2 + \text{H}$   
 $A_{-1}$  factor based upon entropy change fro reverse.  
 (ref: Dean)

b

A factor based upon entropy change for reverse.  
 $A_{-1}$  taken as that for  $\text{CH}_3 + \text{CH}_2\text{CH}_3$  ( $A = 2.0 \text{ E+13}$ ,  $Ea = \Delta\text{Hr}$ )  
 (ref: Dean)

c

see note (c) Table 1-a.  
 (refer to  $\text{CH}_3\text{CH}_2\text{Cl}$ )

d

see note (d) Table 1-a

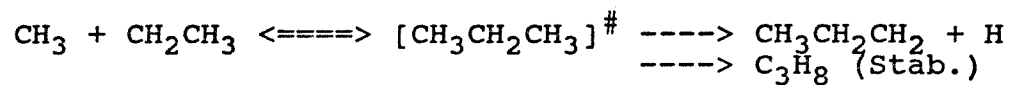
Table 3-b

APPARENT REACTION RATE CONSTANTS PREDICTED  
 USING BIMOLECULAR QRRK ANALYSIS

P (torr)	Reaction	A (cc/mol s)	Ea (Kcal/mol)
7.6	$\text{CH}_2\text{CHCl} + \text{H} = \text{CH}_2\text{CH}_2\text{Cl}$	1.30 E+08	-2.57
76.0		1.30 E+09	-2.55
760.0		1.39 E+10	-2.36
7.6	$\text{CH}_2\text{CHCl} + \text{H} = \text{CH}_2\text{CH}_2 + \text{Cl}$	7.97 E+12	3.29
76.0		8.02 E+12	3.31
760.0		8.51 E+12	3.49



Table 4-a



k	A	Ea	source
1	1.0 E+13	0.0	a
-1	8.0 E+16	84.4	a
2	1.6 E+16	97.6	a
$\langle v \rangle = 1330/\text{cm}$			b
LJ Parameters :			c
$\text{sigma} = 4.84 \text{ \AA}^\circ$		$e/k = 302 \text{ cal}$	

a Dean, A.M., J. Phys. Chem., 98, 4600, 1985

b see note (c) Table 1-a

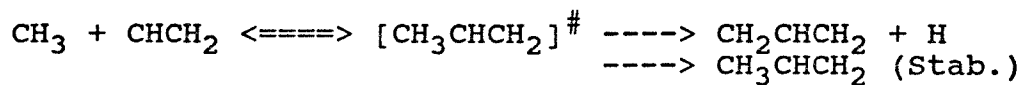
c see note (d) Table 1-a

Table 4-b

APPARENT REACTION RATE CONSTANTS PREDICTED  
 USING BIMOLECULAR QRRK ANALYSIS

P (torr)	Reaction	A (cc/mol s)	Ea (Kcal/mol)
7.6	$\text{CH}_3 + \text{C}_2\text{H}_5 = \text{CH}_3\text{CH}_2\text{CH}_3$	5.45 E+11	-4.63
76.0		2.69 E+12	-2.15
760.0		6.52 E+12	-0.72
7.6	$\text{CH}_3 + \text{C}_2\text{H}_5 = \text{CH}_3\text{CH}_2\text{CH}_2 + \text{H}$	6.55 E+12	16.2
76.0		2.75 E+13	20.2
760.0		1.16 E+14	25.0

Table 5-a



k	A	Ea	source
1	1.8 E+13	0.0	a
-1	8.0 E+16	99.5	a
2	6.3 E+14	89.2	b

$$\langle v \rangle = 1289.5/\text{cm}$$

LJ Parameters :

$$\text{sigma} = 4.685 \text{ \AA}^0$$

$$e/k = 298 \text{ cal}$$

a

Dean, A.M. J. Phys. Chem., 89, 4600, 1985

b

Allara, D.L. and Shaw, R., J. Phys. Chem. Ref. Data, 9, 523, 1980

c

see note (c) Table 1-a

Geometric mean frequency estimated as follows ;

$$\langle v \rangle_{\text{CH}_3\text{CHCH}_2} = ( \langle v \rangle_{\text{CH}_3\text{CH}_2\text{CH}_3} + \langle v \rangle_{\text{CH}_2\text{CCH}_2} )/2$$

d

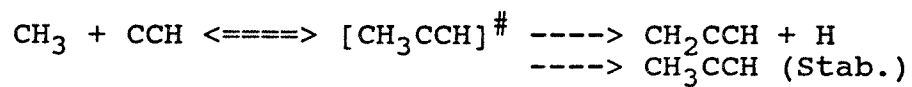
see note (d) Table 1-a

Table 5-b

APPARENT REACTION RATE CONSTANTS PREDICTED  
 USING BIMOLECULAR QRRK ANALYSIS

P (torr)	Reaction	A (cc/mol s)	Ea (Kcal/mol)
7.6	$\text{CH}_3 + \text{CHCH}_2 = \text{CH}_3\text{CHCH}_2$	8.65 E+11	-4.72
76.0		4.59 E+12	-2.21
760.0		1.15 E+13	-0.74
7.6	$\text{CH}_3 + \text{CHCH}_2 = \text{CH}_2\text{CHCH}_2 + \text{H}$	2.27 E+13	5.18
76.0		6.51 E+13	9.66
760.0		9.79 E+13	13.70

Table 6-a



k	A	Ea	source
1	3.2 E+12	0.0	a
-1	5.0 E+15	125.5	a
2	3.0 E+15	101.4	a
$\langle v \rangle = 1238/\text{cm}$			b
LJ Parameters :			c
$\text{sigma} = 4.522 \text{ \AA}^\circ$		$e/k = 333.4 \text{ cal}$	

a  
Dean, A.M., J. Phys. Chem., 89, 4600 (1985)

b  
see note (c) Table 1-a

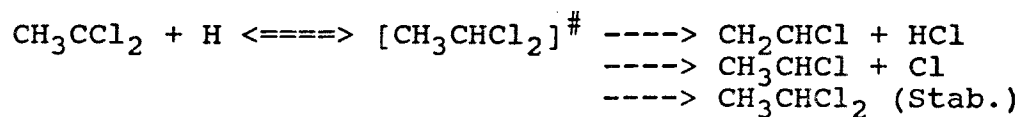
c  
see note (d) Table 1-a

Table 6-a

APPARENT REACTION RATE CONSTANTS PREDICTED  
 USING BIMOLECULAR QRRK ANALYSIS

P (torr)	Reaction	A (cc/mol s)	Ea (Kcal/mol)
7.6	$\text{CH}_3 + \text{CCH} = \text{CH}_3\text{CCH}$	8.11 E+08	-8.05
76.0		1.16 E+10	-6.88
760.0		2.11 E+11	-3.88
7.6	$\text{CH}_3 + \text{CCH} = \text{CH}_2\text{CCH} + \text{H}$	3.36 E+12	0.14
76.0		4.77 E+12	1.10
760.0		1.24 E+13	4.17

Table 7-a



k	A	Ea	source
1	2.0 E+13	0.0	a
-1	4.2 E+14	96.6	a
2	2.9 E+13	55.8	b
3	7.9 E+15	76.8	c
<v> = 797.2/cm			d
LJ Parameters :			e
sigma = 5.103 A°		e/k = 435.9 cal	

a

A factor taken as 1/2 that for H + CH<sub>3</sub>CH<sub>3</sub> (A = 4.0 E+13)  
Reverse reaction (A<sub>-1</sub>) from thermodynamics  
(ref: Allara and Shaw)

b

$$A = 10^{13.55} * 10^{(-4/4.6)} * 6$$

$$Ea = \Delta H + 38.5$$

c

A factor based upon entropy change for reverse.  
A<sub>-3</sub> factor taken as that for C<sub>3</sub>H<sub>7</sub> + CH<sub>3</sub> (A = 4.0E+12)  
Ea = ΔH

d

see note (c) Table 1-a.  
(refer to CH<sub>2</sub>ClCH<sub>2</sub>Cl)

e

see note (d) Table

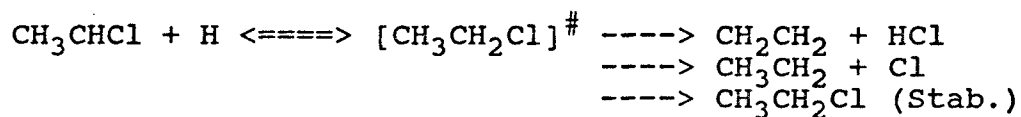
Table 7-b

APPARENT REACTION RATE CONSTANTS PREDICTED  
 USING BIMOLECULAR QRRK ANALYSIS

P (torr)	Reaction	A (cc/mol s)	Ea (Kcal/mol)
7.6	$\text{CH}_3\text{CCl}_2 + \text{H} = \text{CH}_3\text{CHCl}_2$	8.57 E+08	-9.66
76.0		1.12 E+10	-8.89
760.0		2.54 E+11	-6.11
7.6	$\text{CH}_3\text{CCl}_2 + \text{H} = \text{CH}_2\text{CHCl} + \text{HCl}$	2.52 E+12	-2.39
76.0		3.19 E+12	-1.79
760.0		7.50 E+12	0.74
7.6	$\text{CH}_3\text{CCl}_2 + \text{H} = \text{CH}_3\text{CHCl} + \text{Cl}$	3.15 E+13	2.09
76.0		3.72 E+13	2.51
760.0		7.92 E+13	4.59



Table 8-a



k	A	Ea	source
1	2.7 E+13	0.0	a
-1	7.6 E+14	94.0	a
2	3.24E+13	56.6	b
3	1.8 E+15	81.5	c
<v> = 1265.3/cm			d
LJ Parameters : sigma = 4.898 Ao			e
		e/k = 300 cal	

a

A factor as 2/3 that for  $\text{CH}_3\text{CH}_2 + \text{H}$  with  $A = 4.0 \text{ E13}$   
Reverse reaction ( $k_{-1}$ ) from thermodynamics  
(ref: Allara and Shaw)

b

Benson, S. W., "Thermochemical Kinetics", N.Y. John & Son,  
1976 (  $E_a = \Delta H + 39.4$  )

c

A factor based upon entropy change for reverse.  
 $A_{-3}$  taken as that for  $\text{C}_2\text{H}_5 + \text{CH}_3$  ( $A = 2.0 \text{ E13}$ )  
(ref; Allara & Shaw)

d

see note (c) Table 1-a

e

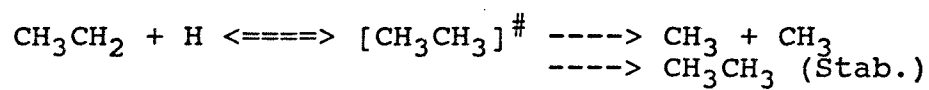
see note (d) Table 1-a

Table 8-b

APPARENT REACTION RATE CONSTANTS PREDICTED  
 USING BIMOLECULAR QRRK ANALYSIS

P (torr)	Reaction	A (cc/mol s)	Ea (Kcal/mol)
7.6	$\text{CH}_3\text{CHCl} + \text{H} = \text{CH}_3\text{CH}_2\text{Cl}$	5.63 E+09	-7.30
76.0		6.89 E+10	-6.67
760.0		1.30 E+12	-4.15
7.6	$\text{CH}_3\text{CHCl} + \text{H} = \text{CH}_2\text{CH}_2 + \text{HCl}$	1.96 E+13	-4.18
76.0		2.38 E+13	0.14
760.0		5.12 E+13	2.65
7.6	$\text{CH}_3\text{CHCl} + \text{H} = \text{CH}_3\text{CH}_2 + \text{Cl}$	3.14 E+13	5.18
76.0		3.67 E+13	5.60
760.0		7.64 E+13	7.75

Table 9-a



k	A	Ea	source
1	1.8 E+14	0.0	a
-1	1.3 E+16	100.7	a
2	8.0 E+16	90.4	a
$\langle v \rangle = 1509/\text{cm}$			b
LJ Parameters :			c
$\text{sigma} = 4.342 \text{ \AA}^\circ$		$e/k = 246.8 \text{ cal}$	

a

Dean, A. M., J. Phys. Chem., 89, 4600, 1985

b

see note (c) Table 1-a

c

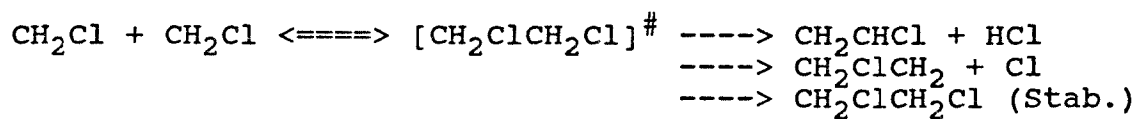
see note (d) Table 1-a

Table 9-b

APPARENT REACTION RATE CONSTANTS PREDICTED  
 USING BIMOLECULAR QRRK ANALYSIS

P (torr)	Reaction	A (cc/mol s)	Ea (Kcal/mol)
7.6	$\text{CH}_3\text{CH}_2 + \text{H} = \text{CH}_3\text{CH}_3$	1.99 E+10	-9.57
76.0		2.91 E+11	-8.21
760.0		4.93 E+12	-5.21
7.6	$\text{CH}_3\text{CH}_2 + \text{H} = \text{CH}_3 + \text{CH}_3$	1.91 E+14	0.16
76.0		2.82 E+14	1.18
760.0		7.65 E+14	4.08

Table 10-a



k	A	Ea	source
1	4.0 E+12	0.0	a
-1	4.8 E+17	89.3	a
2	1.9 E+13	52.4	b
3	6.0 E+15	78.6	c
<v> = 797.2/cm			d
LJ Parameters :			e
sigma = 5.116 A°		e/k = 471.2 cal	

a

A factor taken as that for 1-C<sub>3</sub>H<sub>7</sub> + 1-C<sub>3</sub>H<sub>7</sub>  
 A<sub>-1</sub> factor based upon entropy change for reverse.  
 (ref: Allara & Shaw)

b

A = 10<sup>13.55</sup> \* 10<sup>(-4/4.6)</sup> \* 4  
 Ea = ΔH + 35

c

A factor based upon entropy change for reverse.  
 A<sub>-3</sub> taken as that for C<sub>3</sub>H<sub>7</sub> + CH<sub>3</sub> (A = 2.0E+13)  
 (ref: Allara & Shaw)

d

see note (c) Table 1-a

e

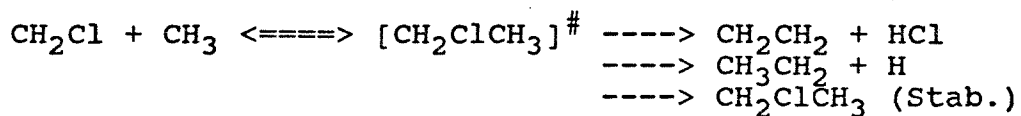
see note (d) Table 1-a

Table 10-b

APPARENT REACTION RATE CONSTANTS PREDICTED  
USING BIMOLECULAR QRRK ANALYSIS

P (torr)	Reaction	A (cc/mol s)	Ea (Kcal/mol)
7.6	$\text{CH}_2\text{Cl} + \text{CH}_2\text{Cl} = \text{CH}_2\text{Cl} + \text{CH}_2\text{Cl}$	4.19 E+08	-9.42
76.0		6.28 E+09	-8.19
760.0		1.34 E+11	-4.98
7.6	$\text{CH}_2\text{Cl} + \text{CH}_2\text{Cl} = \text{CH}_2\text{CHCl} + \text{HCl}$	6.98 E+11	-2.52
76.0		9.96 E+11	-1.53
760.0		2.51 E+12	1.61
7.6	$\text{CH}_2\text{Cl} + \text{CH}_2\text{Cl} = \text{CH}_2\text{ClCH}_2 + \text{Cl}$	2.41 E+12	3.26
76.0		3.05 E+12	3.89
760.0		7.37 E+12	6.46

Table 11-a



k	A	Ea	Source
1	1.67 E+13	0.0	a
-1	1.36 E+17	91.0	a
2	1.44 E+13	56.6	b
3	2.17 E+15	84.0	c
$\langle v \rangle = 1265.3/\text{cm}$			d
LJ Parameters :			e
$\text{sigma} = 4.898 \text{ \AA}$		$e/k = 300 \text{ cal}$	

a

A factor taken as 2/3 that for  $\text{CH}_3 + \text{CH}_3$  ( $A = 2.5 \text{ E}+13$ )  
 $A_{-1}$  based upon entropy change for reverse.

b

$$A = 10^{13.55} * 10^{(-4/4.6)} * 3$$

$$Ea = \Delta H + 39.4$$

d

see note (c) Table 1-a

e

see note (d) Table 1-a

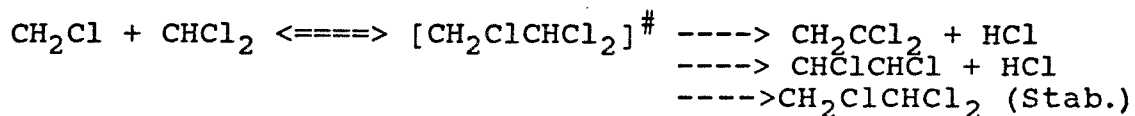
Table 11-a

APPARENT REACTION RATE CONSTANTS PREDICTED  
 USING BIMOLECULAR QRRK ANALYSIS

P (torr)	Reaction	A (cc/mol s)	Ea (Kcal/mol)
7.6	$\text{CH}_2\text{Cl} + \text{CH}_3 = \text{CH}_2\text{ClCH}_3$	5.19 E+09	-7.84
76.0		7.37 E+10	-6.78
760.0		1.30 E+12	-3.75
7.6	$\text{CH}_2\text{Cl} + \text{CH}_3 = \text{CH}_2\text{CH}_2 + \text{HCl}$	5.11 E+12	-1.73
76.0		7.30 E+12	-0.68
760.0		1.67 E+13	2.51
7.6	$\text{CH}_2\text{Cl} + \text{CH}_3 = \text{CH}_3\text{CH}_2 + \text{Cl}$	5.40 E+12	4.35
76.0		7.05 E+12	5.07
760.0		1.76 E+13	7.86



Table 12-a



k	A	Ea	source
-1	8.0 E+12	0.0	a
1	1.0 E+18	86.2	a
2	4.8 E+12	68.1	b
3	2.0 E+13	68.5	c
$\langle v \rangle = 678.7/\text{cm}$			d
LJ Parameters :			e
sigma = 5.72 A <sup>o</sup>		e/k = 498.9 cal	

a

A factor as that for 1-C<sub>3</sub>H<sub>7</sub> + 1-C<sub>4</sub>H<sub>9</sub>  
A<sub>-1</sub> based upon entropy change for reverse.

b

$$A = 10^{13.55} * 10^{(-4/4.6)} * 1$$

$$Ea = \Delta H + 36$$

c

$$A = 10^{13.55} * 10^{(-4/4.6)} * 4$$

$$Ea = \Delta H + 36$$

d

see note (c) Table 1-a  
Geometric mean frequency estimated as folloes:  
 $\langle v \rangle_{\text{CH}_2\text{ClCHCl}_2} = ( \langle v \rangle_{\text{CHCl}_2\text{CHCl}_2} + \langle v \rangle_{\text{CH}_2\text{ClCH}_2\text{Cl}} ) / 2$

e

see note (d) Table 1-a

Table 12-b

APPARENT REACTION RATE CONSTANTS PREDICTED  
USING BIMOLECULAR QRRK ANALYSIS

P (torr)	Reaction	A (cc/mol s)	Ea (Kcal/mol)
7.6	$\text{CH}_2\text{Cl} + \text{CHCl}_2 = \text{CH}_2\text{ClCHCl}_2$	4.84 E+09	-10.60
76.0		5.85 E+10	-7.41
760.0		4.88 E+11	-4.40
7.6	$\text{CH}_2\text{Cl} + \text{CHCl}_2 = \text{CH}_2\text{CCl}_2 + \text{HCl}$	6.54 E+09	-3.65
76.0		1.82 E+10	-0.05
760.0		4.81 E+10	4.05
7.6	$\text{CH}_2\text{Cl} + \text{CHCl}_2 = \text{CHClCHCl} + \text{HCl}$	2.46 E+10	-3.85
76.0		6.91 E+10	0.01
760.0		1.84 E+11	4.12

## APPENDIX 2. ENERGY BALANCE CALCULATION

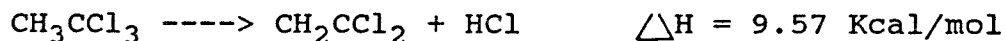
This calculation is based upon the experimental results and detailed reaction mechanism.

## CASE 1.

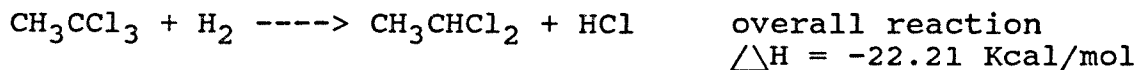
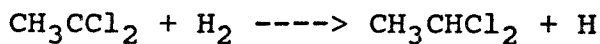
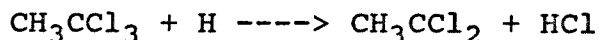
## Reaction conditions

- .Reaction temperature = 572 °C
- .Residence time = 1.0 second
- .Reactor diameter = 1.05 cm
- .Mole fraction for each reagent = 0.0376
- .Mole flow rate = 0.562 l/min \* 1/24.45 \* 0.0376  
= 8.55 x 10<sup>-4</sup> mol/min for each reagent

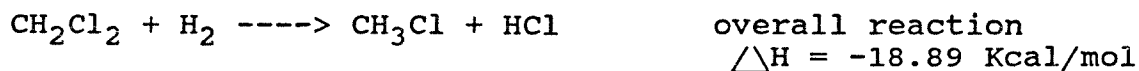
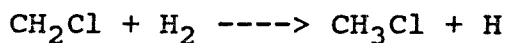
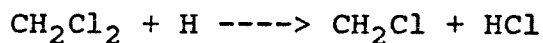
Rxn. 1 90 % conversion



Rxn. 2 10 % conversion



Rxn. 3 17 % conversion



## Total energy balance

$$\text{Rxn. 1} \quad (8.55 \times 10^{-4}) * (9.57) * 0.9 \quad = 7.36 \times 10^{-3}$$

$$\text{Rxn. 2} \quad (8.55 \times 10^{-4}) * (-22.21) * 0.1 \quad = -1.90 \times 10^{-3}$$

$$\text{Rxn. 3} \quad (8.55 \times 10^{-4}) * (-18.89) * 0.17 \quad = -2.75 \times 10^{-3}$$

$$\hline 2.71 \times 10^{-3}$$

$$= (2.71 \text{ cal/min}) * (1/60) * (4.2 \text{ Joule/cal}) = 0.19 \text{ J/sec.}$$

## CASE 2

## Reaction conditions

.Reaction temperature = 720 °C

.Residence time = 1.0 second

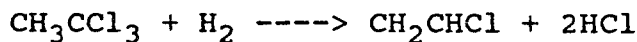
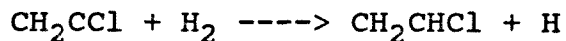
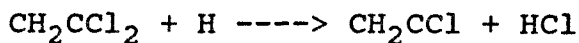
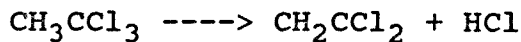
.Reactor diameter = 1.05 cm

.Mole fraction for each reagent = 0.0376

.Mole flow rate = 0.479 l/min \* 1/24.45 \* 0.0376

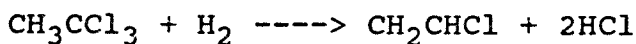
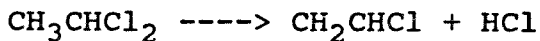
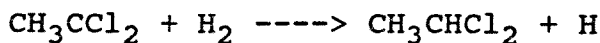
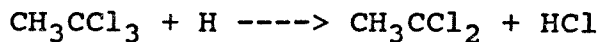
$$= 7.37 \times 10^{-4} \text{ g mol/min for each reagent}$$

Rxn. 1 90 % conversion



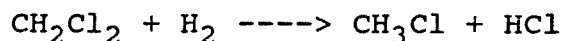
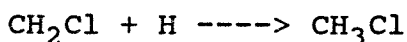
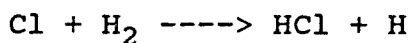
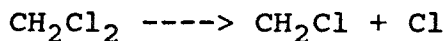
overall reaction  
 $\Delta H = -4.82 \text{ Kcal/mol}$

Rxn. 2 10 % conversion



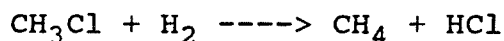
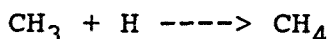
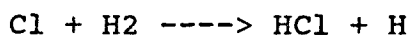
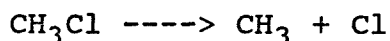
overall reaction  
 $\Delta H = -4.82 \text{ Kcal/mol}$

Rxn. 3      90 % conversion



overall reaction  
 $\Delta\text{H} = -18.9 \text{ Kcal/mol}$

Rxn. 4      10 % conversion



overall reaction  
 $\Delta\text{H} = -20.4 \text{ Kcal/mol}$

Total energy balance

$$\text{Rxn. 1} \quad (7.37 \times 10^{-4}) * (-4.82) * 0.9 = -3.20 \times 10^{-3}$$

$$\text{Rxn. 2} \quad (7.37 \times 10^{-4}) * (-4.82) * 0.1 = -3.55 \times 10^{-4}$$

$$\text{Rxn. 3} \quad (7.37 \times 10^{-4}) * (-18.9) * 0.9 = -1.25 \times 10^{-2}$$

$$\text{Rxn. 4} \quad (7.37 \times 10^{-4}) * (-20.4) * 0.1 = -1.50 \times 10^{-3}$$

$$\text{-----}$$

$$-2.08 \times 10^{-2}$$

$$= (20.8 \text{ cal/min}) * (1/60) * (4.2 \text{ J/cal}) = -1.45 \text{ Joule/sec}$$

#### Heating Element Capacity in Furnace

Position	Length	Watt	Volt	F <sub>time</sub>	Heating Capacity <sup>#</sup>
R	3"	500	50	0.5	114 watt
M	12"	1500	100	0.5	682 watt
L	3"	500	50	0.5	144 watt

<sup>#</sup> see sample calculation.

F<sub>time</sub> = time fraction the furnace element is required to be for designated temperature.

Total heating capacity = 910 watt

Case 1. error in temperature due to endothermic reaction described

$$\text{Error} = \frac{0.19}{910} * (572 \text{ }^{\circ}\text{C}) = 0.12 \text{ }^{\circ}\text{C}$$

Case 2. error due to exothermic reaction described

$$\text{Error} = \frac{-1.45}{910} * (720 \text{ }^{\circ}\text{C}) = -1.14 \text{ }^{\circ}\text{C}$$

NOTE Our temperature is only  $\pm 3 \text{ }^{\circ}\text{C}$ . These error from reaction exo. or endo. thermicity is less than our temperature uncertainty.

SAMPLE CALCULATION

$$\text{Heating capacity} = (500 \text{ watt}) * (50/110) * (0.5) = 114 \text{ watt}$$